ABSTRACT

Title of Document: RESPIRATORY MECHANICS OF FLOW LIMITATION AND CHARACTERIZATION OF RESISTANCE MEASUREMENTS WITH A NON-INVASIVE DEVICE

Derya Calhan Coursey, Ph.D., 2009

Directed By: Professor A. T. Johnson, Department of Bioengineering

Resistance measurements with the airflow perturbation device (APD) were compared to directly measured pulmonary resistances with an esophageal balloon to validate the APD. The APD perturbs the flow and the mouth pressure during regular breathing. The ratio of mouth pressure perturbations to the flow perturbations was used to calculate the inspiratory, expiratory and average respiratory resistance. Six healthy subjects were tested during tidal breathing when known external resistances were added during inspiration, during expiration, and during both inspiration and expiration. The difference between the averaged APD measured and directly measured pulmonary resistances was 0.59 ± 1.25 (mean ± SD) $cmH_2O/L/s$. Compared to the magnitude of the known increase in added resistance, the APD measured resistance increased by 79 %, while the directly measured pulmonary resistance increased only by 56%. During addition of external resistances to both inspiration

and expiration, the changes in inspiratory and expiratory pulmonary resistance were only 36 % and 62 % of the added resistance, respectively. On the other hand, the APD inhalation and exhalation resistance measured between 82 % and 76 % of added resistance change. It was concluded that the APD detects changes in external resistance at least as well and probably better than classical measurements of pulmonary resistance.

Additionally, expiratory isovolume pressure – flow (IVPF) curves, which show the pressure at which the flow becomes limited during forced expiration, were constructed in six healthy subjects with the classical invasive method of esophageal balloon (EB) and the alternative noninvasive method of stop – flow (SF) at 25, 50, and 75 % vital capacity (VC). The difference between the pressures (P_{max}) and flow (Q_{max}) at which flow limitation first occurs and correlation with the stop – flow and esophageal balloon methods were studied. Additionally, the resistance at flow limitation was compared to the APD resistance during forced breathing. On average, $P_{SF,max}$ was 5.6 and 4.4 times $P_{EB,max}$ at 25 %VC and 50 %VC, respectively. $Q_{SF,max}$ was 0.68 and 0.59 times $Q_{EB,max}$ at 25 %VC and 50 %VC, respectively. No correlation was found between the stop – flow and esophageal balloon methods as well as between the resistances at flow limitation.

RESPIRATORY MECHANICS OF FLOW LIMITATION AND CHARACTERIZATION OF RESISTANCE MEASUREMENTS WITH A NON-INVASIVE DEVICE.

By

Derya Calhan Coursey

Dissertation submitted to the Faculty of the Graduate School of the
University of Maryland, College Park, in partial fulfillment
of the requirements for the degree of
Doctor of Philosophy
2009

Advisory Committee:
Professor Arthur T. Johnson, Chair
Professor William J. Higgins
Professor Hubert Montas
Professor Steven M. Scharf, M.D., PhD
Professor Adel Shirmohammadi

To my husband, Jack

Acknowledgements

I would like to thank my advisor Dr. A. Johnson for his support throughout my research. I also would like to thank to my committee members Dr. S. Scharf, Dr. A. Shirmohammadi, Dr. H. Montas, and Dr. W. Higgens. In particular, I appreciate the assistance of Dr. S. Scharf for coming to College Park to help me with my experiments. I also appreciate his guidance throughout my research and taking his time to reply to endless emails from wherever he was. Additionally, I would like to acknowledge Dr. R. McCuen for his help in guiding me in statistical analysis of my data. I also would like to thank Dr. A. Shirmohammadi for saving me from various crises including finding a subject in the last minute.

This dissertation never would have happened without the great cooperation of my subjects. I would like to thank each one of them for their patience. I especially would like to thank Dan, Andrew, and Preston for their willingness to be tested many many times to validate my experimental set up. I also would like to thank Frank, Shaya, and Melissa for always offering their help when necessary.

I would like to acknowledge my family for their support throughout my education. Finally, my journey would have been impossible without intellectual, emotional, editorial, and financial support of my husband, Jack.

Table of Contents

Chapter 1. Introduction 1
1.1 Motivation 1
1.2 Background 2
1.2.1 Maximum Expiratory Flow 2
1.2.2 Pleural Pressure 4
1.2.3 Respiratory Pressures 6
1.2.4 A Simple Respiratory Model 7
1.2.5 The Theory of APD Resistance Prediction 9
1.3 Research Goals and Objectives 10

Chapter 2. Literature Review 12
2.1 Maximum Expiratory Flow 12
2.1.1 Flow Limitation 12
2.1.2 Respiratory Resistance at Maximum Flow 20
2.2 The Stop-Flow Method 24
2.3 Pleural Pressure Measurement with Esophageal Balloon 28
2.4 Pulmonary Resistance 30
2.5 Airflow Perturbation Device (APD) 30
2.6 Detection of Respiratory Resistive Loads 33

Chapter 3. Experimental Setup and Methodology 36
3.1 Equipment and Experimental Apparatus 36
3.1.1 Stop-Flow Experimental Setup 36
3.1.2 The Airflow Perturbation Device (APD) 40
3.1.3 The External Resistances 40
3.1.4 The Esophageal Balloon Catheter 42
3.2 Subject Testing 45
3.2.1 Orientation and Consent 45
3.2.2 Vital Capacity (VC) 46
3.2.3 Stop – Flow Measurements 46
3.2.4 Pleural Pressure 49
3.2.5 The APD Resistance 49

Chapter 4. Data Analysis 51
4.1 Construction of IVPF Curves 51
4.1.1 Stop – Flow Experiments 51
4.1.2 Esophageal Balloon Method 53
4.1.3 Identifying the Limited Flow 54
4.2 Pulmonary Resistance Calculations 55
4.3 The APD Resistance Calculation 58
4.4 Statistical Analysis 58

Chapter 5. The APD Resistance versus Pulmonary Resistance 60
5.1 The APD and Pulmonary Resistance 60

5.1.1 The Baseline Resistances 61
5.1.2 Addition of Inspiratory and Expiratory Resistances 63
5.1.3 High Respiratory Load only on Inhalation or Exhalation 73
5.2 Discussion 77
5.3 Conclusion 83

Chapter 6. Isovolume Pressure - Flow (IVPF) Curves 84
6.1 IVPF Curves 84
6.1.1 Stop – Flow Method 84
6.1.2 Esophageal Balloon Method 89
6.2 Comparing the two Methods 95
6.3 Resistance Calculation at the Onset of Flow Limitation 103
6.4 Discussion 106

Chapter 7. Conclusion and Future Work 109
7.1 Conclusion 109
7.2 Suggestions for Future Work 109

Appendix A: Consent Form and Health Questionnaire 112

Appendix B. Various Lung Volumes and Capacities 118

Appendix C: Matlab Program to Plot IVPF Curves 120

Appendix D: Statistics of Comparison of the APD Resistance to Pulmonary Resistance 123
D.1 Baseline Resistances 123
D.2 Addition of Inspiratory and Expiratory Resistances 124
D.2.1 Average Resistance 124
D.2.1.1 Addition of Low Resistance 124
D.2.1.2 Addition of High Resistance 126
D.2.2 Inhalation Resistance 127
D.2.2.1 Addition of Low Resistance 127
D.2.2.2 Addition of High Resistance 129
D.2.3 Exhalation Resistance 130
D.2.3.1 Addition of Low Resistance 130
D.2.3.2 Addition of High Resistance 132
D.3 High Respiratory Load only on Inhalation or Exhalation 133
D.3.1 High Respiratory Load on Inhalation Side 133
D.3.2 High Respiratory Load on Exhalation Side 134

Appendix E: Average APD and Pulmonary Resistance Plots 136

Appendix F: Inhalation and Exhalation APD and Pulmonary Resistance Plots 139

Appendix G: Statistics of IVPF Curves 143

G1. Comparing the Stop – Flow and Esophageal Balloon Methods 143
G.2 Comparison of Resistances 145

References 148

List of Tables

Table 1: Inspiratory and expiratory resistances for normal subject and patients with COPD (Aldrich et al., 1989). 24

Table 2: Added external resistances in cm H_2O/L/s. Each set contained a low and high resistance..... 41

Table 3: Physiological characteristics of subjects. 46

Table 4: Intrinsic resistances (cm H_2O/L/s) measured with both methods. Only for subject 102, the pulmonary resistance was higher than the APD resistance. 62

Table 5: The mean and standard deviation (SD) of the APD and pulmonary intrinsic resistances. 62

Table 6: Average (av) resistance results with added resistances to both inspiration and expiration in cm H_2O/L/s. 63

Table 7: Table showing whether or not there were any significant differences between the change in average APD resistance, pulmonary resistance, and added resistance when external low and high resistances were added during tidal breathing. Note that statistics were calculated with unpaired t-test for unequal variances at $\alpha = 0.05$..... 66

Table 8: Inspiratory resistance results with added resistances to both inhalation and exhalation in cm H_2O/L/s..... 67

Table 9: Expiratory (exh) resistance results with added resistances to both inspiration and exhalation in cm H_2O/L/s..... 68

Table 10: Table showing whether or not there were any significant differences between the change in inhalation APD resistance, pulmonary resistance, and added resistance when external low and high resistances were added during tidal breathing. Note that statistics were calculated with t-test for unequal variances at $\alpha = 0.05$..... 71

Table 11: Table showing whether or not there were any significant differences between the change in exhalation APD resistance, pulmonary resistance, and added resistance when external low and high resistances were added during tidal breathing. Note that statistics were calculated with t-test for unequal variances at $\alpha = 0.05$..... 72

Table 12: Measured inspiratory (ins) and expiratory (exp) resistances and change in resistances with 5.81 cm H_2O/L/s added only on the inhalation side..... 74

Table 13: Measured inspiratory (ins) and expiratory (exp) resistances and change in resistances with 5.81 cm H_2O/L/s added only on the exhalation side. 74

Table 14: Pressure ($P_{SF,max}$) and flow ($Q_{SF,max}$) values at the point of flow limitation at different lung volumes for all subjects with the stop – flow method..... 88

Table 15: Pressure ($P_{EB,max}$) and flow ($Q_{EB,max}$) values at the point of flow limitation at different lung volumes for all subjects with the esophageal balloon method..... 94

Table 16: Pressure (P) and flow (Q) values at the onset of flow limitation for stop - flow (SF) and esophageal balloon (EB) methods at 25 %VC. 101

Table 17: Pressure (P) and flow (Q) values at the onset of flow limitation for stop - flow (SF) and esophageal balloon (EB) methods at 50 %VC. 101

Table 18: Pearson correlation coefficient values. 102

Table 19: The resistance values (cm H_2O/L/s) at the onset of flow limitation for stop - flow (SF), esophageal balloon (EB), and the APD methods at 25 %VC..... 105

Table 20: The resistance values (cm H_2O/L/s) at the onset of flow limitation for stop - flow (SF), esophageal balloon (EB), and the APD methods at 50 %VC..... 105

Table 21: Pearson correlation coefficient at 25 and 50 %VC..... 105

List of Figures

Figure 1: Plot of volume expired as a function of time 3

Figure 2: Plot of expiratory flow as a function of volume. TLC=Total lung capacity, RV=Residual volume. Curves 1 through 4 show different effort levels. Curve 4 is for the minimum effort and curve 1 is for the maximum effort. Curves A, B, and C show the flow volume curves with different starting volume. 4

Figure 3: Drawing of the respiratory system showing where the various pressures can be measured. 5

Figure 4: Pleural pressure versus change in lung volume during inspiration and expiration. 6

Figure 5: Pressures involved in respiration. P_{pl}= Pleural pressure, P_{alv}= Alveolar pressure, P_{aw}=Airway pressure, P_{mo}=mouth pressure (usually atmospheric), P_{bs}= Pressure at body surface (usually atmospheric). 7

Figure 6: Simplified lumped parameter of the respiratory system. C_{rs} = Respiratory compliance, L/cm H_2O; I_{rs} = Respiratory inertance, cm $H_2O.s^2/L$; R_{rs} = Respiratory resistance, cm H_2O/L/s; P_{mo} = Mouth pressure, cm H_2O; P_{mus} = Muscle pressure, cm H_2O. 7

Figure 7: On the left is the the relationship between the pressure applied to the surface of the lung and the resulting flowrate. On the right is the flow and volume coordinates of the pressure flow curve maxima (Fry ,1958). 13

Figure 8: Left: Maximum expiratory flow volume curves for a subject exhaling through three different resistances. Right: Maximum flow plotted against mouth pressure, P_{ao}, for different resistances and at different lung volumes expressed as % VC (Mead et. al, 1967). 14

Figure 9: Collapse of airways during expiration. P_{pl} = Pleural pressure, P_{el} = elastic recoil pressure 15

Figure 10: Effect of pressure change on flow (Q) at a given lung volume. 16

Figure 11: A graphical representation of flow limitation at wave speed (After Wilson et al., 1980). 18

Figure 12: Viscous flow limitation. An area-pressure curve of a smaller airway is shown in panel a. If the pressure gradient in the flow is described by the Poiseuille equation, then for a fixed pressure P_1 at the upstream end of the tube, flow will depend on P_2, the pressure at the downstream end of the tube, as shown in panel b (Wilson et al., 1980) 20

Figure 13: Waterfall model of the lung. P_{alv} = alveolar pressure, P_{pl} = pleural pressure, P_m = mouth pressure (Pride et al. 1967). 21

Figure 14: Curves showing how the resistance of the total airway, R_{aw}, and upstream from EPP, R_{us}, and downstream from EPP, R_{ds}, change as pleural pressure, P_{pl}, increases (After Mead et al., 1967). 22

Figure 15: Airway resistance-lung volume curves during ten consecutive forced vital capacity maneuvers in a healthy non-smoker (open circles). For comparison the resistance volume curve during panting (closed circles) (Zamel et al., 1974). 23

Figure 16: Plot of flow versus time after shutter opening during the stop-flow method 25

Figure 17: C: The mouth pressure time curve showing the first 2 phases. D: Pleural pressure versus time curve during interruption (Ohya et al., 1988)..... 27

Figure 18: The supramaximal flow is observed as the flow exceeding V_{max} line (Ohya et al., 1988). 28

Figure 19: The Airflow Perturbation Device 31

Figure 20: Pressure and flow versus time as recorded by APD. The ratio of $\Delta P/\Delta V'$ gives the respiratory resistance (Lausted et al., 1999). 31

Figure 21: Presence of perturbations on the chest wall: (1) above pectoral 4 cm right of sternum, (2) below pectoral 4 cm right of sternum, (3) 2 cm right of seventh dorsal vertebra (Lausted et al., 1999). 32

Figure 22: Diagram of the stop-flow experimental setup. 37

Figure 23: Setup of stop-flow experiment. 37

Figure 24: Pressure and flow relationship of the pneumotach..... 38

Figure 25: Solenoid-relay assembly that controls the shutter..... 39

Figure 26: Solenoid shutter assembly 40

Figure 27A: Low and high resistances built with capillary tubes. B: Diagram of another external resistance system to apply higher respiratory load to one side only. If a subject was breathing through side I, during inhalation the valve will close and the flow would follow dashed arrows. During exhalation, flow would follow solid arrows. Therefore, the higher resistance would be on the inhalation side. If a subject breaths through side II, the higher resistance would be on the exhalation side. 41

Figure 28: Pressure-flow characteristics of external rigid resistances used. 42

Figure 29: Esophageal balloon catheter 43

Figure 30: The pressure volume characteristics of the esophageal balloon..... 43

Figure 31: Schematic of the experimental apparatus that was used to measure the frequency response of the esophageal balloon..... 44

Figure 32: Bode plot showing the frequency response of the esophageal balloon 45

Figure 33: Operation of stop-flow data acquisition 48

Figure 34: Flow and mouth pressure recording of a subject during the stop – flow experiment..... 52

Figure 35: The transient flow after shutter opening..... 52

Figure 36: Transpulmonary pressure and flow recording of subject 105 for one effort level at different percent vital capacity. Green circles show the correlated pressure and flow values at each lung volume. 53

Figure 37: The IVPF curves of subject 105 at 25 %, 50 % and 75 %VC. Green circles show the data points obtained from Figure 36. 54

Figure 38: IVPF curves of one subject at 25 %VC. $P_{SF,max}$ and $Q_{SF,max}$: Mouth pressure and flow at flow limitation with the stop – flow method; $P_{EB,max}$ and $Q_{EB,max}$: Transpulmonary pressure and flow at flow limitation with the esophageal balloon method..... 55

Figure 39: Simultaneous recording of lung volume, pleural pressure, and flow during tidal breathing. The change in pressure (ΔP) divided by change in flow (ΔQ) between two points where lung volume is identical provide an estimate of average pulmonary resistance. 57

Figure 40: The Airflow Perturbation Device mouth pressure perturbation during part of the exhalation. $\Delta P/\Delta Q$ gives the resistance calculated with the APD. 58

Figure 41: Added Resistance versus pulmonary and APD resistances for subject 100. The resistance value on the y axis when the added resistance is zero corresponds to the subject's intrinsic resistance..... 64

Figure 42: Measured change in average APD resistance with added resistance. Dashed lines connect the data from an individual subject. Linear regression is drawn with all data. 65

Figure 43: Measured change in average pulmonary resistance with added resistance. Dashed lines connect the data from an individual subject. Linear regression is drawn with all data. 66

Figure 44: The resistance value on the y axis when the added resistance is zero corresponds to the subject's intrinsic resistance. Added Resistance versus pulmonary and APD inhalation and exhalation resistances for subject 100. 69

Figure 45: Measured change in inhalation pulmonary resistance with added resistance for all subjects except 104. Dashed lines connect the data from an individual subject. Linear regression is drawn with all data. 69

Figure 46: Measured change in exhalation pulmonary resistance with added resistance. Dashed lines connect the data from an individual subject. Linear regression is drawn with all data. 70

Figure 47: Measured change in inhalation APD resistance with added resistance. Dashed lines connect the data from an individual subject. Linear regression is drawn with all data. 70

Figure 48: Measured change in exhalation APD resistance with added resistance. Dashed lines connect the data from an individual subject. Linear regression is drawn with all data. 71

Figure 49: Added resistance versus the difference between $R_{APD,ins}$ and $R_{L,ins}$ for each subject. 72

Figure 50: Added resistance versus the difference between $R_{APD,exh}$ and $R_{L,exh}$ for each subject. 73

Figure 51: Inspiratory and expiratory resistances of all subjects with one way valve. Solid circles: Inhalation pulmonary and the APD resistances. Open diamond: Exhalation pulmonary and the APD resistances. 75

Figure 52: Mean change in inspiratory and expiratory resistances. The error bars show the standard deviation. 76

Figure 53: Flow (blue line) and pleural pressure (green line) recording of subject 101 during tidal breathing. The pleural pressure plot clearly shows variation assumed to be cardiac artifacts. Compare this to Figure 54. 79

Figure 54: Flow (blue line) and pleural pressure (green line) recording of subject 100 during tidal breathing. Pleural pressure plot does not show any cardiac artifacts. Compare it to Figure 53. 79

Figure 55: Pleural pressure (green line) and flow curve (blue line) of subject 100 during tidal breathing when the APD was off. 82

Figure 56: Pleural pressure (green line) and flow curve (blue line) of subject 100 when the APD was on. Note that pleural pressure curve is not any different than the curve in Figure 55. There are no identifiable perturbations in the pleural pressure curve..... 82

Figure 57: IVPF curves of subject 100 constructed with stop-flow method. 85

Figure 58: IVPF curves of subject 101 constructed with stop-flow method. 85

Figure 59: IVPF curves of subject 102 constructed with stop-flow method. 86

Figure 60: IVPF curves of subject 103 constructed with stop-flow method. 86

Figure 61: IVPF curves of subject 105 constructed with stop-flow method. 87

Figure 62: Normalized pressure and flow versus lung volume for stop - flow method. 89

Figure 63: IVPF curve of subject 100 with the esophageal balloon method. 90

Figure 64: IVPF curve of subject 101 with the esophageal balloon method. 90

Figure 65: IVPF curve of subject 102 with the esophageal balloon method. 91

Figure 66: IVPF curve of subject 103 with the esophageal balloon method. 91

Figure 67: IVPF curve of subject 104 with the esophageal balloon method. 92

Figure 68: IVPF curve of subject 105 with the esophageal balloon method. 92

Figure 69: Normalized pressure and flow versus lung volume for the esophageal balloon method..... 95

Figure 70: IVPF curve of subject 100 at 25 %VC with the stop – flow and esophageal balloon methods. 96

Figure 71: IVPF curve of subject 101 at 25 %VC with the stop – flow and esophageal balloon methods. 96

Figure 72: IVPF curve of subject 102 at 25 %VC with the stop – flow and esophageal balloon methods. 97

Figure 73: IVPF curve of subject 103 at 25 %VC with the stop – flow and esophageal balloon..... 97

Figure 74: IVPF curve of subject 105 at 25 %VC with the stop – flow and esophageal balloon methods. 98

Figure 75: IVPF curve of subject 100 at 50 %VC with the stop – flow and esophageal balloon methods. 98

Figure 76: IVPF curve of subject 101 at 50 %VC with the stop – flow and esophageal balloon methods. 99

Figure 77: IVPF curve of subject 102 at 50 %VC with the stop – flow and esophageal balloon methods. 99

Figure 78: IVPF curve of subject 103 at 50 %VC with the stop – flow and esophageal balloon methods. 100

Figure 79: R_{APD} versus %VC for subject 100 for three different runs are represented by the open symbols. The esophageal balloon, stop –flow, and APD resistances are also plotted at 25 and 50 %VC, and are represented by solid symbols. 100 %VC corresponds to TLC..... 104

Figure 80: Comparison of different methods of measuring resistance. For example, the body plethysmograph measures airways resistance as $P_1/\dot{V}_1$. On the other hand the APD measures resistance at point 1 as $\Delta P_1/\Delta \dot{V}_1$ (Johnson et al., 1984). 107

Figure 81: Pressure-Flow curve of a subject during forced breathing when the APD was connected to the mouth. The black line drawn by connecting the peaks of the flow is the virtual flow curve. This curve does not follow the real flow curve (green line) that was observed without the APD being connected to the mouth. 108

Nomenclature

APD	The Airflow Perturbation Device
A	Cross Sectional Area, m^2
C_{rs}	Respiratory Compliance, L/cm H_2O
C_{lt}	Lung – Tissue Compliance, L/cm H_2O
C_{cw}	Chest Wall Compliance, L/cm H_2O
c	Wave speed, m/s
COPD	Chronic Obstructive Pulmonary Disease
EB	Esophageal Balloon Method
EPP	Equal Pressure Point
FVC	Forced Vital Capacity, L
FEV_1	Volume of Gas Expired in First Second of Forced Expiration, L
FEV1%	Ratio of FEV_1/FVC
I_{rs}	Respiratory Inertance, cm $H_2O.s^2/L$
I_{aw}	Airway Inertance, cm $H_2O.s^2/L$
I_{cw}	Chest Wall Inertance, cm $H_2O.s^2/L$
IVPF	Isovolume Pressure – Flow Curves
P	Pressure, cm H_2O
P_{aw}	Airway Pressure, cm H_2O
P_{alv}	Alveolar Pressure, cm H_2O
P_{mo}	Mouth Pressure, cm H_2O
P_{pl}	Pleural Pressure, cm H_2O
P_{bs}	Pressure at Body Surface, cm H_2O

P_{mus}	Muscle Pressure, cm H_2O
P_L	Lung Elastic Recoil Pressure, cm H_2O
P_{cw}	Chest Wall Elastic Recoil Pressure, cm H_2O
P_{el}	Elastic Recoil Pressure, cm H_2O
$P_{tp,MI}$	Transpulmonary Pressure at Mid Inspiration, cm H_2O
$P_{tp,ME}$	Transpulmonary Pressure at Mid Expiration, cm H_2O
$P_{SF,max}$	Stop – Flow Pressure at Flow Limitation, cm H_2O
$P_{EB,max}$	Esophageal Balloon Pressure at Flow Limitation, cm H_2O
Q	Flow, L/s
Q_{max}	Maximum Flow, L/s
Q_{MI}	Flow at mid inspiration, L/s
Q_{ME}	Flow at mid expiration, L/s
$Q_{EB,max}$	Esophageal Balloon Limited Flow, L/s
$Q_{SF,max}$	Stop – Flow Limited Flow, L/s
R_{APD}	The APD Resistance, cm H_2O/L/s
$R_{APD,ins}$	Inspiratory APD Resistance, cm H_2O/L/s
$R_{APD,exp}$	Expiratory APD Resistance, cm H_2O/L/s
R_{aw}	Airway Resistance, cm H_2O/L/s
R_d	Resistance Downstream From Collapsible Segment, cm H_2O/L/s
R_u	Resistance Upstream From Collapsible Segment, cm H_2O/L/s
R_{lt}	Lung – Tissue Resistance, cm H_2O/L/s
R_{cw}	Chest Wall Resistance, cm H_2O/L/s
R_{SF}	Stop – Flow Resistance, cm H_2O/L/s

R_{EB}	Esophageal Balloon Resistance, cm H_2O/L/s
R_{rs}	Respiratory Resistance, cm H_2O/L/s
R_L	Average Pulmonary Resistance, cm H_2O/L/s
$R_{L,ins}$	Inspiratory Pulmonary Resistance, cm H_2O/L/s
$R_{L,exp}$	Expiratory Pulmonary Resistance, cm H_2O/L/s
RV	Residual Volume, L
SF	Stop – Flow Method
TLC	Total Lung Capacity, L
V	Volume, L
V'	Rate of Change of Volume, flow, L/s
V''	Rate of Change of Flow, L/s^2
VC	Vital Capacity, L
V_{MI}	Lung volume at mid inspiration, L
V_{ME}	Lung volume at mid expiration, L
ρ	Gas Density, kg/m^3
μ	Viscosity, Pa.s
$\Delta P_{L,ER}$	Lung Elastic Recoil Pressure Difference, cm H_2O
$\Delta R_{APD,av}$	Change in average APD resistance relative to average baseline resistance, cm H_2O /L/s
$\Delta R_{APD,ins}$	Change in inspiratory APD resistance relative to inspiratory baseline resistance, cm H_2O /L/s
$\Delta R_{APD,exh}$	Change in expiratory APD resistance relative to expiratory baseline resistance, cm H_2O /L/s

$\Delta R_{L,av}$	Change in average pulmonary resistance relative to average baseline resistance, cm H_2O /L/s
$\Delta R_{L,ins}$	Change in inspiratory pulmonary resistance relative to inspiratory baseline resistance, cm H_2O /L/s
$\Delta R_{L,exh}$	Change in expiratory pulmonary resistance relative to expiratory baseline resistance, cm H_2O /L/s

Chapter 1. Introduction

This thesis focuses on characterization of the Airflow Perturbation device together with flow limitation. The motivation of this work, background, and the objectives are discussed below. A detailed review of the literature follows in Chapter 2.

1.1 Motivation

Every year, almost 400,000 Americans die due to lung disease, which is the number three killer in America. Additionally, most lung disease is also chronic. More than 35 million Americans are now living with chronic lung disease (American Lung Association, Lung Disease Data, 2008).

In a diseased lung that was not diagnosed at an early stage, properties of the tissue change in such a way that it cannot be repaired. One of the important components of the work of breathing is flow-resistive forces. Resistance to airflow changes with the severity of obstructive airways disease. However, resistance to airflow is not easy to measure. Various techniques have been used to measure flow-resistive pressure drops down the airway and estimate resistance to airflow. Airway resistance is routinely measured by body plethysmograph (DuBois et al., 1956). A body plethysmograph is an airtight chamber where compression and expansion of lungs cause pressure changes in the chamber. Changes in chamber pressure with respect to changes in airflow measured at the mouth indicate airway resistance. This is usually expressed as specific conductance, a volume corrected measure of airway conductance. Total pulmonary resistance is another measure of respiratory resistance and includes airway plus lung tissue resistance and may be measured using the

techniques of Von Neergard and Wirz (Von Neergard et al., 1927). It is assumed that esophageal pressure measured with a balloon catheter reflects the pleural pressure (Baydur et al., 1982, Dechman et al., 1992, Peslin et al., 1993). Current methodology was first introduced by Buytendijk in 1949 (Dechman et al. 1992) and later standardized by Milic-Emili et al., 1964.

An important disadvantage of the body plethysmograph or esophageal balloon techniques for measurements of airways or total pulmonary resistance is that these require expensive equipment, great cooperation of the patient, and a trained technical staff, thus rendering the assessment of resistance-based measurements impossible in the home or ambulatory setting outside the pulmonary function laboratory. Thus, there remains a need for a non-invasive, easy to use device for monitoring of respiratory resistances.

This study focuses on the validation of respiratory resistance measurements with the Airflow Perturbation Device (APD) and prediction of the flow limitation at any given lung volume using the stop-flow and esophageal balloon methods. These three methods are used to understand the characteristics of the APD to be used as a diagnostic tool.

1.2 Background

1.2.1 Maximum Expiratory Flow

Maximum expiratory flow is a useful measurement of lung mechanics because of its reproducibility, ease of measurement, and sensitivity to changes in the lung's mechanical properties. The simplest measurement method is the forced expiratory vital capacity test. This method involves the subject inhaling to total lung capacity (TLC) and then exhaling as completely and with as much force as possible i.e. with

maximum effort. From this test, the volume expired versus time curve (Figure 1) and the maximal expiratory flow-volume curve can be produced (Figure 2). Curves 1, 2, 3, and 4 in Figure 2 show different effort levels. Curve 1 is the flow versus volume curve for a maximum effort. When maximum flow is reached, flow falls regardless of starting volume (curves A, B, and C) or effort (curves 1, 2, 3, and 4). As seen in Figure 2, flow is high at early expiration, reaches its peak and falls as expiration continues and lung volume decreases. Another commonly used parameter that could be obtained from Figure 1 is the FEV_1. FEV_1 is the volume of gas expired in the first second of forced expiration. For example, significantly reduced FEV_1 could indicate a chronic obstructive pulmonary disease.

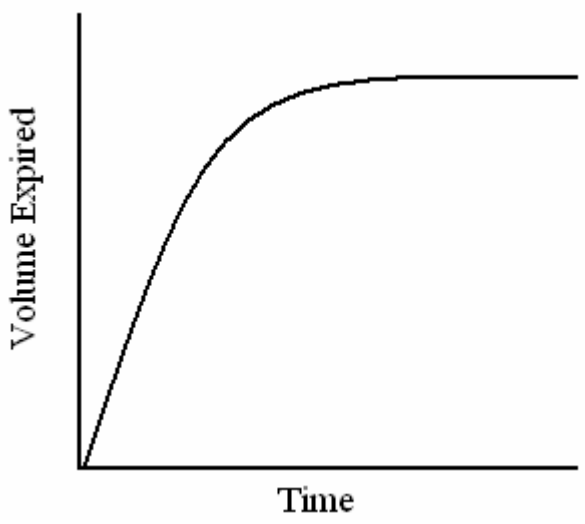

Figure 1: Plot of volume expired as a function of time

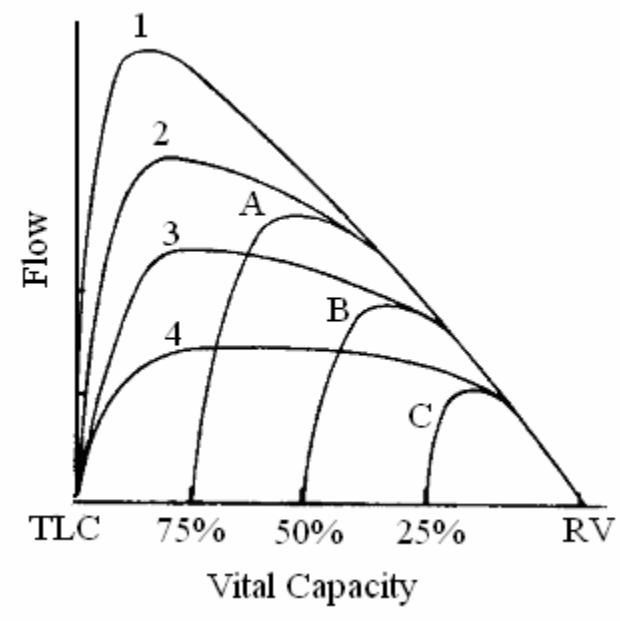

Figure 2: Plot of expiratory flow as a function of volume. TLC=Total lung capacity, RV=Residual volume. Curves 1 through 4 show different effort levels. Curve 4 is for the minimum effort and curve 1 is for the maximum effort. Curves A, B, and C show the flow volume curves with different starting volume.

It has been known that flow limitation during the maximum expiratory effort is related to narrowing of airways. When maximum flow is reached at a certain lung volume, regardless of the effort, flow decreases (Figure 2). One of the reasons is that the resistance in the airways increases in the same proportion as increase in pressure due to the change in shape of the airways. One of the ways of finding the change of resistance at the onset of flow limitation is to construct the isovolume pressure - flow curves with pleural pressure (Hyatt et al., 1958; Fry, 1958; Mead et al., 1967).

1.2.2 Pleural Pressure

The pleural space surrounding the lung is a fluid filled medium. Pleural pressure can be defined as the pressure in the pleural space with respect to the atmosphere (Figure 3). Knowledge of the pleural pressure is important to assess the mechanical and physical state of the lung airways and tissue. During inspiration,

muscular tension in the diaphragm creates subatmospheric pleural pressure, which results in subatmospheric alveolar pressure. This in turn causes the inspiratory flow to start. The flow continues until the alveolar pressure is atmospheric again. Expiratory flow starts when alveolar pressure exceeds atmospheric. The flow will continue until the inward recoil of the lung (i.e. tendency of the lung to collapse) is balanced by the outward recoil of the chest wall (i.e. tendency of the chest wall to expand). The changes in pleural pressure with lung volume during inspiration and expiration are shown in Figure 4. Note that even though alveolar pressure changes from being subatmospheric to atmospheric, pleural pressure is always negative during tidal breathing.

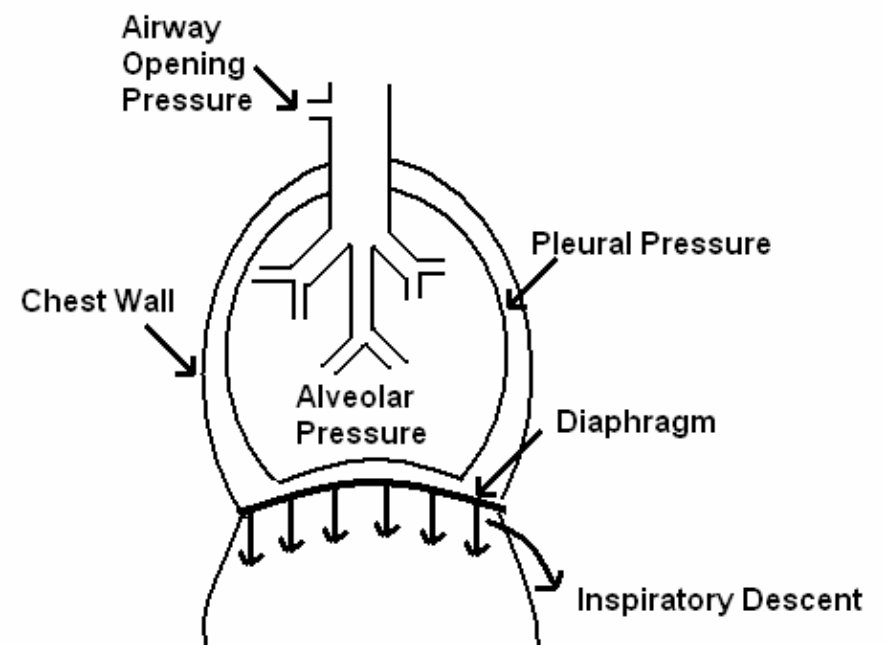

Figure 3: Drawing of the respiratory system showing where the various pressures can be measured.

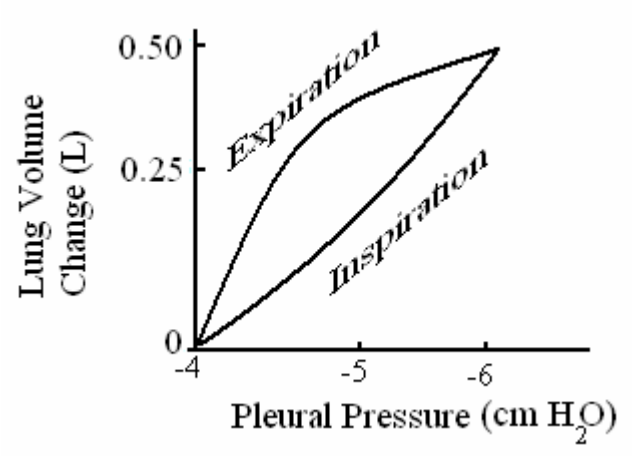

Figure 4: Pleural pressure versus change in lung volume during inspiration and expiration.

Pleural pressure is also used to calculate the pulmonary resistance. The most commonly used method to measure pleural pressure is the use of an esophageal balloon catheter (Milic-Emili et al, 1964). This method assumes that there is no pressure difference from the pleural space to esophagus, and the pleural pressure around the lung is distributed evenly. Esophageal balloons are typically 10 cm long with a 1.4 mm internal diameter. The balloon is swallowed into the esophagus by inserting the tubing through the nasal passageway. Very little air (~1 ml) is put into the balloon. The pressure within the balloon is the same as local pleural pressure, assuming that the pressure drop across the wall of the balloon itself is negligible when the balloon volume is small. The pressure transducer is connected to the other end of the tubing to measure the esophageal (pleural) pressure.

1.2.3 Respiratory Pressures

Figure 5 shows the pressures involved during respiration. The pressure acting across the elastic airways is the transmural pressure, which is the difference between the airway pressure (P_{aw}) and the intrapleural pressure (P_{pl}). Due to the elasticity of

the airways, the transmural pressure changes the shape of the airways. One can write the balance of forces as:

$$P_{alv} - P_{bs} + P_{mus} = P_L + P_{cw} \quad (1.1)$$

where P_{alv}= alveolar pressure, P_{bs}= pressure at body surface, P_{mus} = the muscle pressure, P_L = the lung elastic recoil pressure and P_{cw} = the chest wall elastic recoil pressure.

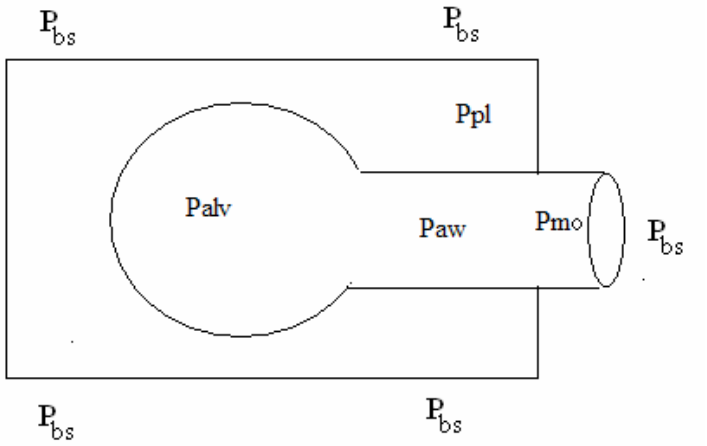

Figure 5: Pressures involved in respiration. P_{pl}= Pleural pressure, P_{alv}= Alveolar pressure, P_{aw}=Airway pressure, P_{mo}=mouth pressure (usually atmospheric), P_{bs}= Pressure at body surface (usually atmospheric).

1.2.4 A Simple Respiratory Model

A simplified model of the respiratory system is given in Figure 6.

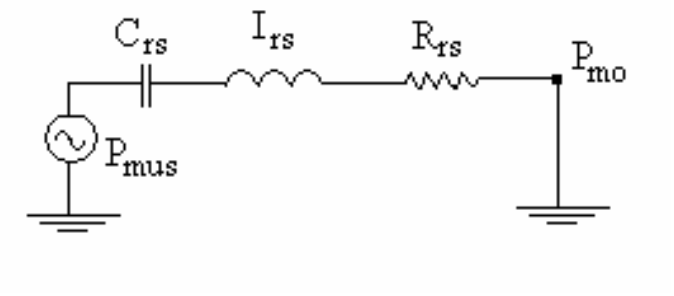

Figure 6: Simplified lumped parameter of the respiratory system. C_{rs} = Respiratory compliance, L/cm H_2O; I_{rs} = Respiratory inertance, cm $H_2O.s^2/L$; R_{rs} = Respiratory resistance, cm $H_2O/L/s$; P_{mo} = Mouth pressure, cm H_2O; P_{mus} = Muscle pressure, cm H_2O.

Respiratory compliance is related to the elasticity of the respiratory system. As pressure rises in this biological system, the walls of the vessels, bronchi, and alveoli expand and as pressure falls, the walls contract. The elastic quality is analogous to a capacitor in an electrical system. Therefore, the compliance could be defined as the added volume that can be accommodated for any given increment in pressure. The respiratory capacitance (C_{rs}) has the following components:

$$C_{rs} = \frac{C_{lt} C_{cw}}{C_{lt} + C_{cw}} \tag{1.2}$$

Where C_{lt} = lung – tissue compliance, L/cm H_2O

C_{cw} = chest wall compliance, L/cm H_2O

When a mass of any kind is accelerated, a certain force is required to overcome the inertia. The mass impedes the motion, and the greater the mass, the larger the impedence to acceleration. The respiratory inertance (I_{rs}) could be expressed as:

$$I_{rs} = I_{aw} + I_{lt} + I_{cw} \tag{1.3}$$

Where I_{aw} = Airway inertance, cm $H_2O.s^2/L$

I_{lt} = Lung – tissue inertance, cm $H_2O.s^2/L$

I_{cw} = Chest wall inertance, cm $H_2O.s^2/L$

The respiratory resistance also includes airway, lung tissue, and chest wall resistances. They all depend on flowrate, lung volume, and frequency. Also note that the pulmonary resistance is the airway resistance plus lung - tissue resistance.

Therefore, respiratory resistance (R_{rs}) is the pulmonary resistance plus chest wall resistance, and can be defined as:

$$R_{rs} = R_{aw} + R_{lt} + R_{cw} \tag{1.4}$$

Where R_{aw} = Airway resistance, cm H_2O/L/s

R_{lt} = Lung - tissue resistance, cm H_2O/L/s

R_{cw} = Chest wall resistance, cm H_2O/L/s

This first order linear system could be described by the equation

$$P_{mus} - P_{mo} = \frac{1}{C_{rs}} V + R_{rs} V' + I_{rs} V'' \tag{1.5}$$

Where V = volume (L), V' = rate of change of volume (L/s), V" = rate of change of air flow (L/s^2).

1.2.5 The Theory of APD Resistance Prediction

The APD periodically perturbs the air flow. For the calculation of resistance, two data sets are considered. Real data are the pressure and flow values recorded during perturbations. The second set of data is called virtual data and obtained by interpolating pre- and post-perturbational values of pressure and flow. Then the pressure drop for two data sets could be written as:

$$P_{mus} - P_{mo1} = \frac{1}{C_{rs}} V + R_{rs} V_1' + I_{rs} V_1'' \tag{1.6}$$

$$P_{mus} - P_{mo2} = \frac{1}{C_{rs}} V + R_{rs} V_2' + I_{rs} V_2'' \tag{1.7}$$

The subscript 1 describes the real data, and the subscript 2 describes the virtual data. Subtracting equation 1.7 from 1.6 will result in

$$P_{mo2} - P_{mo1} = R_{rs}(V_1' - V_2') + I_{rs}(V_1'' - V_2'') \tag{1.8}$$

The term V_2" is zero at the instant of minimum flow rate. Also $I_{rs}V_1$" can be dropped since during normal breathing the contribution of pressure drop due to inertance effects are negligible (Bates et al., 1988). Therefore the equation 1.8 could be simplified to:

$$\Delta P = R_{rs}\Delta V' \tag{1.9}$$

$$R_{rs} = \frac{\Delta P}{\Delta V'} \tag{1.10}$$

Where $\Delta P=P_{mo2}-P_{mo1}$ is mouth pressure perturbation magnitude and $\Delta V'= V_1"-V_2"$ is flow perturbation magnitude. Therefore, the APD resistance is calculated as the ratio of the mouth pressure perturbation magnitude to the flowrate perturbation magnitude (equation 1.10).

1.3 Research Goals and Objectives

This dissertation focuses on validation of the APD and prediction of flow limitation and, therefore, addresses the following two objectives:

1. Determine the difference and similarities between the APD resistance and pulmonary resistance.
2. Determine the predictability of flow limitation with isovolume pressure - flow curves (IVPF) when constructed with the stop-flow and esophageal balloon catheter methods.

In order to achieve the first objective, the APD resistance and pulmonary resistance were measured during tidal breathing with and without addition of rigid external resistances to both inspiration and expiration or just to inhalation or

exhalation. The calculated pulmonary resistance and the APD resistance were compared.

For the second objective, IVPF curves were constructed and the pressure and flow at the onset of flow limitation were compared. Additionally, the inverse of the slope of the line drawn to the point of flow limitation in IVPF curves at different lung volumes were compared to the APD resistance during forced breathing to determine the ability of the APD to predict the resistance at flow limitation.

Chapter 2. Literature Review

The following section reviews the literature on maximum expiratory flow, the stop flow method, respiratory resistance and the airflow perturbation device (APD).

2.1 Maximum Expiratory Flow

2.1.1 Flow Limitation

Hyatt et al. (1958) and Fry (1958) were the first ones to construct maximum expiratory flow-volume curves and showed the effort independent portion of flow vs. volume curves. Hyatt et al. determined that there is an upper limit to expiratory flow at any lung volume. They showed that the limit to expiratory flow is altered with disease and is essentially independent of upper airway resistance. In order to understand the mechanisms behind the flow limitation, Fry constructed isovolume pressure-flow curves (Figure 7). Curves 1, 2, 3, and 4 in Figure 7 show the isovolume line. Therefore, each curve represents the pressure-flow relationship at a constant degree of lung inflation. From these curves, they realized that flow increased as pressure increased. But when it reached a maximum, a further increase in pressure or effort did not cause an increase in flow. They showed that the pressure at which the maximum flowrate is reached depends on the volume. For example, the pressure at maximum flowrate is higher for curve 4 than for curve 1, which is at a lower volume (Figure 7).

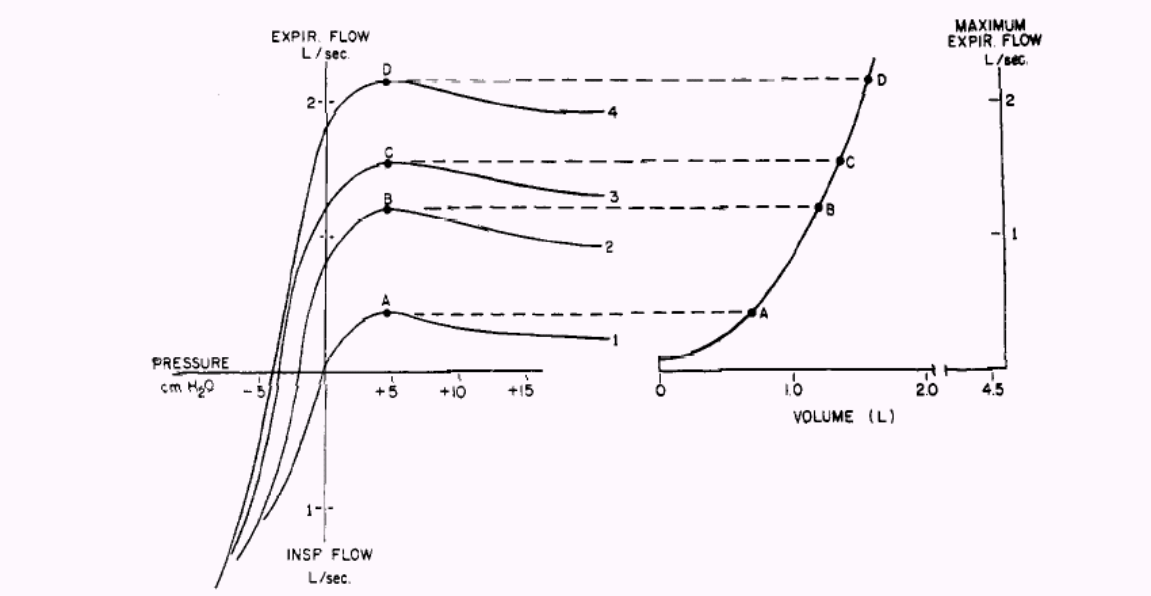

Figure 7: On the left is the the relationship between the pressure applied to the surface of the lung and the resulting flowrate. On the right is the flow and volume coordinates of the pressure flow curve maxima (Fry ,1958).

Mead et al. (1967) examined the effort-independent range of the maximum flow curve with a different approach. The idea was based on the fact that addition of external resistance to the mouth would not change the maximum flow as long as the new decreased transpulmonary pressure due to additional resistance is above or equal to the pressure required to achieve the maximum flow. They tested this hypothesis by adding different external resistances to the mouth during forced breathing and comparing the maximum expiratory flow volume curves. Even though they did not report the magnitude of each resistance added, they reported that addition of as high as 5 cm H_2O/L/s did not change the maximal flow at volumes below 50% of vital capacity (Figure 8).

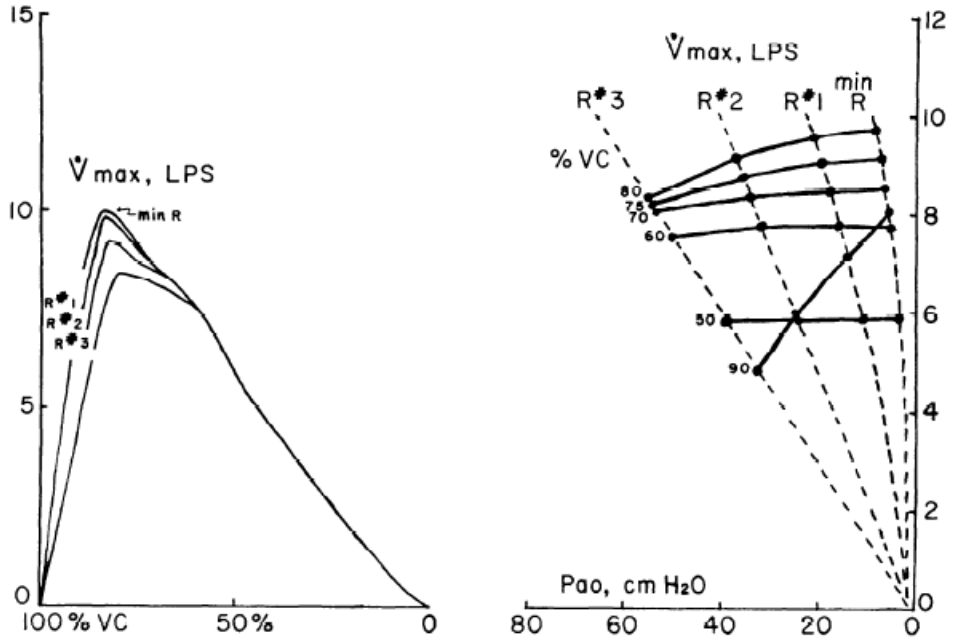

Figure 8: Left: Maximum expiratory flow volume curves for a subject exhaling through three different resistances. Right: Maximum flow plotted against mouth pressure, P_{ao}, for different resistances and at different lung volumes expressed as % VC (Mead et. al, 1967).

Although Fry et al. (1960) and Hyatt et al. (1958) observed that the main mechanism responsible for the expiratory flow limitation is the dynamic compression of the elastic airways, the parameters that determined the flow were not known. Their theory was that when the transmural pressure becomes zero during maximal expiratory flow, an equal pressure point (EPP) in the airways develops, where the pressure inside is equal to the pleural pressure. Downstream from EPP, the airways will tend to collapse since now the transmural pressure is less than zero (Figure 9).

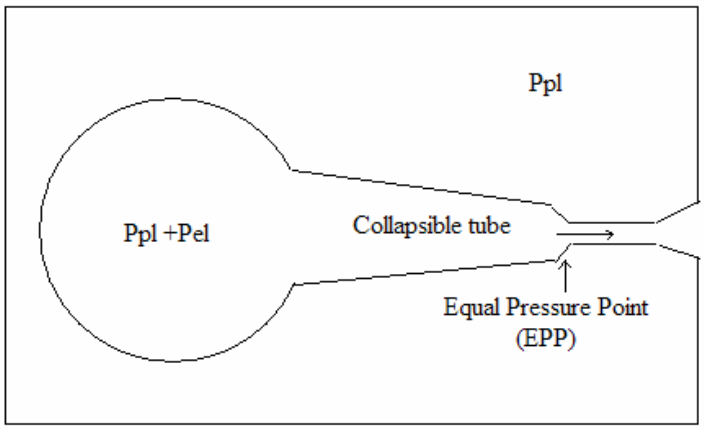

Figure 9: Collapse of airways during expiration. P_{pl} = Pleural pressure, P_{el} = elastic recoil pressure

Mead et al. (1967) showed that once maximum flowrate is reached, flow is dependent on the difference between the driving alveolar pressure,P_{alv}, and surrounding pressure (P_{pl}) and is independent of the total pressure drop from alveolus to atmosphere. In order to understand this theory, one needs to understand the relationship between P_{alv}, the elastic recoil pressure (P_{el}) and EPP (Figure 9). The difference between P_{alv} and P_{pl} gives the elastic recoil pressure (P_{el}). P_{el} varies with lung volume and at a given lung volume, P_{el} is constant. Therefore, when EPP is reached for a given lung volume, the pressure drop between the alveoli and EPP does not change. Increased effort will cause similar increases in alveolar pressure and pressure at EPP. The pressure difference and thus flow will be unchanged (Figure 10).

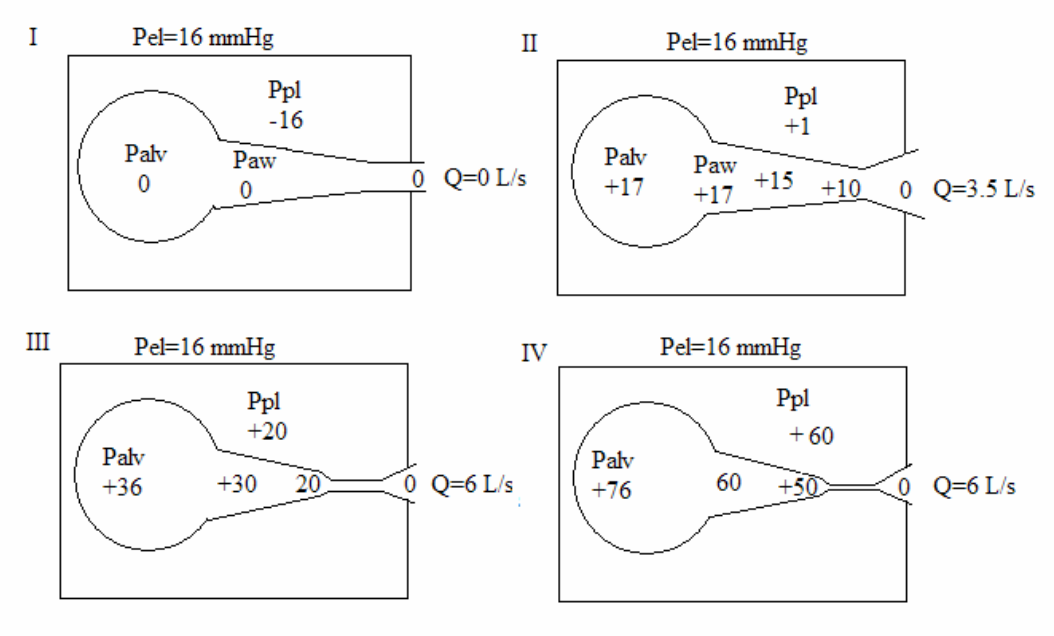

Figure 10: Effect of pressure change on flow (Q) at a given lung volume.

Pride et al. (1967) attempted to explain the mechanism of flow limitation with the difference between P_{alv} and mouth pressure when flow initially reached maximum, the maximum flow, and airway resistance. Their study showed that when the maximum flow is reached in an isovolume pressure-flow curve, a waterfall effect develops, where the flow is independent of the height of the falls, just as the maximal expiratory flow is independent of the total driving pressure between alveoli and the mouth.

Macklem et al. (1965) investigated the location of expiratory airway compression during limited flow. Their results showed that at volumes between 75% and 25% VC, the EPP develops in the trachea, moves upstream, and becomes fixed at the level of segmental bronchi when the maximum flow is reached. Since airways are compliant tubes, the EPP stops moving due to compression of airways downstream from it. The stiffer the airway, the further out the EPP will move. The location of the

EPP is determined by a balance between accelerative resistance (inertia), the distribution of frictional resistance, and airway compliance.

Dawson and Elliot (1977) made a very important contribution by explaining flow limitation with wave – speed. This approach shows that flow through an airway segment becomes maximum when the velocity reaches the speed of pressure-wave propagation at a point along the airway, which is called the "choke point." They have also shown that once the flow is limited, the downstream area continues to decrease as the pleural pressure increases, whereas the airway area upstream from the choke point remains unchanged. In this case, any lowering of downstream pressure below what is required to achieve a flow velocity equal to the speed of wave propagation has no effect on maximum flowrate. This only determines the pattern downstream from the choke point. The reason is that the downstream pressure disturbance cannot travel upstream if the velocity of flow is faster than the wave speed. The wave speed (c) in a compliant tubes with a cross-sectional area (A), transmural pressure (P) and gas density (ρ) is:

$$c = \left(\frac{A}{\rho} \frac{dA}{dP} \right)^{1/2} \tag{2.1}$$

In this equation, dA/dP is the slope of the area-pressure curve for the airway. Therefore, maximal flow (Q_{max}) is the product of the fluid velocity at wave speed and cross-sectional area of the airway:

$$Q_{\max} = cA = \left(\frac{A^3}{\rho} \frac{dA}{dP} \right)^{1/2} \tag{2.2}$$

The mechanism can also be described graphically (Figure 11). If convective acceleration were the only cause of a pressure drop in the flow, the Bernoulli equation

could be used to describe the relation between the transmural pressure and airway area for a given flow (Q). Figure 11 shows the graphical representation of the relationship between transmural pressure and the cross-sectional area of the airway and the plots of the Bernoulli equation at different flow rates Q_1 and Q_2. For flow to pass from the alveoli through the critical airway, two simultaneous conditions must be met: the pressure-area relationship of the flow, and the pressure-area relationship of the airway. There is a maximum flow for which a point common to both curves exists. As it can be seen in Figure 11, flow of Q_2 is tangent to the airway area curve and therefore satisfies both conditions. Flows higher than Q_2 do not intersect the airway pressure curve and, therefore, cannot occur.

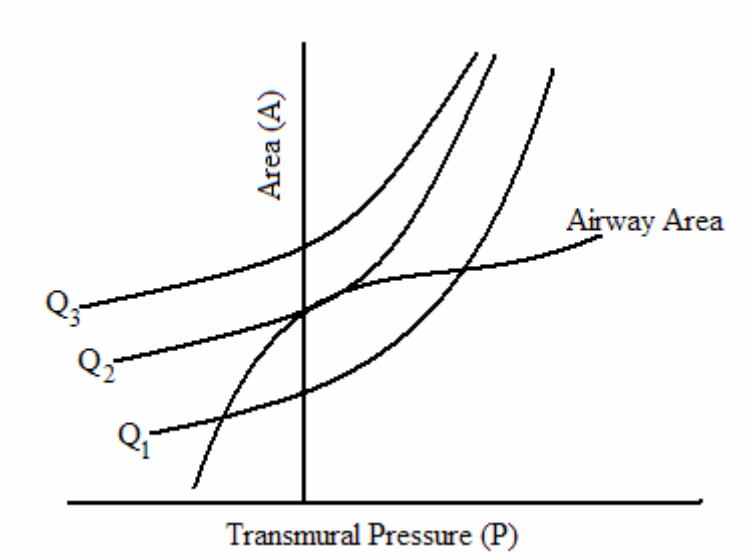

Figure 11: A graphical representation of flow limitation at wave speed (After Wilson et al., 1980).

Elliott and Dawson (1977) tested their hypothesis by trying to locate the choke point in excised dog tracheas. Their experiment showed that the calculated maximum flow was larger than the actual flow. The main reason was the underestimation of the

measured choke point area for the excised dog tracheas. However, within the experimental error, the results supported the wave-speed theory.

Hyatt et al. (1980) tested the prediction of maximum flow by the wave-speed theory in excised human lungs. Their study showed that the wave-speed theory predicts the flow limitation over the upper 75% of the vital capacity. On the other hand, for over 25% of the vital capacity other mechanisms were involved.

Wilson et al. (1980) described the flow limiting mechanisms for low lung volumes. They stated that at low lung volumes, the maximum flow mostly depends on viscosity rather than the density and therefore the predictive capability of the wave speed concept was lost (Figure 12). For a purely viscous flow in a compliant tube, flow limitation could be described by the Poiseuille equation,

$$\frac{dp}{dx} = -a\frac{\mu Q}{A^2} \tag{2.3}$$

Where a is a numerical constant, p is pressure, Q is flow, A is area, and μ is viscosity. Then the limited flow could be described as,

$$Q = -\frac{1}{a\,\mu\,L}\int_{p_1}^{p_2} A^2 dp \tag{2.4}$$

Where L is the distance between the upstream pressure, P_1, and the downstream pressure, P_2. They also pointed out that maximum flow at low lung volumes would depend on the properties of the airways with diameters of about 1 mm.

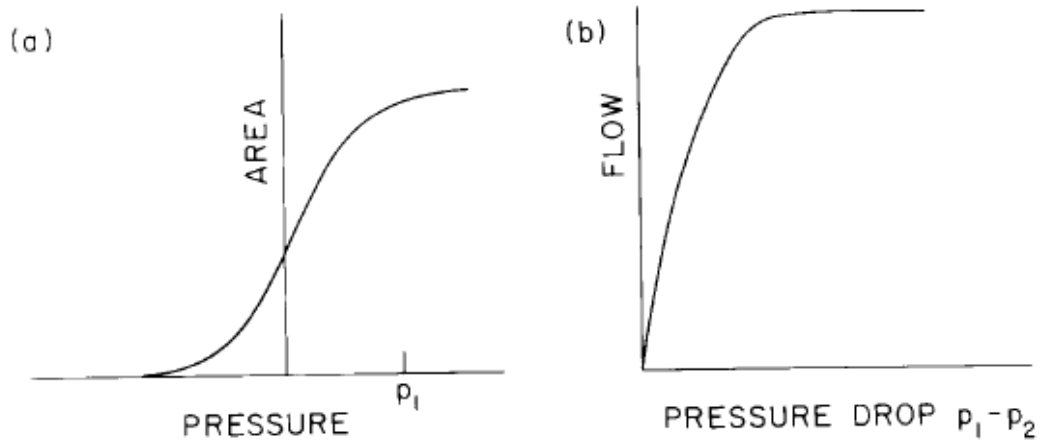

Figure 12: Viscous flow limitation. An area-pressure curve of a smaller airway is shown in panel a. If the pressure gradient in the flow is described by the Poiseuille equation, then for a fixed pressure P_1 at the upstream end of the tube, flow will depend on P_2, the pressure at the downstream end of the tube, as shown in panel b (Wilson et al., 1980).

2.1.2 Respiratory Resistance at Maximum Flow

The change in resistance when maximum flow is reached has been investigated for many years. Many studies divided the airways as upstream and downstream of EPP and studied the change in resistance when maximum flow is reached (Pride et al. 1967, and Mead et al. 1967).

Pride et al. (1967) used the waterfall model of the lung (Figure 13) and defined the resistance downstream from the collapsible segment as R_d and upstream resistance as R_s. They modeled the maximum flow in relation to the resistances as follows:

$$Q_{\max} = \left(\frac{1}{R_s + R_d} \right) \Delta P' \qquad (2.5)$$

where Q_{max} is the maximum achievable flow at a given lung volume, and $\Delta P'$ is the pressure difference between the alveoli and mouth at the onset of maximum flow. They considered R_s to be fixed when flow becomes limited with a fixed pressure

producing this flow. They also claimed airway obstruction could result from an increase in R_s, which would limit the maximum flow at a given lung volume. But, the magnitude of R_d has no influence on the maximum flow because it is downstream from the waterfall.

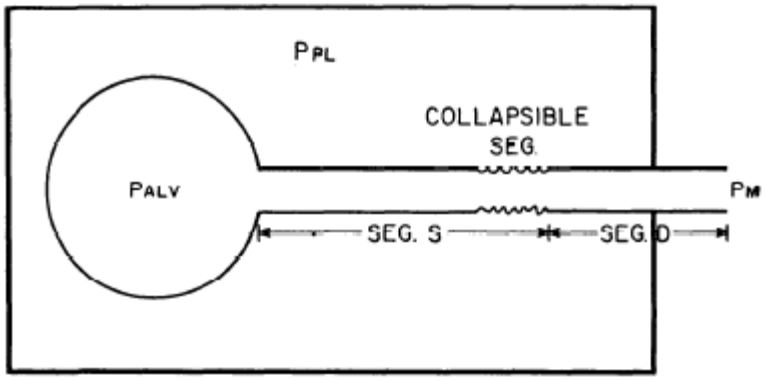

Figure 13: Waterfall model of the lung. P_{alv} = alveolar pressure, P_{pl} = pleural pressure, P_m = mouth pressure (Pride et al. 1967).

Mead et al. (1967) measured esophageal pressures and simultaneous expiratory flows at the same lung volume. Figure 14 shows how they defined the change in total resistance, R_{aw}, and resistance in the upstream, R_{us}, and downstream from EPP, R_{ds}. The driving pressure for the upstream segment was described as the static recoil pressure of the lung and that for the downstream segment was pleural pressure. When the maximum flow is reached, EPP is fixed and resistance of the upstream segment does not change even though resistance of the downstream segment is increasing due to the narrowing of airways downstream of EPP. Therefore, total airway resistance increases even though maximum flow does not change.

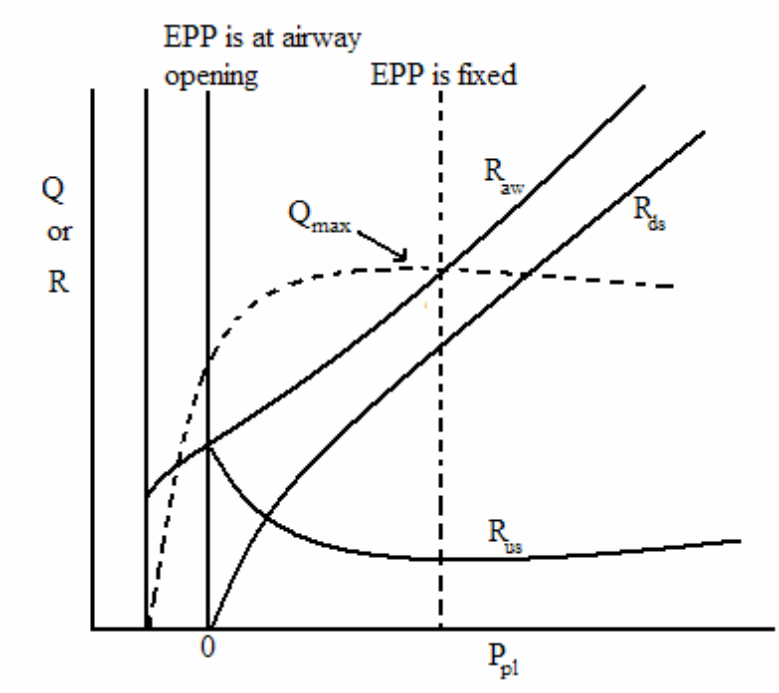

Figure 14: Curves showing how the resistance of the total airway, R_{aw}, and upstream from EPP, R_{us}, and downstream from EPP, R_{ds}, change as pleural pressure, P_{pl}, increases (After Mead et al., 1967).

Zamel et al. (1974) observed the alveolar pressures to calculate the airway resistance during maximum expiratory flow by using a volume displacement body plethysmograph. They also calculated the alveolar pressures by using esophageal pressures and compared both methods. Their results of airway resistance calculations by both methods were in good agreement especially for high lung volumes. Their plot of airway resistance versus lung volume showed resistances as high as 100 cm H_2O/L/s (Figure 15).

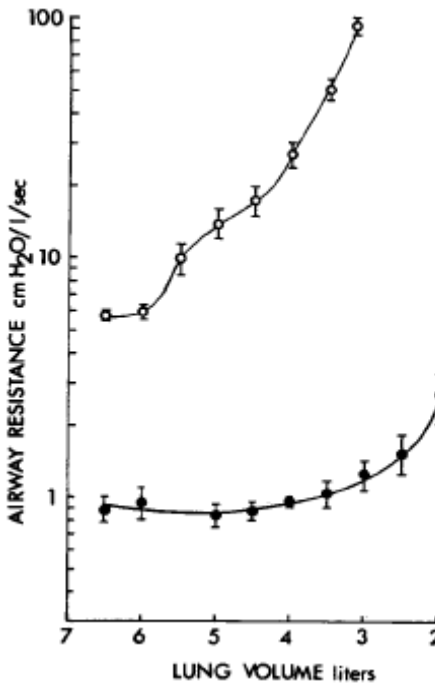

Figure 15: Airway resistance-lung volume curves during ten consecutive forced vital capacity maneuvers in a healthy non-smoker (open circles). For comparison the resistance volume curve during panting (closed circles) (Zamel et al., 1974).

Smaldone et al. (1976) studied the resistance upstream from the flow limiting segment by comparing the calculated values from the slope and intercept of maximum flow, Q_{max}, vs. lung elastic recoil pressure, P_{el}, to derived values from isovolume flow-pressure curves in excised dog and human lungs. Their results showed that the resistance between the alveoli and EPP can be calculated indirectly from the slope of a graph of Q_{max} vs. P_{el} as first suggested by Mead et al. (1967).

Aldrich et al. (1989) studied the airway resistance during forced inspiratory and expiratory vital capacity maneuvers with a body plethysmograph. This study was similar to the study done by Zamel et al. (1974). They monitored the airflow, mouth pressure and the plethysmograph pressure. Their results showed that maximum expiratory resistances varied with volume. However, inspiratory resistances did not

show volume dependence for normal subjects. They observed expiratory resistance as high as 112.4 cm H_2O/L/s. They also tested the patients with chronic obstructive pulmonary disease, COPD. For COPD patients both inspiratory and expiratory resistance values changed with lung volume. Table 1 below summarizes their findings.

Table 1: Inspiratory and expiratory resistances for normal subject and patients with COPD (Aldrich et al., 1989).

COMPARISON OF MAXIMAL EXPIRATORY AND INSPIRATORY RESISTANCES AT 75, 50, AND 25% OF VITAL CAPACITY AND AT MAXIMUM* DURING FORCED EXPIRATORY AND INSPIRATORY VITAL CAPACITY MANEUVERS IN SIX NORMAL SUBJECTS†

Subject No.	Age (yr)	Sex	FEV_1 (% pred)	RI_{75}	RI_{50}	RI_{25}	RImax	PAmin‡	RE_{75}	RE_{50}	RE_{25}	REmax	PAmax‡
Normal subjects													
1	37	M		3.0	4.5	4.5	5.8	−45.5	13.8	37.9	76.7	112.4	217.0
2	27	M		3.2	3.2	2.1	3.2	−22.0	7.5	10.0	22.5	33.3	57.0
3	33	M		2.3	2.1	1.0	2.8	−18.3	12.0	21.6	32.3	61.0	108.4
4	29	M		3.0	3.1	2.4	3.1	−35.2	12.8	20.3	35.1	90.2	116.5
5	29	F		2.1	2.2	1.0	2.4	−11.4	9.2	13.3	20.3	33.6	54.8
6	33	M		1.9	1.6	0.4	2.1	−14.3	6.2	12.1	16.5	17.0	61.5
Mean				2.58	2.81	1.91	3.23	−24.5	10.2	19.2	33.9	57.9	102.5
± SEM				0.23	0.42	0.60	0.54	5.4	1.2	4.2	9.0	15.2	25.4
Patients with COPD													
1	58	F	17	6.1	8.4	11.6	19.4	−19.4	30.7	233	310	394.0	49.8
2	57	M	25	1.8	4.5	9.6	26.7	−18.6	4.5	6.4	101.8	226.0	53.8
3	61	M	32	5.2	6.4	9.0	26.7	−37.9	112.5	91.9	121.7	145.0	90.7
4	73	F	53	1.5	2.0	2.3	5.2	−7.8	21.5	215.8	309.0	508.0	119.7
5	61	M	36	3.8	4.4	5.0	8.4	−12.3	32.9	221.9	295.9	332.9	136.0
6	59	F	45	1.4	1.2	1.8	4.1	−4.6	20.9	37.4	13.3	38.7	31.3
Mean			35	3.31	4.49	6.55	15.08	−16.8	37.2	134.4	191.9	274.1	80.2
± SEM			5	0.83	1.10	1.67	4.29	4.81	15.6	41.5	52.7	70.0	17.1
p Value				NS	NS	< 0.05	< 0.05	NS	NS	< 0.02	< 0.02	< 0.02	NS

* Excluding the very high resistances calculated when flow rates were less than 0.02 L/s.
† ANOVA indicated significant effects on the resistance measurement of group (normal versus COPD), phase of respiration, and volume at which the measurement was made. The p value refers to the differences between normal subjects and patients with COPD using Student's *t* test.
‡ Maximal expiratory and inspiratory alveolar pressures (PAmax and PAmin) are also shown.

2.2 The Stop-Flow Method

Pressure measurements to construct isovolume pressure-flow (IVPF) curves require rather complicated techniques such as use of an intraoesophageal balloon. Pride et al. (1967) developed an alternative method for measuring IVPF curves, which is a modification of the classical flow-interruption technique (Mead et al. 1954, Shephard 1963, Jackson et al. 1974, Ohya et al. 1989).

The interrupter method was first introduced by Von Neergaard and Wirz in 1927 (Mead et al. 1954) and was later improved by Clements et al. (1959). This technique is based on the fact that during brief airway occlusion, alveolar pressures,

P_{alv}, are assumed to equilibrate with mouth pressure. As subjects breathe through a pneumotachograph, airflow and mouth pressure is recorded continuously. During the respiratory cycle, the mouth is occluded briefly. This causes airflow to fall to zero as the mouth pressure changes. This pressure change represents the pressure difference that existed between the mouth and alveoli just prior to interruption. With many interruptions, numerous pressure changes could be recorded. When the flow immediately before the interruption is plotted against the pressure change, the flow-pressure relationship in the respiratory tract could be obtained (Mead et al. 1954).

Pride et al. (1967) used the same principle to construct IVPF curves by interrupting the flow at a selected lung volume and instructing the subject to increase alveolar pressure against a closed shutter until it reached a preset value. The flowrate just after shutter opening is correlated with the pressure. Since the pressure and flow cannot be measured at the same time, the flow measured after the shutter opening had a transient region (Figure 16), which lasted 30 to 50 ms (Pride et al. 1967, Miyamoto et al. 1978). They explained that this transient region was due to the collapse of the airways during expiration and the dead-space of the instrument and lungs.

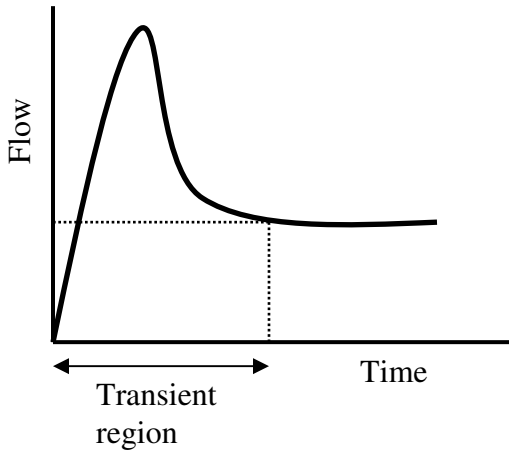

Figure 16: Plot of flow versus time after shutter opening during the stop-flow method

The main assumption of this method is that flow can be measured quickly enough after valve opening so that P_{alv} before the valve opening represents the measured flow at the end of the transient region. Pride et al. (1967) tested this hypothesis by measuring the esophageal pressure after valve opening in two normal subjects. They observed that during the 30ms of transient region, P_{alv} fell by 17 to 19% of the initial levels. They concluded that this change is mostly due to a decrease in expiratory muscle force immediately after valve opening.

Ohya et al. (1989) studied the relationship between the mouth pressure during abrupt interruption of airflow and the process of air flowing into the collapsed segment downstream from the choke point by using the stop-flow method. Each subject performed the maximum expiratory flow-volume maneuver and at a preselected lung volume the shutter was closed for different durations up to 100 ms. During this period, the subject continued with the maneuver regardless of opening or closing of the shutter. In addition to monitoring mouth pressure, they monitored the pleural pressure with an esophageal balloon. During the interruption, the pleural pressure did not change. Their assumption was that the flow greater than the maximum achievable flow after the shutter opening reflected the behavior of the downstream segment. Their results showed that the mouth pressure curve after the shutter closing had three phases. During phase 1, mouth pressure showed a step-functional increase (Figure 17). Phase 2 was the slower rise in pressure, and phase 3 was the equilibration of mouth pressure with the alveolar pressure. They predicted that during phase 2, the airway is releasing from the collapsed state. Therefore, when

the length of the interruption was increased, the supramaximum flow also became larger.

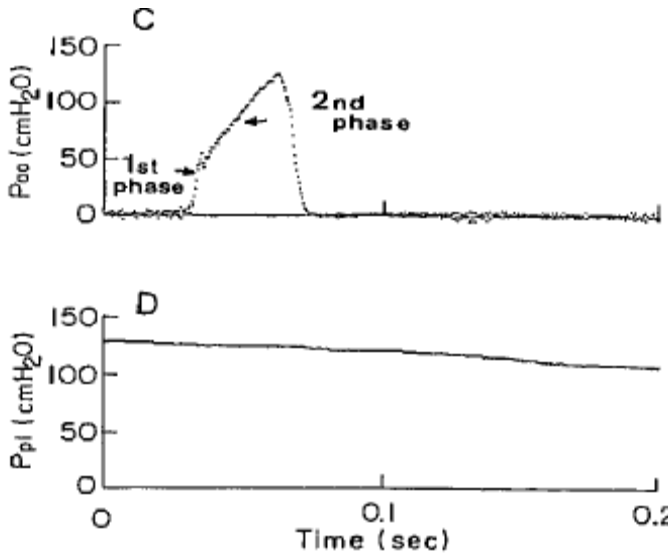

Figure 17: C: The mouth pressure time curve showing the first 2 phases. D: Pleural pressure versus time curve during interruption (Ohya et al., 1988).

Ohya et al. (1989) also compared the gas volume interrupted area (*area A*) to the volume of supramax flow after shutter opening (*area B*) Figure 18. When the flow was restored during phase 2, *area A* was equal to *area B*. On the other hand, when the shutter was opened during phase 3, namely after the alveolar pressure equilibrated with the mouth pressure, *area A* was greater than *area B*. Their explanation was that after flow restored during phase 2, the choke point was preserved at the same point. Therefore, the downstream disturbance could not travel upstream. During phase 3, the choke point disappeared. Restoring the flow after interruption caused the downstream disturbance to travel upstream.

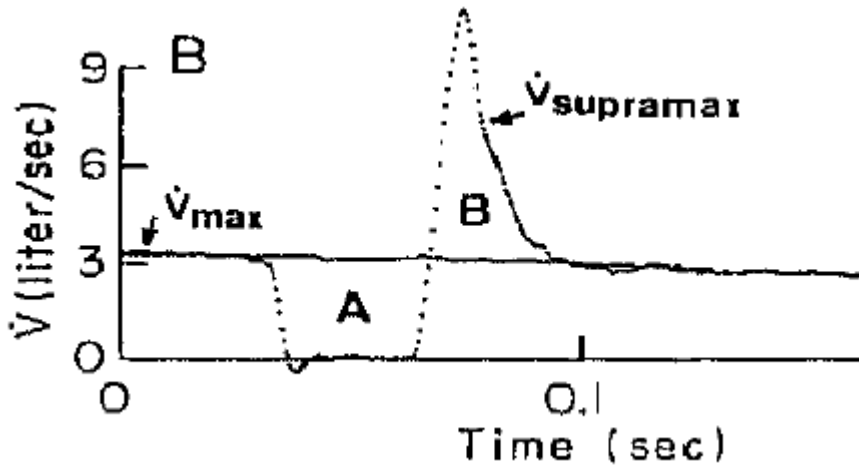

Figure 18: The supramaximal flow is observed as the flow exceeding V_{max} line (Ohya et al., 1988).

2.3 Pleural Pressure Measurement with Esophageal Balloon

Esophageal pressure has been used to reflect the pleural pressure since it was first introduced by Buytendijk in 1949 (Dechman et al., 1992). Milic-Emili et al. (1964) perfected the esophageal balloon catheter method to measure the pleural pressure. They studied the effect of lung volume on the measured esophageal pressure and found that the esophageal pressure increased with balloon volume, and this effect was larger at large lung volumes. From this, they concluded that when lung volume is above 20% of the vital capacity, the esophageal pressure reflects the local pleural pressure when the balloon volume is close to zero.

Baydur et al. (1982) studied the validation of the esophageal balloon technique in normal subjects in sitting, supine, and lateral positions by using the occlusion test. They occluded the airway opening at end-expiration and asked the subjects to perform inspiratory efforts against the occluded airway and compared the change in esophageal pressure (ΔP_{es}) with the corresponding changes in mouth pressure (ΔP_m). The same procedure was repeated at different body positions and

esophageal balloon location. The ratio of $\Delta P_{es}/\Delta P_m$ in the sitting and reclining on one side position was close to one when the esophageal balloon was 10 cm above the cardia (the sphincter between the esophagus and stomach). In the supine position, the ratio was less than one for most subjects. The ratio with the balloon positioned at three different levels (5, 10, and 15 cm above cardia) did not show any systematic change except in the supine position. The ratio increased as the balloon was positioned closer to cardia. Therefore, they suggested that repositioning the balloon in the esophagus for supine position measurements to make the ratio closer to one would make the measurement more accurate.

Dechman et al. (1992) measured the esophageal pressure (P_{es}) and tracheal pressure (P_{tr}) in spontaneously breathing dogs and paralyzed dogs. The theory was that if P_{es} reflected pleural pressure (P_{pl}), the slope of P_{es} vs. P_{tr} should be 1. Their study showed that the slope was closer to unity for paralyzed dogs. The slopes of non-paralyzed sate were less that unity. The results were also different between supine and side lying. Therefore, they concluded that the accuracy of P_{es} to reflect P_{pl} changes with lung volume, balloon position, and posture for spontaneously breathing dogs.

Peslin et al. (1993) investigated the reliability of the esophageal balloon technique in measuring high frequency changes in pleural pressure (P_{pl}). They concluded that esophageal pressure (P_{es}) measured with a standard esophageal balloon-catheter system provides a good estimate of P_{pl} at frequencies as high as 32 Hz in humans. The amplitude distortion was very small and the time delay was of the order of 1 ms. They also concluded that the esophageal balloon-catheter system could be used to observe the change in P_{pl} following airway interruption since the time

delay of 1ms is short compared to the time required to operate the valve which is usually around 10-30 ms.

2.4 Pulmonary Resistance

Frank et al. (1957) studied the pulmonary flow resistance in healthy elderly subjects as well as young adults. They reported that in 28 young adults, the average pulmonary resistance was 1.2 to 3.4 cm H_2O/L/s. Among the elderly subjects it ranged from 1.3 to 4.4 cm H_2O/L/s.

Ferris et al. (1964) tried to partition the respiratory flow resistance. Their studies showed that total pulmonary resistance was 65% of total respiratory resistance during exhalation and 68% of total resistance during inhalation.

Vincent et al. (1970) investigated the influence of lung volume on total and lower pulmonary resistance and resistance upstream from equal pressure points. They demonstrated that inspiratory airway and pulmonary resistance was higher at a given lung volume when inflation was started from a smaller volume than when it was started from a larger one. Also, they concluded that lower pulmonary resistance was lower (less than 0.25 cm H_2O/L/s) over the upper half of the vital capacity.

2.5 Airflow Perturbation Device (APD)

A noninvasive way of measuring the respiratory resistance is the APD (Johnson et al. 1984, Lausted et al. 1998, Lausted et al. 1999, Johnson et al. 2004). It is a very easy to use device and does not require any special breathing maneuvers (Figure 19). A rotating wheel in the flow path perturbs air flow and mouth pressure by a small amount. The ratio of pressure perturbation to flow perturbation is used to calculate the respiratory resistance (Figure 20).

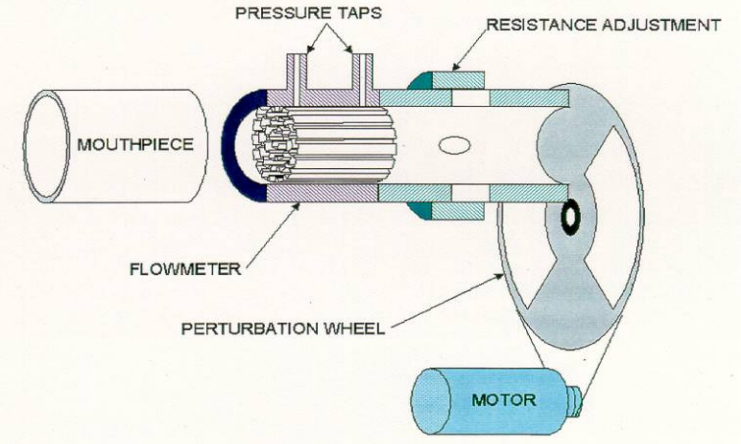

Figure 19: The Airflow Perturbation Device

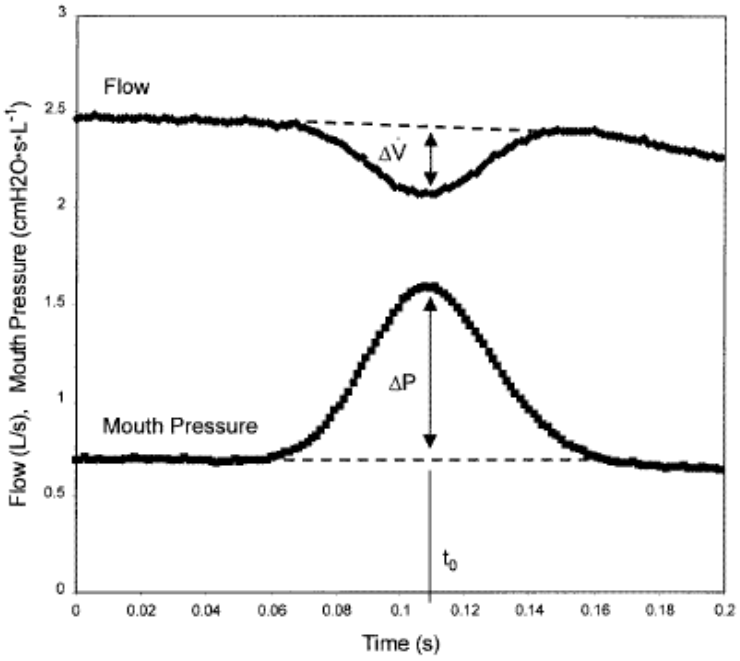

Figure 20: Pressure and flow versus time as recorded by APD. The ratio of ΔP/ΔV' gives the respiratory resistance (Lausted et al., 1999).

Lausted et al. (1999) investigated how far the perturbations travel by placing three accelerometers on the chest wall: one centered on the right pectoral muscle 4 cm from the sternum, another 5 cm below it, and a third 2 cm right of the seventh dorsal

vertebra. The analysis of data from the accelerometers indicated the presence of perturbations on the chest wall (Figure 21). They concluded that the APD measures respiratory resistance.

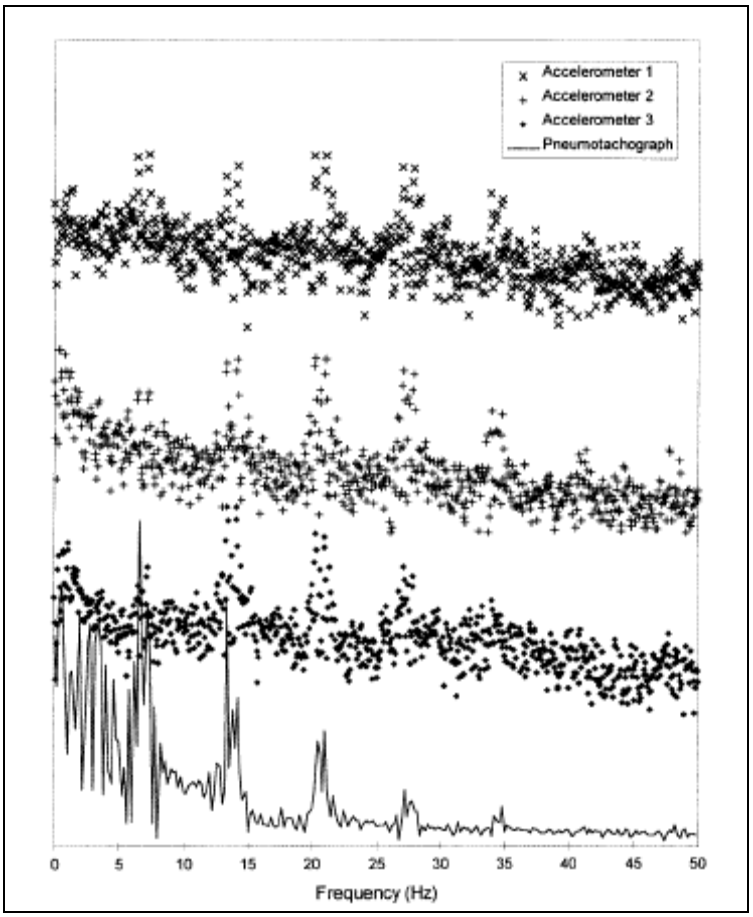

Figure 21: Presence of perturbations on the chest wall: (1) above pectoral 4 cm right of sternum, (2) below pectoral 4 cm right of sternum, (3) 2 cm right of seventh dorsal vertebra (Lausted et al., 1999).

Lausted et al. (1999) also investigated the APD perturbation frequency dependence. Average inhalation and exhalation resistances were measured at wheel rotational speed of 2.2, 4.4, and 6.7 revolutions per second. Their result showed that the calculated APD resistances did not vary significantly with wheel speed.

Johnson et al. (2004) used excised sheep lungs within a respiratory chamber to compare the APD resistance to the resistance calculated with the forced oscillation (FO) method. The conventional setup of FO technique is based on superimposing a small pressure oscillation (~1 cmH_2O) at the mouth during quiet breathing. The forced oscillation is applied at a frequency much higher than the patient's breathing rate. Therefore, at this frequency the activity of the muscle pump is negligible since it operates at the breathing rate. The only driving pressure is the pressure applied at the mouth.

The APD resistance was found to be 1.7 to 1.9 times the airway resistance. On the other hand, resistances calculated by using FO were 1.4 times the airway resistance. Additionally, the APD pressure perturbations were observed in the respiratory chamber. They also concluded that the APD resistance included not only airway resistance but also lung tissue resistance.

2.6 Detection of Respiratory Resistive Loads

Detection of added respiratory resistance has been studied extensively (Bennet et al. (1962), Wiley et al (1966), Mahutte et al. (1983)) to understand the sensory process involved with the perception of mechanical events related to breathing. Bennet et al. (1962) provided resistive loads ranging from 0.2 cm H_2O/L/s to 1.2 cmH_2O/L/s to the subjects and asked the subjects to signal when the load was detected. The threshold for detection was 0.59 cm H_2O/L/s, which was approximately 25% of subject's intrinsic resistance. Wiley et al. (1966) found the threshold resistance for perception varied from subject to subject. But when thresholds were expressed in terms of the ratio of added resistance to subject's initial background resistance, the threshold resistance ratios were found to be 0.25-0.3. The

background resistance included the subject's intrinsic resistance and resistance of the apparatus. Therefore, subjects with higher intrinsic resistance required addition of larger resistance to reach the threshold of perception. This implies that resistive load detection follows Weber psychophysical law.

Weber psychophysical law states that the perception of difference between two products was a constant, related to the ratio of difference. This could be expressed mathematically as:

$$k = \frac{\Delta I}{I} \tag{2.6}$$

where k= a constant, I=background intensity, and ΔI= difference between intensity of the just noticeable stimulus and background intensity.

Mahutte et al. (1983) tried to understand the mechanism behind respiratory load detection. They theorized that when a small external resistance creates a phase angle greater than the critical phase angle, the detection occurs. Basically, when there is a delay in the expected rate of rise of airflow for the previously preset muscle pressure, the resistive load is detected.

Killian et al. (1980) investigated the threshold detection when loads were applied at different times during inspiration, with different inspiratory flows, at different lung volumes, and with different background loads. When loads were applied during inspiratory flow suddenly, the mean detection threshold was 0.94 cm H_2O/L/s. On the other hand, when loads were applied before inspiration the mean detection threshold was 0.42 cm H_2O/L/s. This implied that the information generated at the beginning of inspiration is significant for the resistive load detection. They

concluded that detection of resistive loads requires the relation of pressure to flow which occurs early in the breath.

Chapter 3. Experimental Setup and Methodology

Resistance measurements with the APD were compared to directly measured pulmonary resistances with an esophageal balloon. Six healthy subjects were tested during tidal breathing when known external resistances were added during inspiration, during expiration, and during both inspiration and expiration.

Additionally, isovolume pressure – flow curves were constructed with an esophageal balloon and the stop – flow methods to find the resistance at flow limitation to compare to the APD resistance during forced breathing. These methods and the experimental apparatus are described in detail below.

3.1 Equipment and Experimental Apparatus

3.1.1 Stop-Flow Experimental Setup

Figure 22 and Figure 23 show the setup of the stop-flow experiment. The shutter positioned behind the pneumotach was built to control the mouth pressure at a desired lung volume, and was controlled by two solenoids. There was a second monitor in front of the subject for him to see his mouth pressure signal. This helped subjects to keep the desired mouth pressure constant.

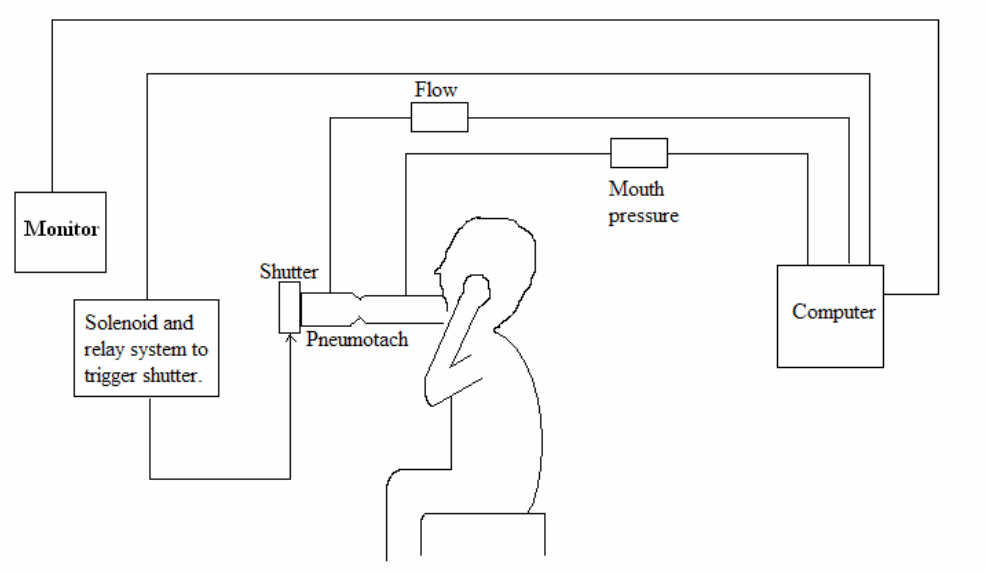

Figure 22: Diagram of the stop-flow experimental setup.

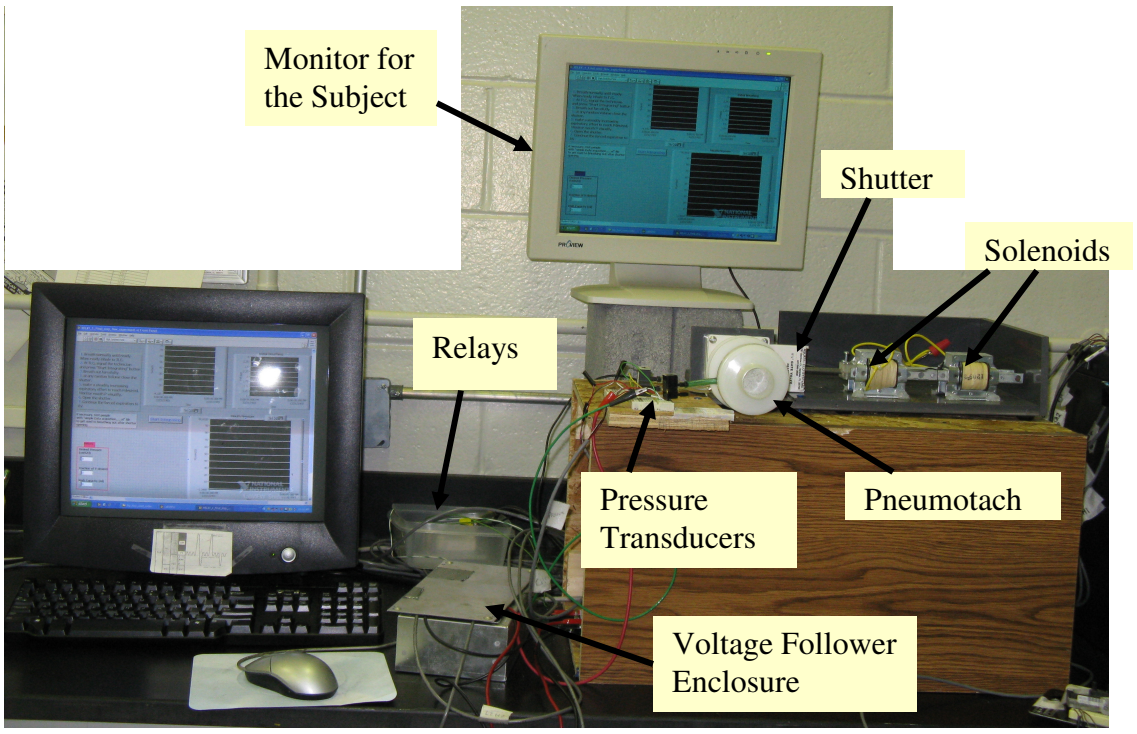

Figure 23: Setup of stop-flow experiment.

The measurement of airflow during breathing was achieved with a pneumotach that was originally used in a 1993 model Collins constant volume body

plethysmograph. A pneumotach consists of a plastic tube with a fine wire mesh inside. As air moves through the mesh, a small differential pressure is generated that is proportional to flow. Figure 24 shows the relationship between the flow and pressure for the pneumotach, which is linear. The pneumotach was calibrated with a 3L syringe daily. A differential pressure transducer (model 5inch-D-4V, All Sensors, Morgan Hill, CA) with a range ± 12.7 cm H_2O was used to correlate the pressure change along the pneumotach to flow. The mouth pressure was also measured with a differential pressure transducer (model ASCX05DN, +350 cm H_2O, Honeywell, Morristown, NJ). Data acquisition was achieved by a 14-bit data acquisition device (NI USB-6009, National Instruments, Austin, TX). Labview 7 (National Instruments, Austin, TX) was used to manipulate the signal.

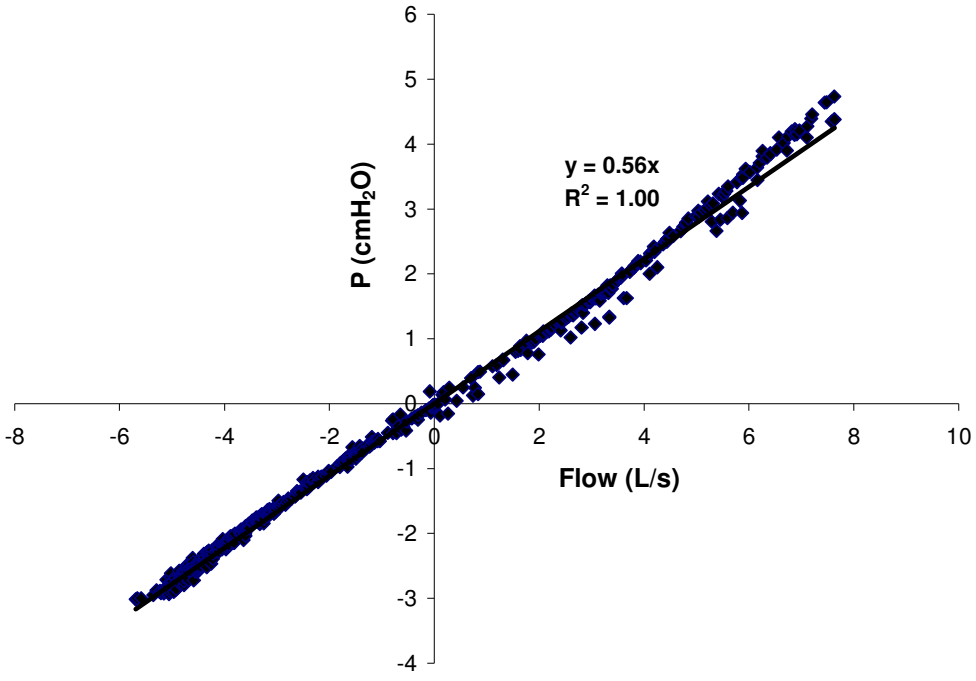

Figure 24: Pressure and flow relationship of the pneumotach

The shutter was triggered with a solenoid relay assembly (Figure 25). The digital output signal came from the data acquisition card. Since the signal did not have enough power to trigger the relays, voltage followers were used. This signal fed into two solid state relays (model SSRL240, Omega, Stamford, CT), which eventually controlled the movement of the solenoids.

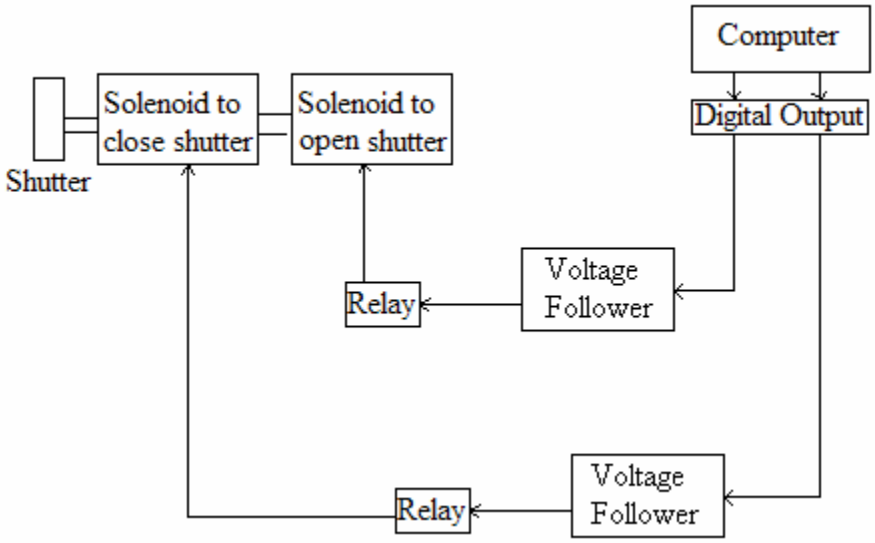

Figure 25: Solenoid-relay assembly that controls the shutter

Two push-pull type solenoids (model 7110-2A, Dormeyer, Vandalia, OH) were connected to a modified 1 ½" knife gate valve, which was used as the shutter (Figure 26). The valve had a plunger whose back and forth movement controlled the valve opening. This plunger was attached to a push type solenoid to close the opening when the solenoid was triggered. Another pull type solenoid was attached to the push-type solenoid. When the pull type solenoid was triggered, the plunger was moved back to the open position. By taking a high speed movie, the time it took to open and close the valve was investigated. The movie showed that the valve was closed in 27 ms and was opened in 19 ms.

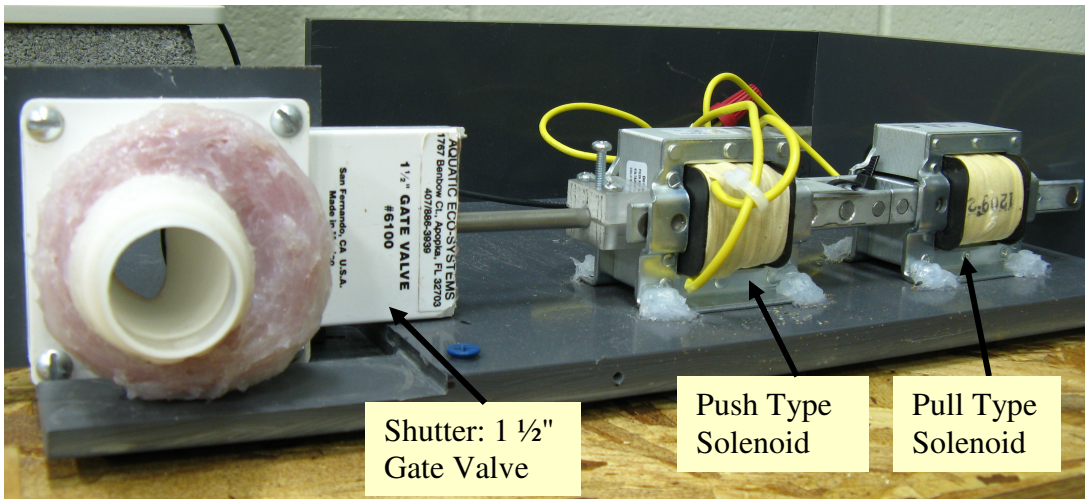

Figure 26: Solenoid shutter assembly

3.1.2 The Airflow Perturbation Device (APD)

The APD body was connected to a screen type pneumotach, which was originally used in a 1993 model Collins constant volume body plethysmograph, and to two pressure transducers to measure flow and mouth pressure during tidal breathing and forced expiration. A differential pressure transducer (model 5inch-D-4V, All Sensors, Morgan Hill, CA) with a range ± 12.7 cm H_2O was used to correlate the pressure change along the pneumotach to flow. Mouth pressure was measured with a differential pressure transducer (model ASCX05DN, + 350 cm H_2O, Honeywell, Morristown, NJ). The detailed description of the APD was given in the paper by Johnson et al., 1984.

3.1.3 The External Resistances

Two sets of linear external resistances were built by using capillary tubes (Figure 27A) to imitate mild impairment of upper airways. Each set contained both a low and high resistance (Table 2). The first set had resistances of 1.12 cm H_2O/L/s and 2.10 cm H_2O/L/s, respectively. The second set had resistance values of 1.26 cm H_2O/L/s and 2.30 cmH_2O/L/s. Each subject was tested with either the first or second

set of resistances. Additionally, another external resistance was built to apply a higher respiratory load limited to either the inspiration or expiration side during tidal breathing. (Figure 27B). The resistance on one side of this one way valve was 5.81 cm H_2O/L/s. The other side (no added resistance) had a resistance of 0.91 cm H_2O/L/s. This one way valve resistance system was designed such that it could be turned around to put the high resistance on either inhalation or exhalation side (Figure 27B). The pressure versus flow characteristics of these systems are shown in Figure 28.

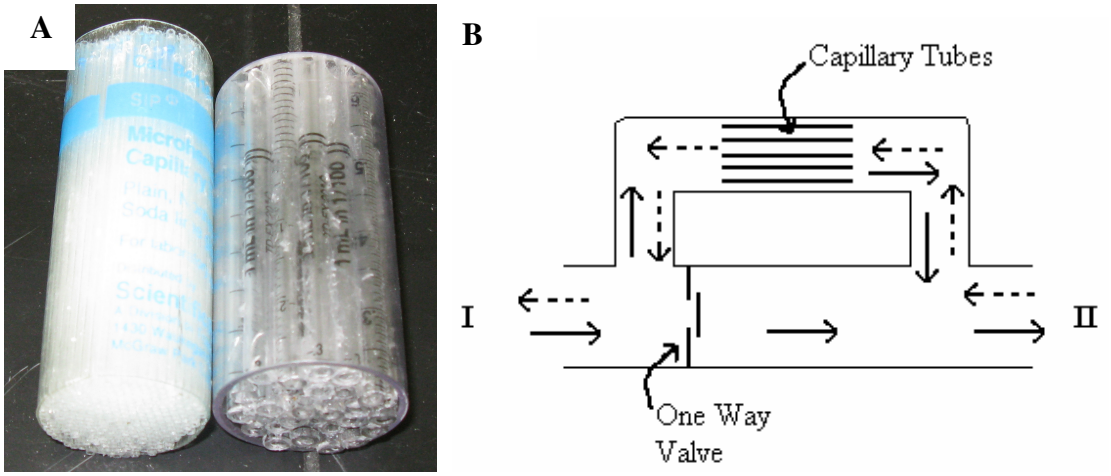

Figure 27A: Low and high resistances built with capillary tubes. B: Diagram of another external resistance system to apply higher respiratory load to one side only. If a subject was breathing through side I, during inhalation the valve will close and the flow would follow dashed arrows. During exhalation, flow would follow solid arrows. Therefore, the higher resistance would be on the inhalation side. If a subject breaths through side II, the higher resistance would be on the exhalation side.

Table 2: Added external resistances in cm H_2O/L/s. Each set contained a low and high resistance.

	Set 1	**Set 2**
Low R	1.12	1.26
High R	2.10	2.30

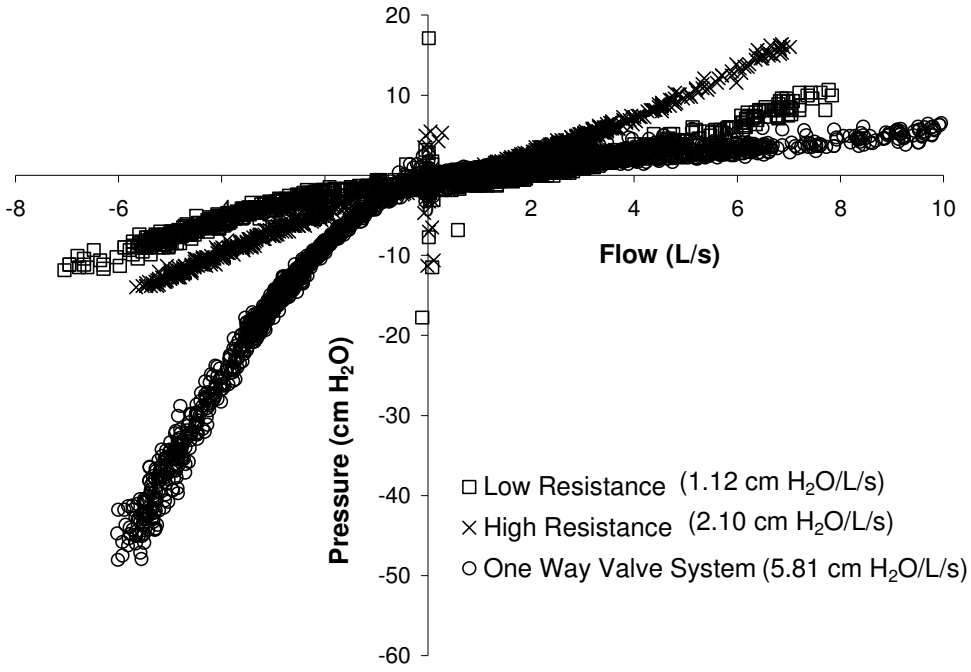

Figure 28: Pressure-flow characteristics of external rigid resistances used.

3.1.4 The Esophageal Balloon Catheter

Pleural pressure was measured with an 86-cm closed-end catheter with a balloon of 9.5 cm length (Cooper Surgical, Trumbull, CT) (Figure 29). The catheter was connected to a differential pressure transducer (model 143PC03D, Honeywell, ± 176 cm H_2O). The pressure - volume characteristic of the balloon was measured (Figure 30) so that the minimum volume of air to be introduced into the balloon would be in the flat part of its pressure-volume curve (i.e. dP/dV~0). The esophageal balloon catheter had a flat pressure response up to 3 ml. Unless otherwise stated, 1 ml of air was injected to the balloon during all trials. The air was necessary in order to measure pressure with the transducer. Transpulmonary pressure (P_{tr}) was taken as the difference between esophageal pressure and air pressure measured at the mouth.

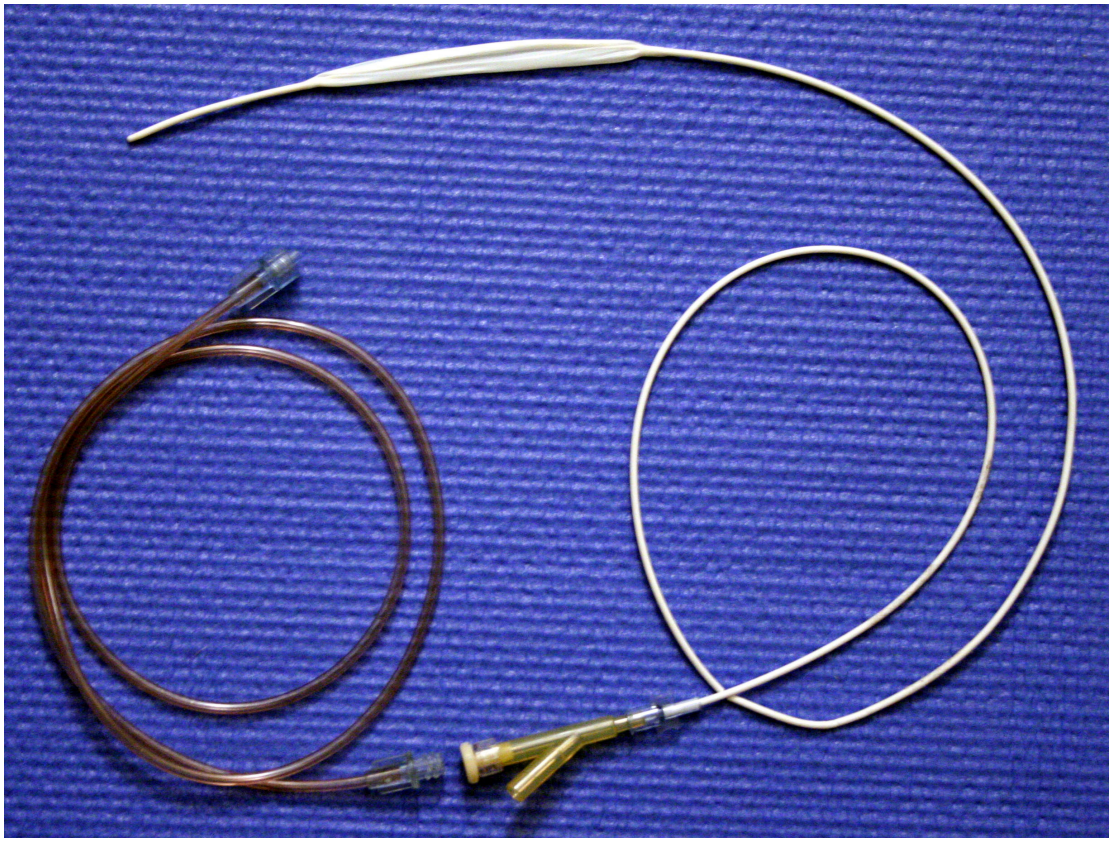

Figure 29: Esophageal balloon catheter

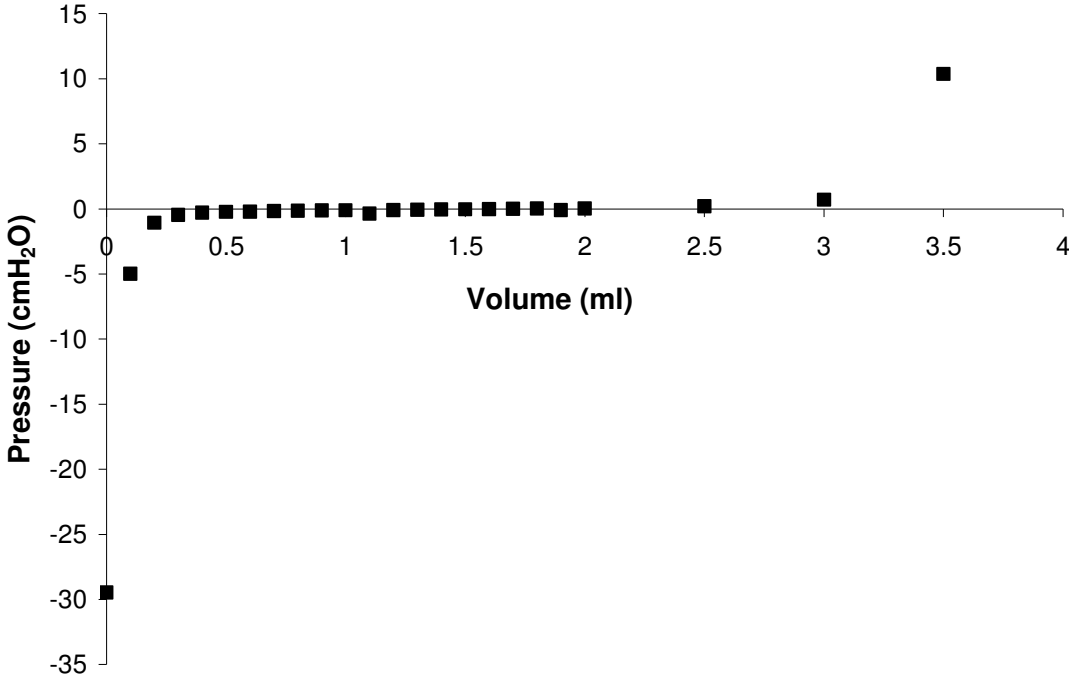

Figure 30: The pressure volume characteristics of the esophageal balloon

The frequency response of the esophageal balloon catheter was also measured from 1 Hz to 50 Hz. The apparatus consisted of a function generator, amplifier, loudspeaker and an oscilloscope (Figure 31). There were two main steps. First, the frequency response of the pressure transducer was found by connecting the pressure transducer to the loudspeaker, and then feeding a sinusoidal wave into the speaker with a function generator. The amplitude ratio of the signal coming from the speaker and the pressure transducer were calculated by reading the values through the oscilloscope.

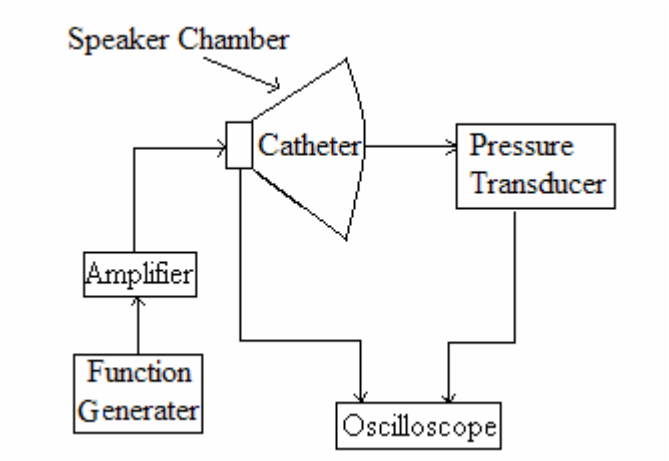

Figure 31: Schematic of the experimental apparatus that was used to measure the frequency response of the esophageal balloon.

For the second step, the esophageal balloon catheter was placed in the closed chamber and 1 ml of air was injected into the balloon. Afterwards, it was connected to the same pressure transducer used in the first step. Again, a sinusoidal wave was fed into the speaker with a function generator. Then, the amplitude ratio of the signal coming from the speaker and the pressure transducer that was connected to the balloon was calculated. This ratio was divided by the ratio found at the first step. This gave the frequency response of the balloon. The esophageal balloon catheter was a

second order system with a flat frequency response up to 5 Hz (Figure 32). Due to inadequate frequency response of the balloon, it was not possible to see the APD perturbations in the pleural space during the experiments.

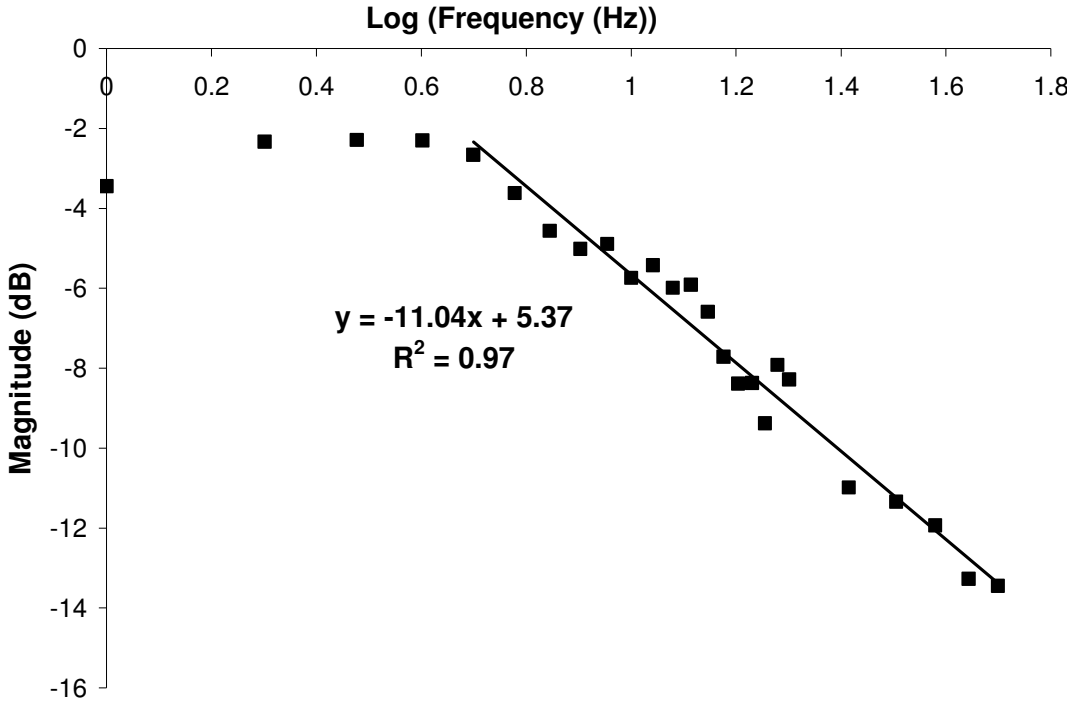

Figure 32: Bode plot showing the frequency response of the esophageal balloon

3.2 Subject Testing

3.2.1 Orientation and Consent

Institutional Review Board (IRB) approval on IRB application # 06-0338 was received on April 23, 2008 (Appendix A). Six male subjects without any history of respiratory disease were recruited from among laboratory personnel (Table 3). The subjects read and signed the informed consent document and medical history questionnaire (Appendix A). An orientation session provided the subject with a detailed description of their rights and the procedure, and it provided the investigators with information about the subjects' health. Any demographic or experimental data

collected corresponds only to a subject number and may not be traced back to the individual. The first subject (104) was tested to evaluate the experimental setup. Therefore, not all measurements were done with this subject.

Table 3: Physiological characteristics of subjects.

				FVC (L)		FEV1 (L)		FEV1/FVC (%)
Subject No	Age	Height (in)	Weight (lb)	Meas	%Pred	Meas	%Pred	Meas
100	22	73	195	5.95	98	4.24	84	71
101	21	72	150	5.07	86	3.78	77	75
102	29	72	200	4.57	79	3.98	84	87
103	20	66	230	5.53	112	4.51	108	82
104	61	70	230	4.38	97	3.81	107	87
105	21	74	200	5.57	89	4.86	94	87

FVC: forced vital capacity; FEV1: volume of gas expired in the first second of forced expiration. Predicted (Pred) values are Hankinson reference values (Hankinson et al., 1999) and are compared to measured (Meas) values.

3.2.2 Vital Capacity (VC)

The first measurement was the vital capacity. The diagram of various lung volumes and definitions are given in Appendix B. Vital capacity is the maximum amount of air expired after a full inspiration. The test procedure required that the subject be seated with a mouthpiece attached to his mouth while wearing a nose clip. He was instructed to breathe to total lung capacity (TLC) and signal the technician when at TLC. Then, he breathed out forcefully to his residual volume. The same procedure was repeated three times and the average was taken. Exhaled volume percentage was used as a reference point when closing the shutter at a specified lung volume to construct isovolume pressure-flow curves with the stop – flow method.

3.2.3 Stop – Flow Measurements

One method used to construct isovolume pressure-flow curves was the stop flow method (Figure 33). The test procedure required that the subject be seated with a

mouthpiece attached to his mouth while wearing a nose clip. The subject was instructed to inhale to TLC and signal the technician. During expiration, at a preselected lung volume, the shutter was closed. The subject made a steadily increasing effort to increase the pressure against a closed shutter until the pressure reached a preset value. At this point, the shutter was opened again. The pressure just before the shutter opening was correlated with the flow just after shutter opening. At each lung volume, pressure measurements were obtained in 10 cm H_2O increments up to 80 cm H_2O. Not all subjects were capable of generating mouth pressures as high as 80 cm H_2O. For those subjects, the experiment was ended at the highest achievable mouth pressure.

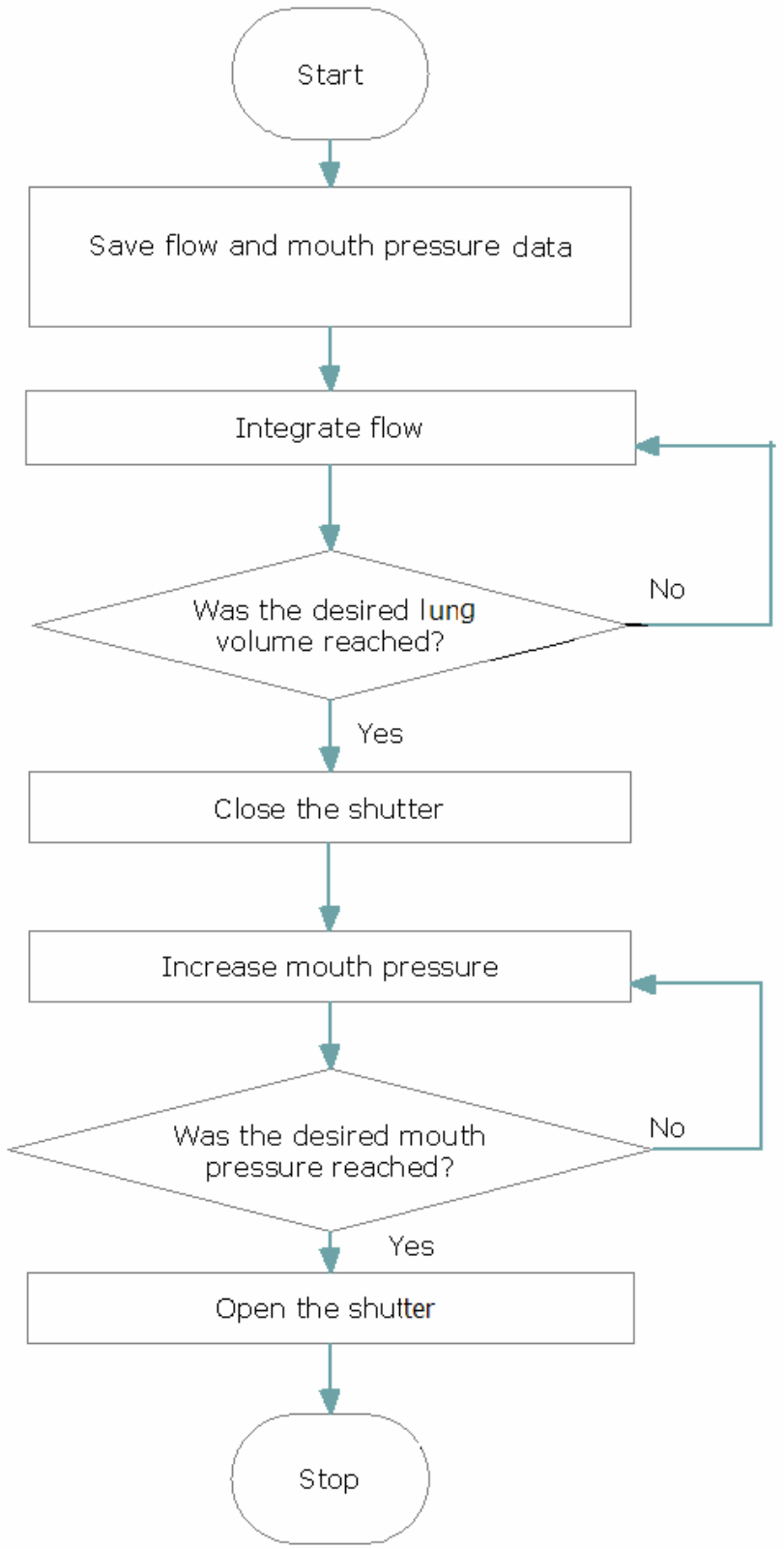

Figure 33: Operation of stop-flow data acquisition

3.2.4 Pleural Pressure

Pleural pressure measurements were made with the esophageal balloon catheter. The balloon was passed through the nose into the lower third of the esophagus. The subject was asked to swallow the balloon as follows. First, 1 % lidocaine, which is a local anesthetic and a numbing agent, was injected into one of the nostrils using a syringe without a needle. After the subject sniffed this back, the balloon, with all air removed, was inserted to the back of the nose while the subject was asked to drink water from a cup through a straw. This helped with the movement of the balloon along the esophagus. After lowering it to approximately 30 cm from the nostrils, very little air (~1 ml) was put into the balloon and the end of the catheter was connected to a pressure gage. A three – way valve prevented air from escaping during the transition from syringe to the pressure transducer.

Pleural pressure measurements were used to construct IVPF curves during forced expiration with different effort levels and to calculate pulmonary resistance during tidal breathing when external resistances added to the mouth.

To construct the IVPF curves, subjects were instructed to take a full breath in and breathe out to residual volume with different effort levels. During this time, pleural pressure, mouth pressure and flow were recorded for at least eight different effort levels, for each subject.

3.2.5 The APD Resistance

The APD resistance was measured during tidal breathing and forced expiratory flow. For forced expiratory flow measurements, the subject was instructed to breathe to TLC and signal the technician. He breathed out to the residual volume with forced expiratory flow. During this time, pressure and flow was recorded. This

data was used to calculate the APD resistance at different lung volumes during forced vital capacity. More detailed description of the APD resistance calculations are given in Chapter 4.

Chapter 4. Data Analysis

The resistance calculations with the APD and an esophageal balloon as well as construction of isovolume pressure-flow (IVPF) curves are explained in detail below.

4.1 Construction of IVPF Curves

4.1.1 Stop – Flow Experiments

The flow and mouth pressure recording of one subject tested with the stop – flow method is given in Figure 34. The stop – flow experimental setup required that the subject breathes out forcefully after a deep inspiration. Then, the shutter was closed at a desired lung volume and mouth pressure was increased to again a preselected value. When the desired mouth pressure was reached, the shutter was opened. The flow after shutter opening had a transient region varying between 30 to 70 ms. The length of the transient region was relatively constant for each subject but varied from one subject to another (Figure 35). The length of this transient region was identified by inspection to determine the flow at the end of the transient region and to correlate it with mouth pressure before shutter opening.

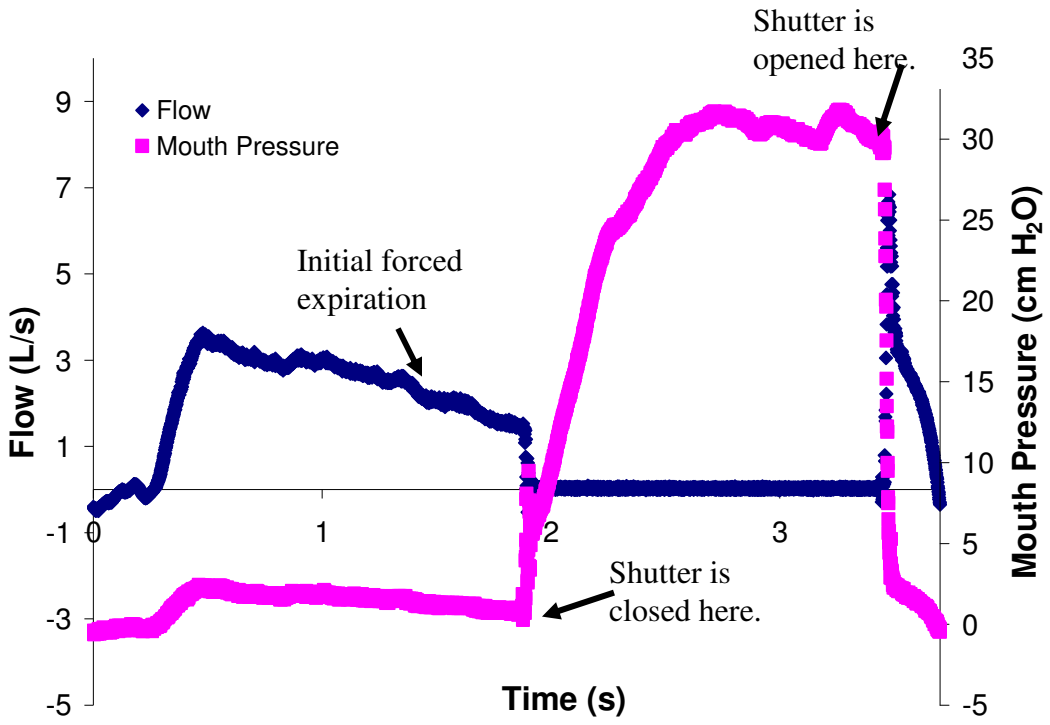

Figure 34: Flow and mouth pressure recording of a subject during the stop – flow experiment.

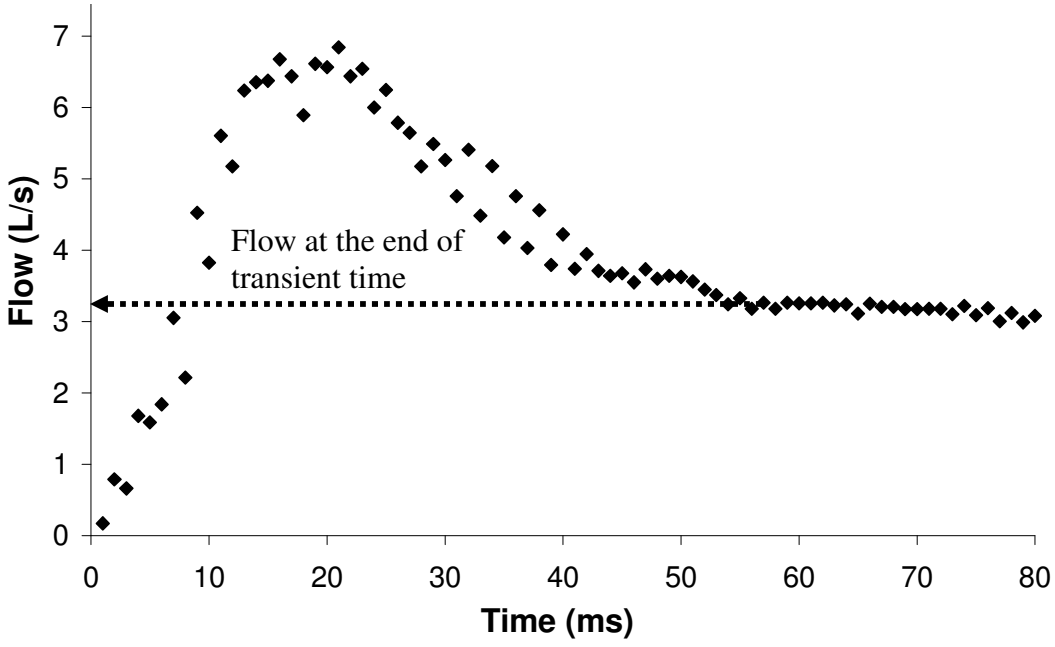

Figure 35: The transient flow after shutter opening.

4.1.2 Esophageal Balloon Method

IVPF curves were constructed at 25, 50, and 75 % VC by correlating the flow to the pleural pressure minus mouth pressure (i.e. transpulmonary pressure) at various effort levels of forced expiratory flow. All subjects started at TLC, and amount of exhaled air was calculated by integrating the flow. Figure 36 shows the transpulmonary pressure and flow recording of a subject for one effort level. In this plot, green circles show the correlated pressure and flow values at each lung volume. A correlated pressure and flow pair was obtained from each effort level for each lung volume. By testing the same subject many times with different effort levels, eventually enough data points were obtained to construct the IVPF curves like the ones shown in Figure 37.

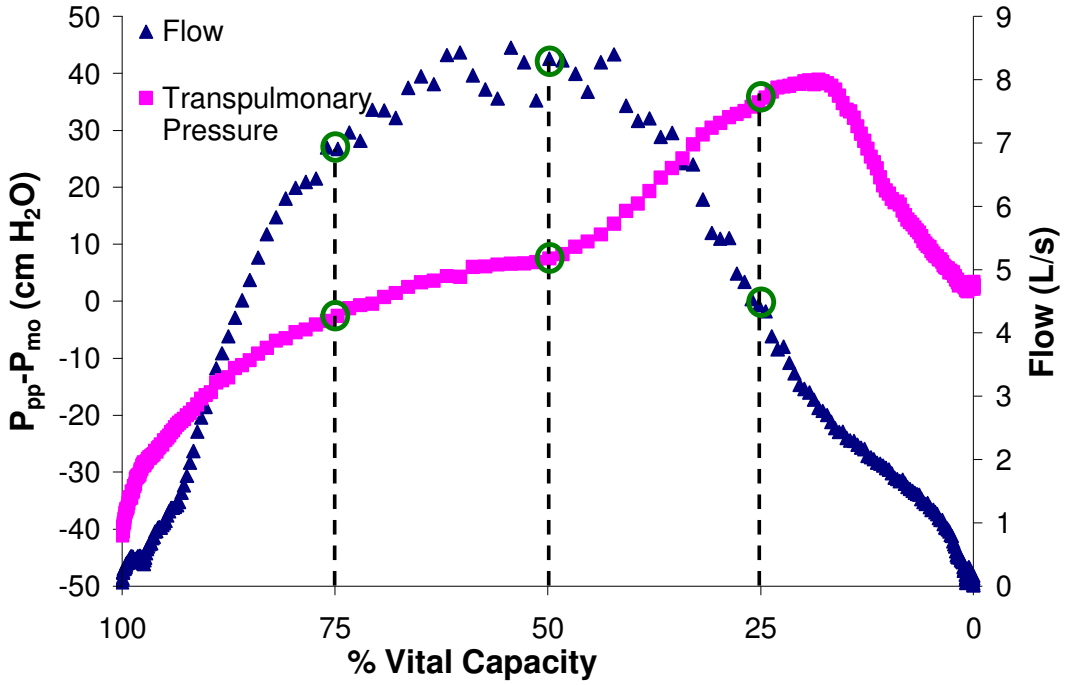

Figure 36: Transpulmonary pressure and flow recording of subject 105 for one effort level at different percent vital capacity. Green circles show the correlated pressure and flow values at each lung volume.

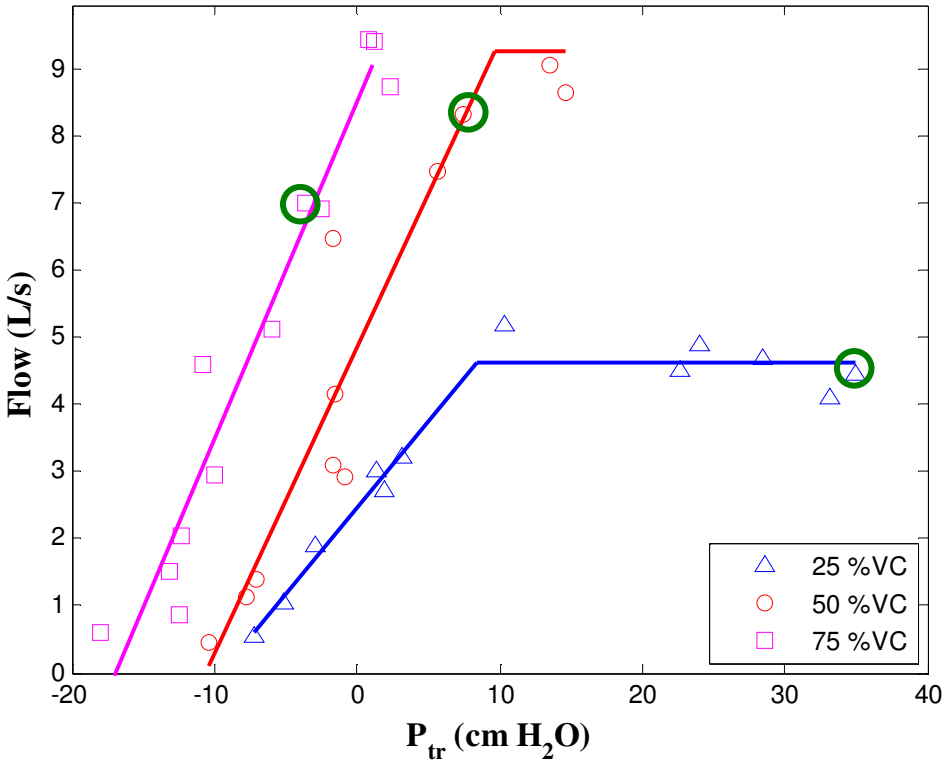

Figure 37: The IVPF curves of subject 105 at 25 %, 50 % and 75 %VC. Green circles show the data points obtained from Figure 36.

4.1.3 Identifying the Limited Flow

IVPF curves are formed of two linear lines intersecting at the point where the flow becomes limited. The line drawn through points after the limited flow has a slope of zero. In order to be able to identify the pressure and flow at the limited flow condition, a MATLAB program was written to optimize the best fit in a least square sense that could be drawn through the points (Appendix C). Figure 38 shows the fitted lines for the two methods that show the limited flow and the pressures at the onset of flow limitation.

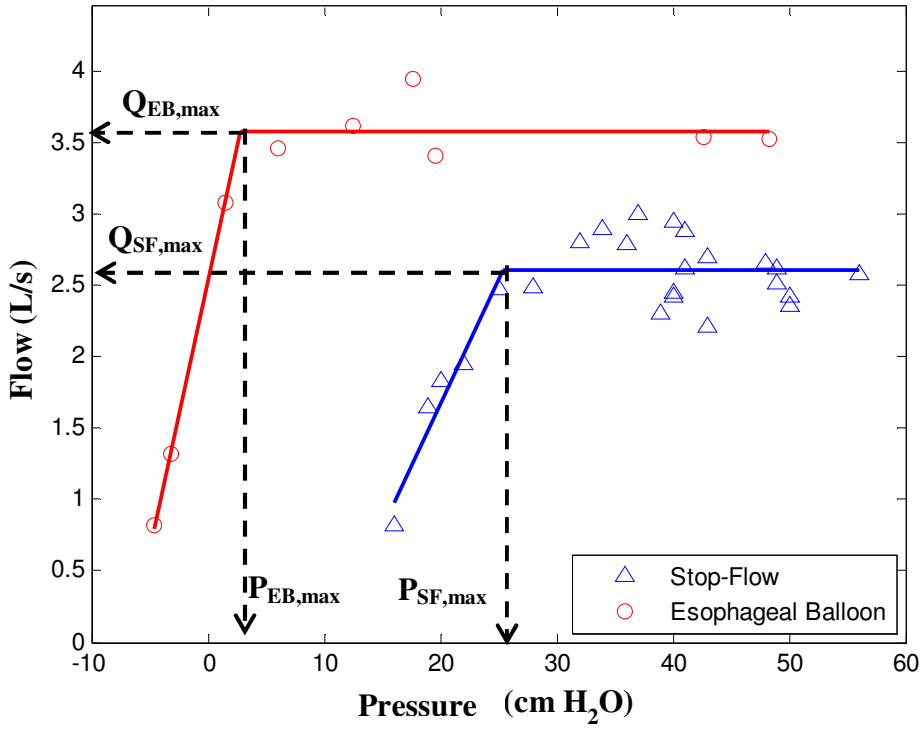

Figure 38: IVPF curves of one subject at 25 %VC. $P_{SF,max}$ and $Q_{SF,max}$: Mouth pressure and flow at flow limitation with the stop – flow method; $P_{EB,max}$ and $Q_{EB,max}$: Transpulmonary pressure and flow at flow limitation with the esophageal balloon method.

4.2 Pulmonary Resistance Calculations

The pulmonary resistance, (R_L), measurements required continuous recording of transpulmonary pressure, (P_{tp}), flow, (Q), and lung volume, (V) during tidal breathing. It was assumed that at the beginning of inspiration and end of expiration, all subjects were at their functional residual capacity. Average pulmonary resistance was calculated by dividing the pleural pressure difference between mid inspiration (MI) and mid expiration (ME) by the flow difference at mid tidal volume (MTV) (Figure 39). Flow was integrated during tidal breathing to calculate the lung volume. Mid inspiration and mid expiration lung volumes were assumed to be the same, and were taken as half of the tidal volume at the end of inspiration. The theory is

explained below. During inspiration and expiration, transpulmonary pressures can be described as:

$$P_{tp,MI} = V_{MI}/C + Q_{MI} R_L \quad (4.1)$$

$$P_{tp,ME} = V_{ME}/C + Q_{ME} R_L \quad (4.2)$$

The lung compliance, C, is assumed to be the same during inspiration and expiration. Therefore if $V_{MI}/C = V_{ME}/C$, then equation (4.2) is subtracted from equation (4.1) to find the average pulmonary resistance as:

$$R_{L,av} = \frac{P_{tp,MI} - P_{tp,ME}}{Q_{MI} - Q_{ME}} \quad (4.3)$$

In order to calculate inspiratory (or expiratory) pulmonary resistance separately, the effect of lung elastic recoil needs to be subtracted since the transpulmonary pressure reflects the pressure required to overcome the resistance to airflow in addition to the elastic recoil pressure required to inflate the lung. At the beginning of inspiration and expiration the flow is zero. The flow resistive pressure drop is thus zero. Therefore, the measured transpulmonary pressures at the beginning and end of the inspiration represented only elastic recoil of the lungs. These pressures were interpolated to calculate the elastic pressures at mid tidal volume assuming a linear relationship between elastic pressures and lung volume.

To calculate the inspiratory (or expiratory) pulmonary resistances separately, lung elastic pressure at mid inspiration (or expiration) is subtracted from the transpulmonary pressure at mid inspiration (or expiration). Then, the resulting flow resistive pressure was divided by flow at mid inspiration (or expiration). Equations

4.4 and 4.5 show how to calculate the inspiratory and expiratory pulmonary resistance values separately.

$$R_{L,ins} = \frac{P_{tp,MI} - P_{L,MTV}}{Q_{MI}} \qquad (4.4)$$

$$R_{L,exh} = \frac{P_{L,MTV} - P_{tp,ME}}{Q_{ME}} \qquad (4.5)$$

$R_{L,ins}$ = Inspiratory pulmonary resistance, cm H_2O/L/s

$R_{L,exh}$= Expiratory pulmonary resistance, cm H_2O/L/s

$P_{L,MTV}$= Lung elastic recoil pressure at mid tidal volume, cm H_2O

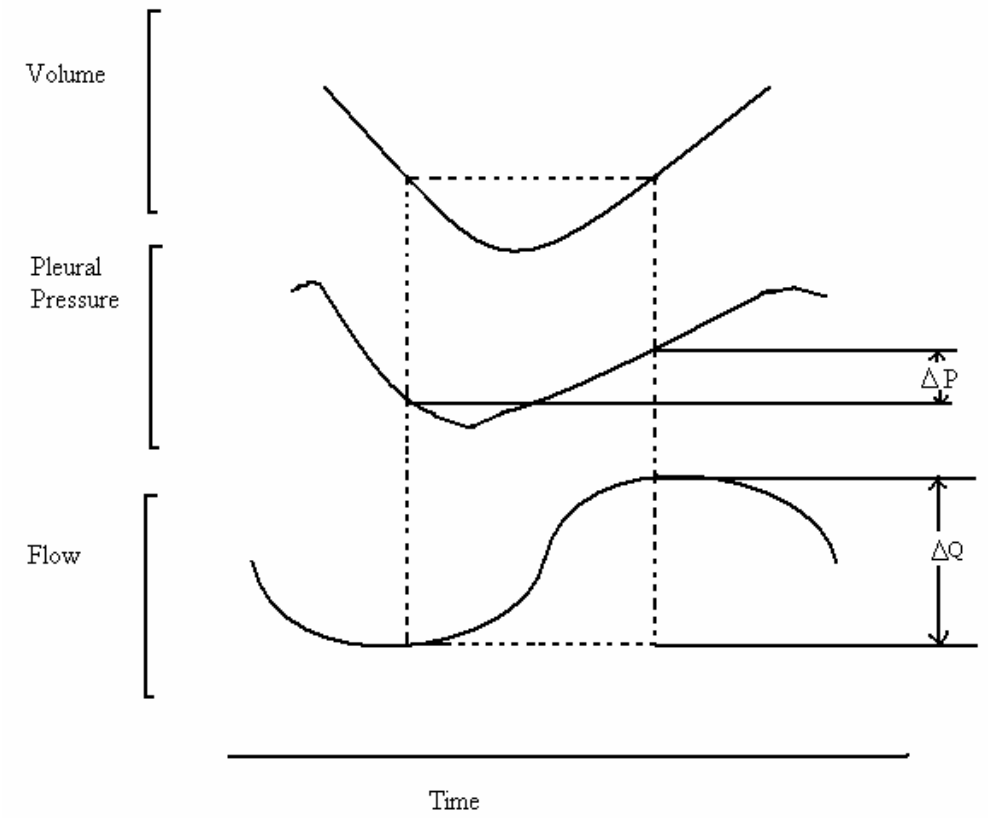

Figure 39: Simultaneous recording of lung volume, pleural pressure, and flow during tidal breathing. The change in pressure (ΔP) divided by change in flow (ΔQ) between two points where lung volume is identical provide an estimate of average pulmonary resistance.

4.3 The APD Resistance Calculation

A wheel in the flow path rotating at 10 Hz perturbs air flow and mouth pressure by a small amount during tidal breathing. There are many perturbations during inhalation and exhalation depending on the duration of breathing. The ratio of pressure perturbation to flow perturbation was calculated for each perturbation (Figure 40). Then, resistances calculated from perturbations occurring during inhalation (or exhalation) are averaged to find the APD inhalation (or exhalation) resistance. The average of inhalation and exhalation resistances gives the average APD resistance.

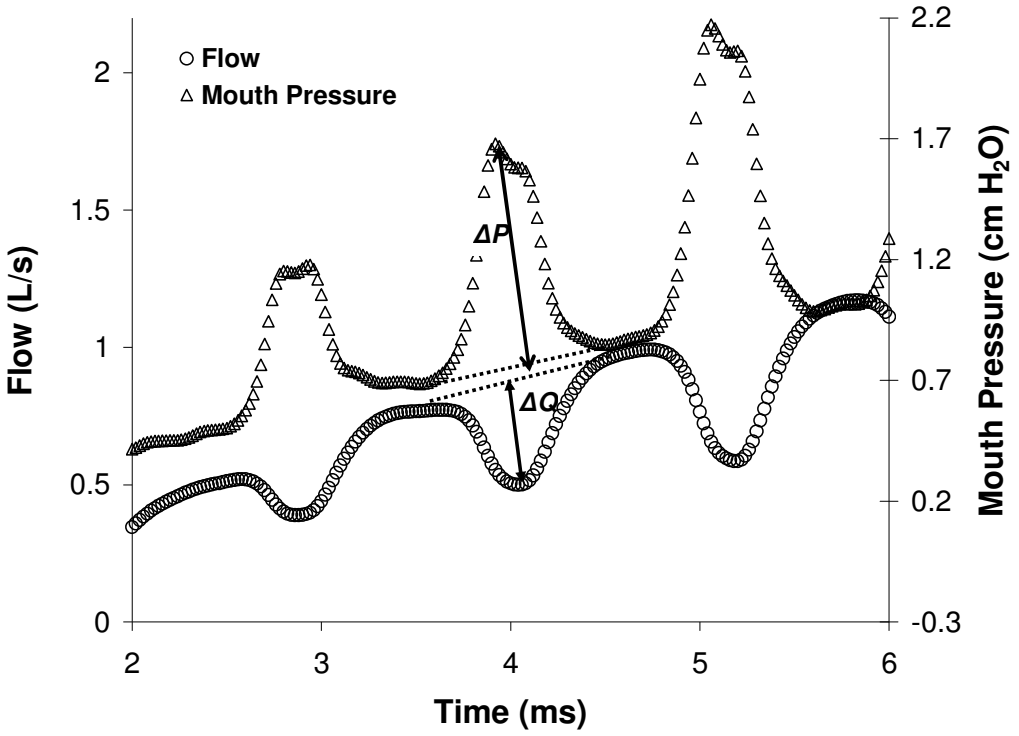

Figure 40: The Airflow Perturbation Device mouth pressure perturbation during part of the exhalation. ΔP/ΔQ gives the resistance calculated with the APD.

4.4 Statistical Analysis

The unpaired t-test for unequal variances was used to compare the APD resistance and pulmonary resistance and the stop – flow and esophageal balloon

methods at 95 % confidence. The statistics were calculated in Excell (Microsoft, Redmond, WA), and the detailed statistical results are given in appendices D and G. The difference between the methods was given as mean ± standard deviation.

The Pearson correlation coefficient (r) (Mendenhall et al., 1992) was used to investigate the strength of a linear relationship between various variables in this study. For example, if r was calculated for two variables, x and y, a positive r means y increases as x increases. A negative r means y decreases as x increases. A r value between 0 and 1 means that a linear trend *may* exist between x and y. While r = ± 1 shows a perfect relationship, r near "0" reflects little or no linear relationship between the variables.

Chapter 5. The APD Resistance versus Pulmonary Resistance

Six healthy subjects were tested with the APD and an esophageal balloon during tidal breathing when known external resistances were added during inspiration, during expiration, and during both inspiration and expiration. In this chapter, the term "APD resistance" represents the resistance measured using the APD device, and "pulmonary resistance" represents the resistance measured using airflow and esophageal pressure as described in Chapter 4. Detailed statistical results are given in Appendix D, and all statistical calculations were made at $\alpha = 0.05$.

5.1 The APD and Pulmonary Resistance

A detailed explanation of the results is given in sections 5.1.1 through 5.1.3. In summary, the key differences and similarities between the APD and pulmonary resistances are as follows:

- The APD resistance was higher than the pulmonary resistance for most of the subjects tested.
- Using the APD resistance was a better predictor of the added external resistance than using the pulmonary resistance.
- The variance in the APD resistance was lower than that in the pulmonary resistance.
- When the external resistance was added only on the inhalation or exhalation side, the APD resistance showed a larger change on the side where the resistance was added.

- With larger added resistance, the difference between the APD and pulmonary resistance decreased for most of the subjects.
- The differences between the APD resistance and the pulmonary resistance were not statistically significant.

5.1.1 The Baseline Resistances

A subject's baseline or "intrinsic" resistance is defined as the measured resistance during tidal breathing when no external resistances were added. The average intrinsic APD resistance was always higher than the average pulmonary intrinsic resistance for all subjects except for subject 102, who had a higher pulmonary intrinsic resistance than APD intrinsic resistance (Table 4). However, there was no statistically significant difference between average resistances measured by the two techniques and the average difference between two methods was 0.92 ± 1.25 cm H_2O/L/s.

Table 5 shows the mean and standard deviation (SD) for the APD and pulmonary resistances. In general, the variance of the APD resistance was lower than that of pulmonary resistance.

Table 4: Intrinsic resistances (cm H_2O/L/s) measured with both methods. Only for subject 102, the pulmonary resistance was higher than the APD resistance.

Subject No	$R_{APD,av}$	$R_{L,av}$	$R_{APD,ins}$	$R_{L,ins}$	$R_{APD,exh}$	$R_{L,exh}$
100	1.89	1.00	1.58	1.06	2.20	1.23
101	1.76	0.53	1.70	0.80	1.82	0.95
102	2.94	4.18	2.64	3.19	3.24	5.43
103	3.46	2.10	3.57	1.77	3.36	2.31
104	3.81	1.23	3.58	0.39	4.03	2.40
105	2.26	1.57	2.21	1.41	2.31	1.76

R_{APD}: The APD resistance; R_L: Pulmonary resistance; Average (av), inspiratory (ins), and expiratory (exp) resistances were shown.

Table 5: The mean and standard deviation (SD) of the APD and pulmonary intrinsic resistances.

	Mean	SD
$R_{APD,av}$	2.69	0.85
$R_{L,av}$	1.77	1.29
$R_{APD,ins}$	2.55	0.88
$R_{L,ins}$	1.44	0.98
$R_{APD,exh}$	2.83	0.85
$R_{L,exh}$	2.35	1.62

The APD inhalation and exhalation resistances were higher than pulmonary inhalation and exhalation resistances in five out of the six subjects tested. The difference between intrinsic inhalation resistances with both methods was 1.11 ± 1.27 cm H_2O/L/s, and the difference between exhalation resistances was 0.48 ± 1.35 cm H_2O/L/s. There was no statistically significant difference between the APD and pulmonary inhalation resistances. Similarly, the exhalation resistances measured with both methods were not statistically significantly different.

5.1.2 Addition of Inspiratory and Expiratory Resistances

Average pulmonary resistance was always lower than the average APD resistance for all subjects when external resistances were added to both inspiration and expiration (Table 6). Measured APD resistance also increased for all subjects with increased added resistance. This shows the ability of the APD to detect the added resistance. When the measured average APD and pulmonary resistances were plotted against added resistance for each subject separately, it was clear that the APD was more consistent at predicting the added resistance than the pulmonary resistance. Figure 41 shows this for subject 100. The plots of the rest of the subjects are given in Appendix E.

Table 6: Average (av) resistance results with added resistances to both inspiration and expiration in cm H_2O/L/s.

Subject No	Added Resistance	$R_{APD,av}$	$R_{L,av}$	$\Delta R_{APD,av}$	$\Delta R_{L,av}$
100	1.12	2.95	1.30	1.06	0.30
	2.10	4.02	2.49	2.13	1.49
101	1.26	2.41	0.77	0.65	0.24
	2.30	2.92	2.27	1.16	1.74
102	1.26	5.33	3.34	2.39	-0.84
	2.30	5.79	4.37	2.85	0.19
103	1.12	4.22	3.67	0.76	1.57
	2.10	5.37	5.01	1.91	2.91
104	1.12	4.34	NM	0.54	NM
	2.10	4.73	NM	0.93	NM
105	1.12	2.50	1.56	0.24	-0.01
	2.10	3.41	2.57	1.15	1.00

R_{APD}: APD resistance; R_L: Pulmonary resistance; ΔR: Change in measured resistance relative to baseline resistance; NM: Not Measured.

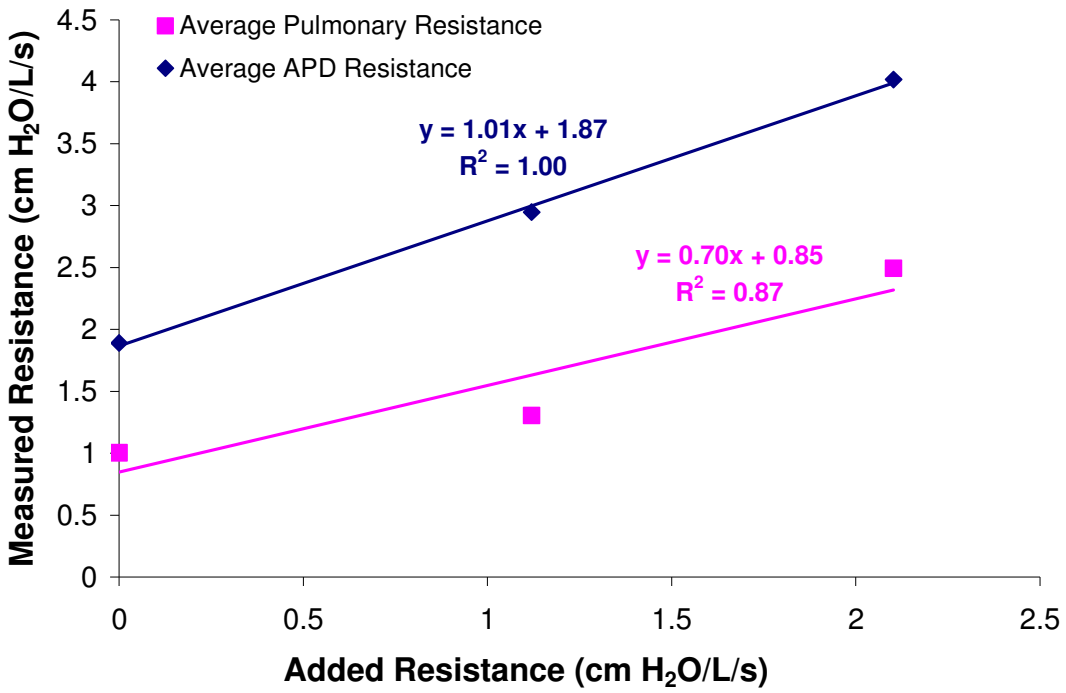

Figure 41: Added Resistance versus pulmonary and APD resistances for subject 100. The resistance value on the y axis when the added resistance is zero corresponds to the subject's intrinsic resistance.

When all data were combined, the regression plot showed that the measured average APD resistance increased by 79 % of the expected magnitude (Figure 42). The change in pulmonary average resistance was only 56 % of expected resistance change (Figure 43).

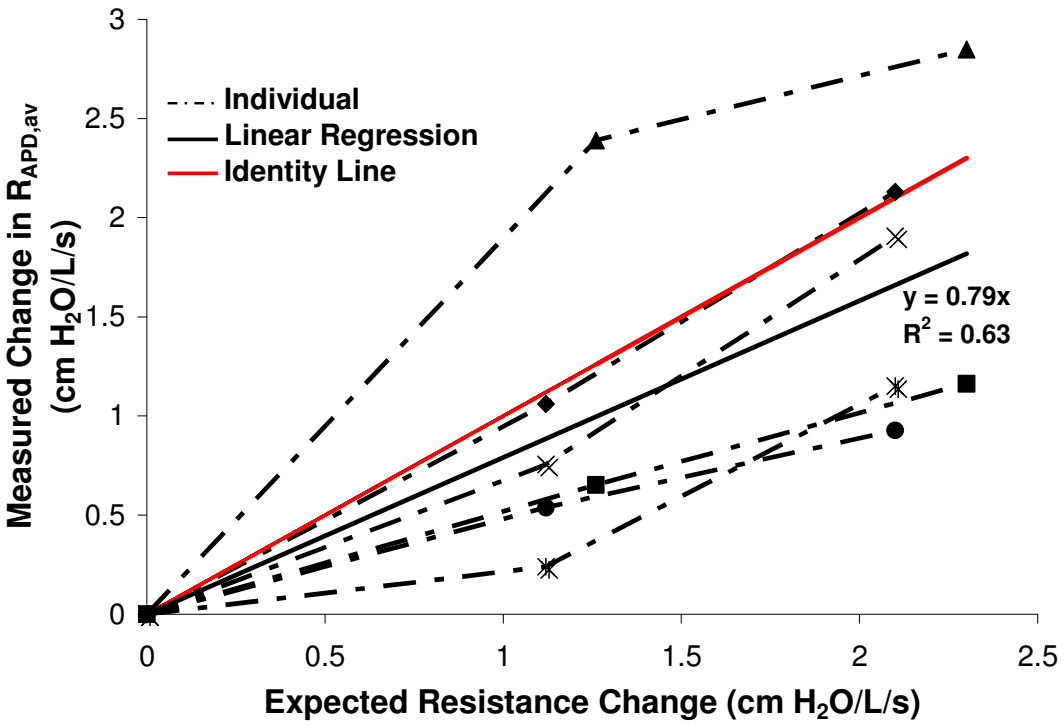

Figure 42: Measured change in average APD resistance with added resistance. Dashed lines connect the data from an individual subject. Linear regression is drawn with all data.

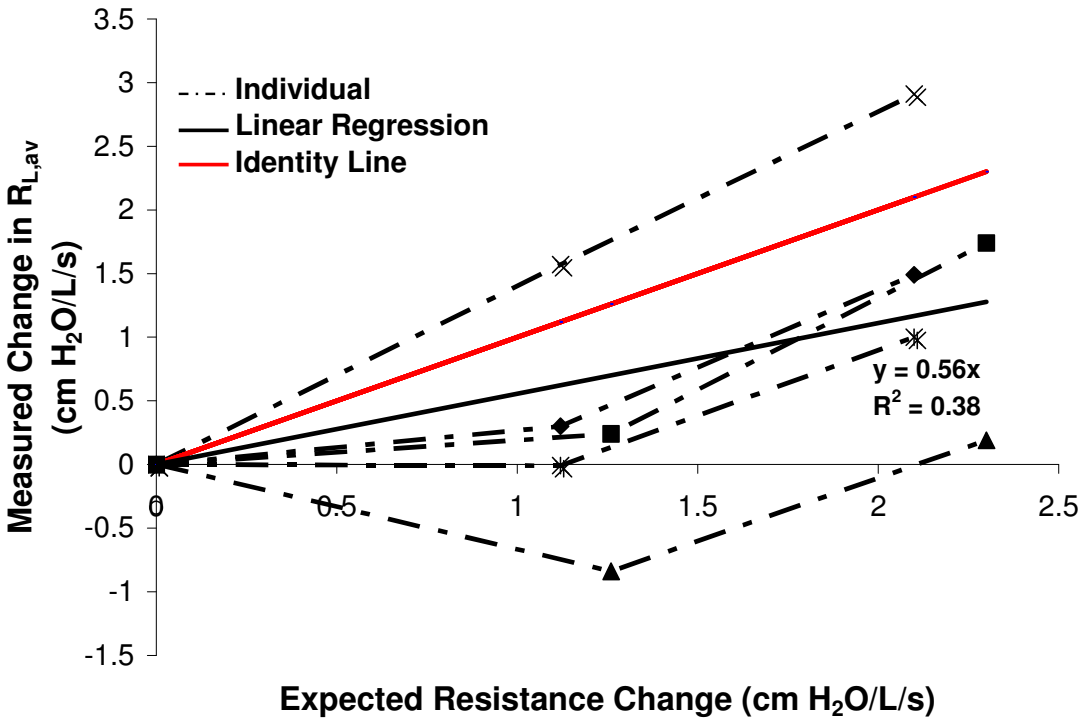

Figure 43: Measured change in average pulmonary resistance with added resistance. Dashed lines connect the data from an individual subject. Linear regression is drawn with all data.

Additionally, the comparison of measured change in $R_{APD,av}$, measured change in $R_{L,av}$, and added resistance showed that they were not statistically significantly different (Table 7).

Table 7: Table showing whether or not there were any significant differences between the change in average APD resistance, pulmonary resistance, and added resistance when external low and high resistances were added during tidal breathing. Note that statistics were calculated with unpaired t-test for unequal variances at $\alpha = 0.05$.

	Significant Difference (Yes/No)	
	Low Resistance	*High Resistance*
$\Delta R_{APD,av}$ *vs.* $\Delta R_{L,av}$	No	No
Added Resistance vs. $\Delta R_{APD,av}$	No	No
Added Resistance vs. $\Delta R_{L,av}$	No	No

With added resistances, both high and low, the APD inhalation resistance increased for all subjects (Table 8). When the high resistance was added, pulmonary inhalation resistance increased for all subjects. However, when the low resistance was added, measured pulmonary inhalation resistance decreased for two out of five subjects tested (Table 8).

The APD exhalation resistance also increased for all subjects with added resistances (Table 9). Pulmonary exhalation resistance, calculated as described in Chapter 4, decreased for one subject when low resistance was added, and for another when both low and high resistances were added. For the rest, pulmonary exhalation resistance increased.

Table 8: Inspiratory resistance results with added resistances to both inhalation and exhalation in cm H_2O/L/s.

Subject No	Added Resistance	$R_{APD,ins}$	$R_{L,ins}$	$\Delta R_{APD,ins}$	$\Delta R_{L,ins}$
100	1.12	3.11	1.15	1.53	0.09
	2.10	4.23	2.03	2.65	0.97
101	1.26	2.44	1.26	0.74	0.46
	2.30	2.97	1.72	1.27	0.92
102	1.26	4.71	2.26	2.07	-0.93
	2.30	5.31	3.58	2.67	0.39
103	1.12	4.02	2.89	0.45	1.12
	2.10	5.21	4.38	1.64	2.61
104	1.12	4.26	NM	0.68	NM
	2.10	4.93	NM	1.35	NM
105	1.12	2.49	0.61	0.28	-0.80
	2.10	3.31	1.75	1.10	0.34

R_{APD}: APD resistance; R_L: Pulmonary resistance; ΔR: Change in measured resistance relative to baseline resistance; NM: Not Measured.

Table 9: Expiratory (exh) resistance results with added resistances to both inspiration and exhalation in cm H_2O/L/s.

Subject No	Added Resistance	$R_{APD,exh}$	$R_{L,exh}$	$\Delta R_{APD,exh}$	$\Delta R_{L,exh}$
100	1.12	2.79	1.49	0.59	0.26
	2.10	3.81	2.98	1.61	1.75
101	1.26	2.39	0.22	0.57	-0.73
	2.30	2.87	2.86	1.05	1.91
102	1.26	5.95	4.21	2.71	-1.22
	2.30	6.27	4.99	3.03	-0.44
103	1.12	4.41	4.63	1.05	2.32
	2.10	5.53	5.78	2.17	3.47
104	1.12	4.43	NM	0.40	NM
	2.10	4.54	NM	0.51	NM
105	1.12	2.50	2.50	0.19	0.74
	2.10	3.51	3.33	1.20	1.57

R_{APD}: APD resistance; R_L: Pulmonary resistance; ΔR: Change in measured resistance relative to baseline resistance; NM: Not Measured.

When the measured inhalation and exhalation APD and pulmonary resistances were plotted against added resistances for each subject separately (Figure 44 and Appendix F), again there was larger variation in pulmonary resistance measurements compared to the APD resistances.

The changes in inspiratory and expiratory pulmonary resistance were only 36 % and 61 % of expected resistance change, respectively (Figure 45 and Figure 46). The regression line showed that the change in inspiratory and expiratory APD resistances were 82 % and 76 % of the expected resistance change, respectively (Figure 47 and Figure 48).

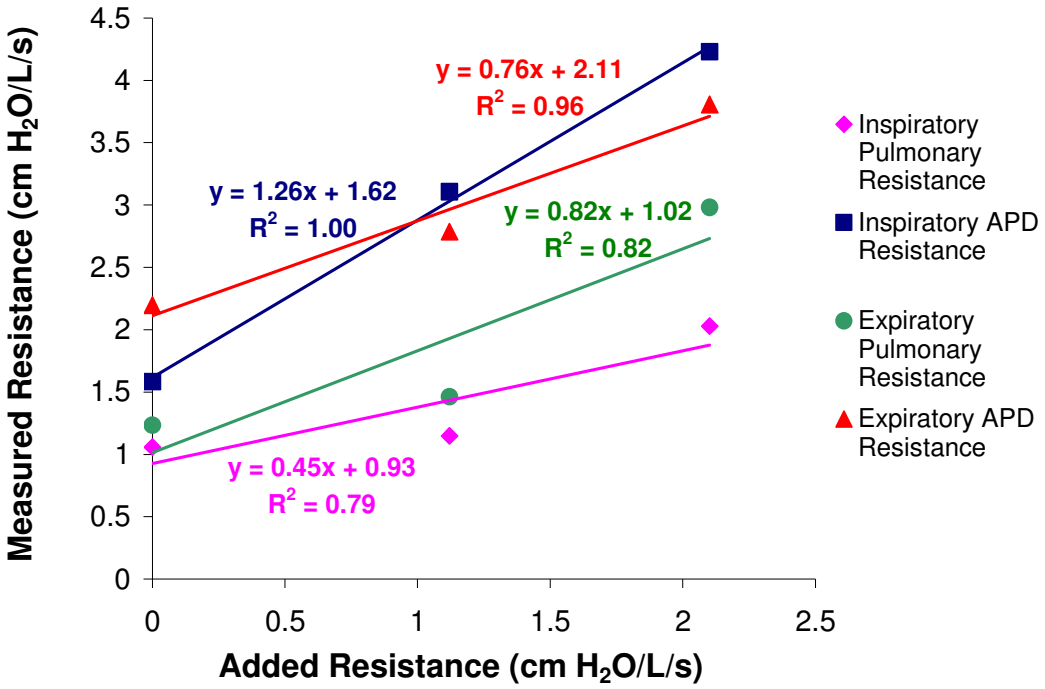

Figure 44: The resistance value on the y axis when the added resistance is zero corresponds to the subject's intrinsic resistance. Added Resistance versus pulmonary and APD inhalation and exhalation resistances for subject 100.

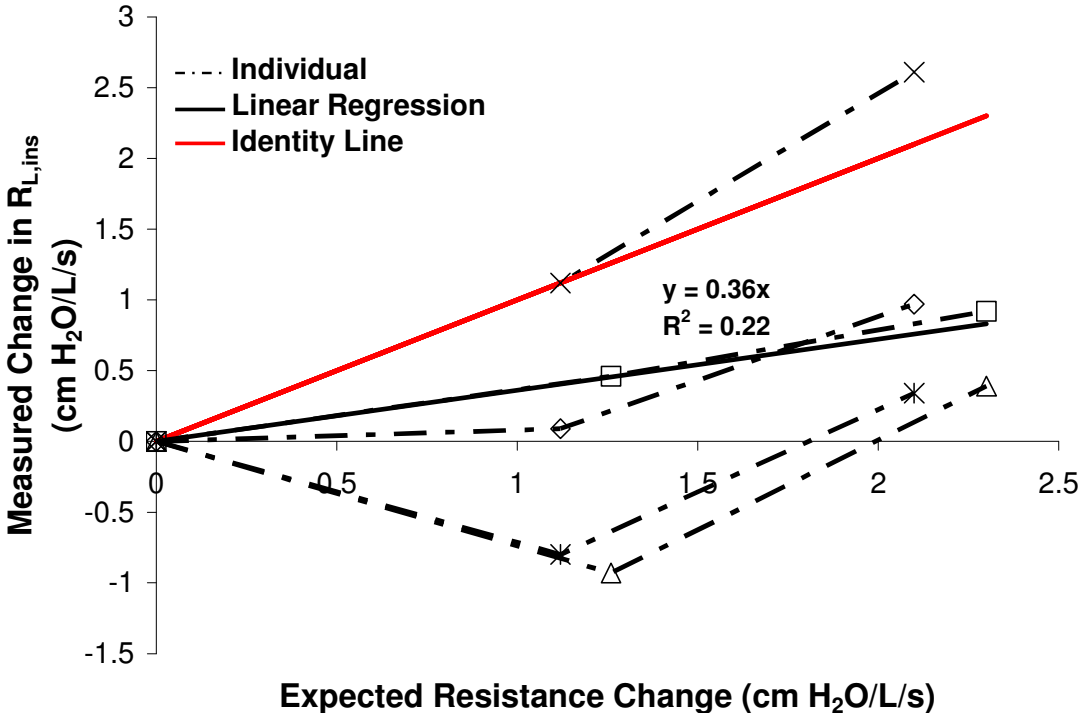

Figure 45: Measured change in inhalation pulmonary resistance with added resistance for all subjects except 104. Dashed lines connect the data from an individual subject. Linear regression is drawn with all data.

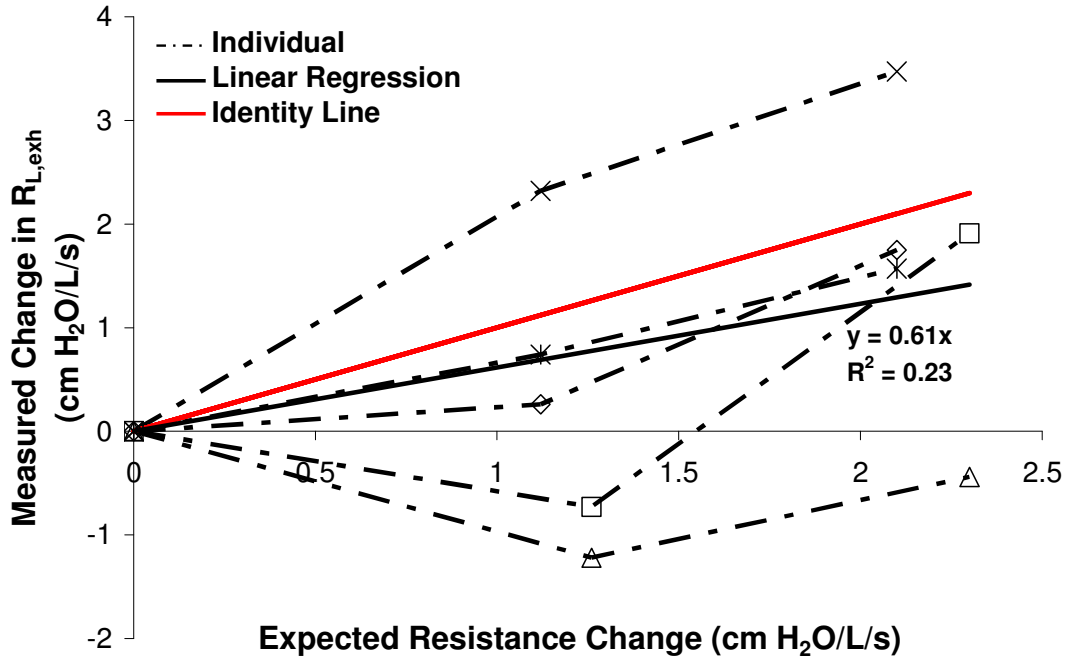

Figure 46: Measured change in exhalation pulmonary resistance with added resistance. Dashed lines connect the data from an individual subject. Linear regression is drawn with all data.

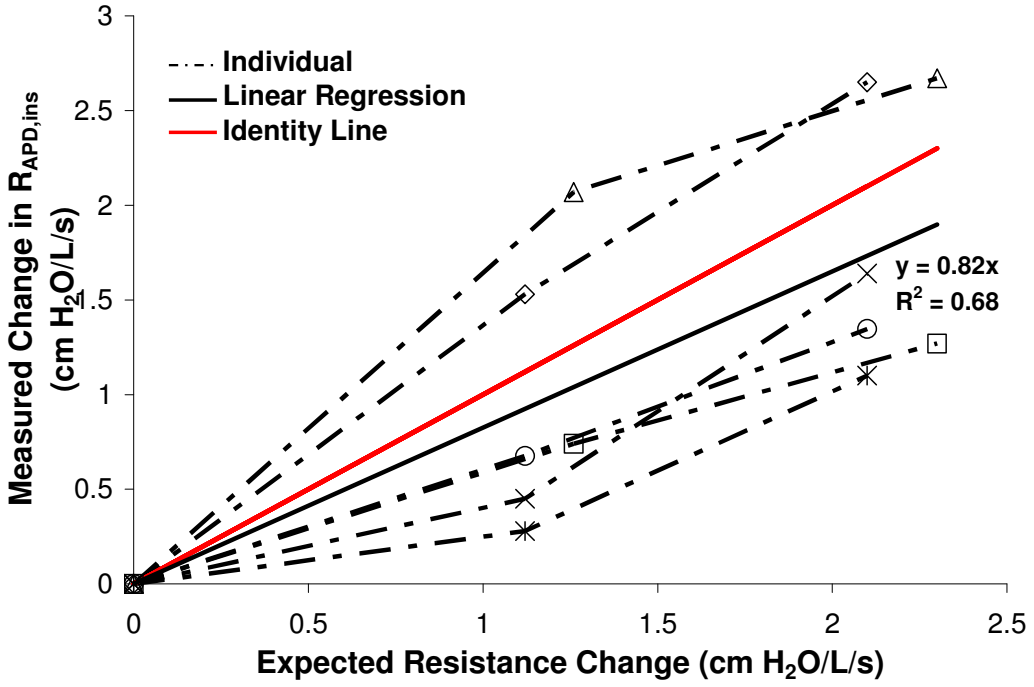

Figure 47: Measured change in inhalation APD resistance with added resistance. Dashed lines connect the data from an individual subject. Linear regression is drawn with all data.

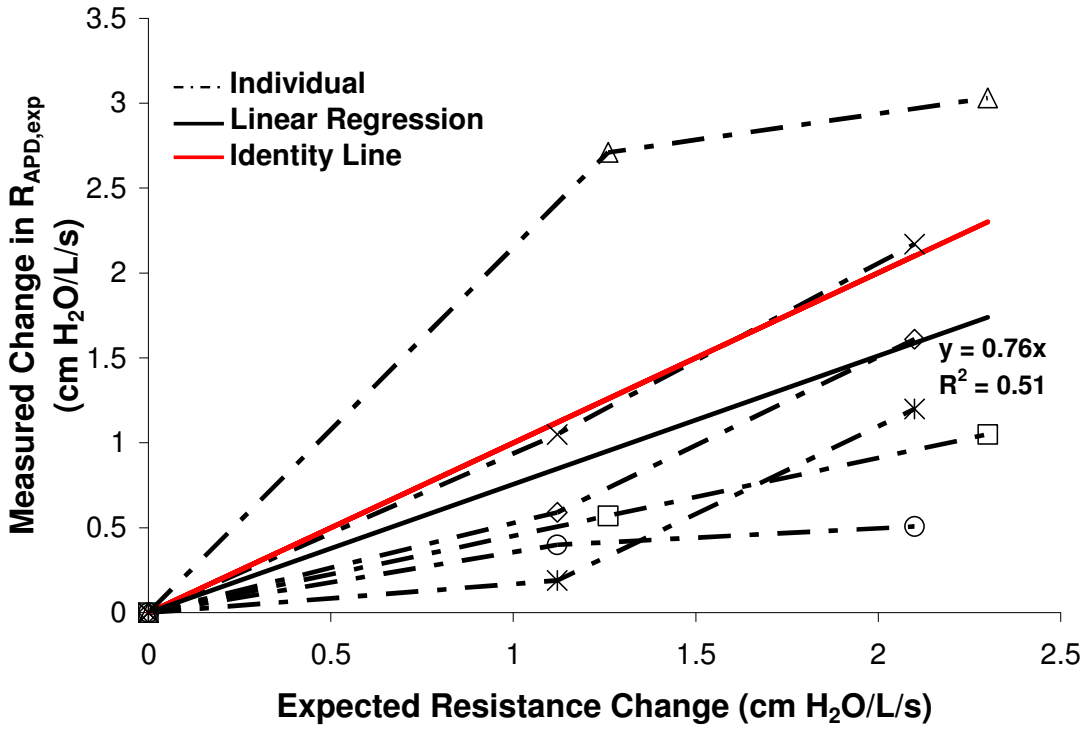

Figure 48: Measured change in exhalation APD resistance with added resistance. Dashed lines connect the data from an individual subject. Linear regression is drawn with all data.

Additionally, the comparison of measured change in $R_{APD,ins}$, measured change in $R_{L,ins}$, and added resistance showed that only added resistance and measured change in $R_{L,ins}$ were significantly different (Table 10). When exhalation resistances were compared, there were no significant differences (Table 11).

Table 10: Table showing whether or not there were any significant differences between the change in inhalation APD resistance, pulmonary resistance, and added resistance when external low and high resistances were added during tidal breathing. Note that statistics were calculated with t-test for unequal variances at $\alpha = 0.05$.

	Significant Difference (Yes/No)	
	Low Resistance	*High Resistance*
$\Delta R_{APD,ins}$ *vs.* $\Delta R_{L,ins}$	No	No
Added Resistance vs. $\Delta R_{APD,ins}$	No	No
Added Resistance vs. $\Delta R_{L,ins}$	Yes	No

Table 11: Table showing whether or not there were any significant differences between the change in exhalation APD resistance, pulmonary resistance, and added resistance when external low and high resistances were added during tidal breathing. Note that statistics were calculated with t-test for unequal variances at $\alpha = 0.05$.

	Significant Difference (Yes/No)	
	Low Resistance	*High Resistance*
$\Delta R_{APD,exh}$ *vs.* $\Delta R_{L,exh}$	No	No
Added Resistance vs. $\Delta R_{APD,exh}$	No	No
Added Resistance vs. $\Delta R_{L,exh}$	No	No

When the difference between the APD resistance and pulmonary resistance for inhalation and exhalation were plotted against added resistance (Figure 49 and Figure 50), the difference between resistances decreased as the added resistance increased.

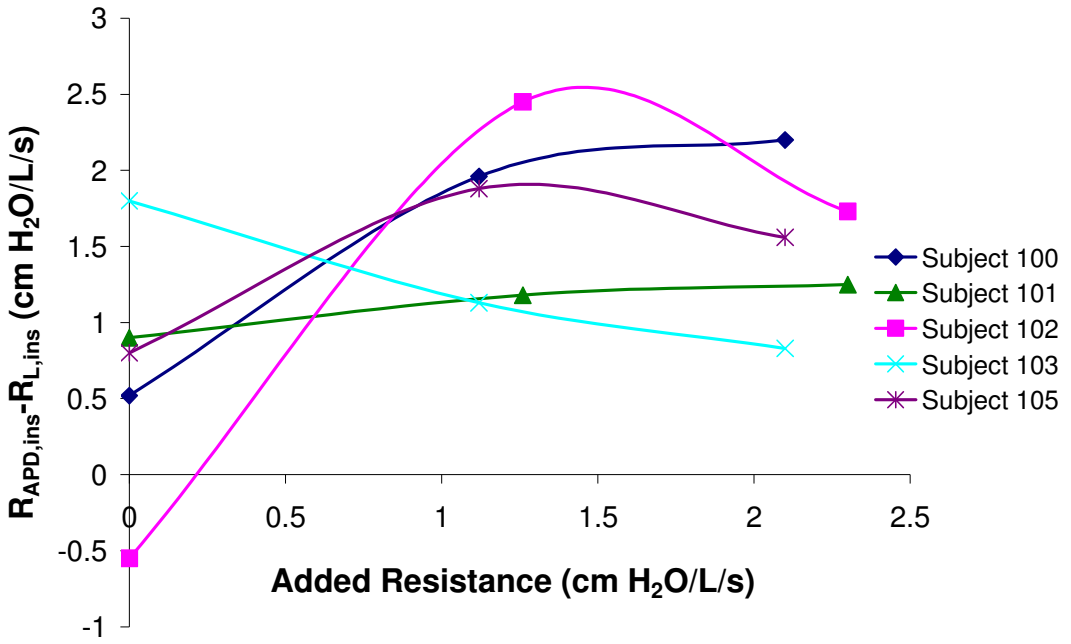

Figure 49: Added resistance versus the difference between $R_{APD,ins}$ and $R_{L,ins}$ for each subject.

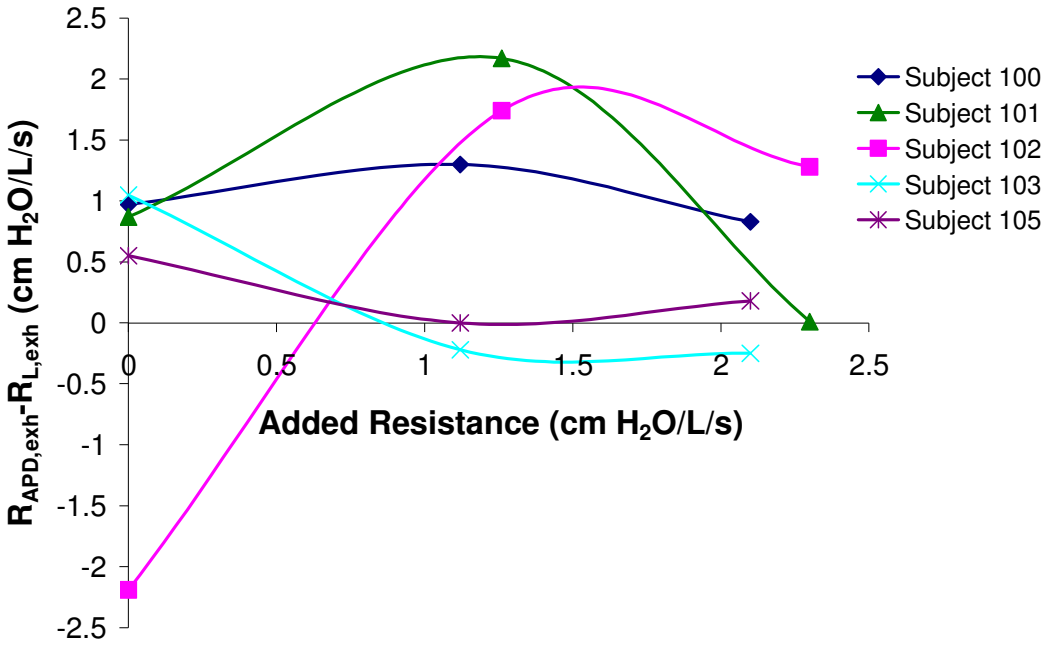

Figure 50: Added resistance versus the difference between $R_{APD,exh}$ and $R_{L,exh}$ for each subject.

5.1.3 High Respiratory Load only on Inhalation or Exhalation

When the high respiratory load was only on the inhalation side, the APD inspiratory resistance was more than the inspiratory pulmonary resistance for all subjects (Table 12). Additionally, when the high load was on the exhalation side only, five out of six subjects showed that the APD exhalation resistance was higher than the pulmonary exhalation resistance (Table 13). Figure 51 shows that having the high respiratory load only on the inhalation or exhalation side affected the measured APD resistance relative to pulmonary resistance similarly regardless of the load direction.

Table 12: Measured inspiratory (ins) and expiratory (exp) resistances and change in resistances with 5.81 cm H_2O/L/s added only on the inhalation side.

Subject No	$R_{APD,ins}$	$R_{L,ins}$	$R_{APD,exh}$	$R_{L,exh}$	$\Delta R_{APD,ins}$	$\Delta R_{L,ins}$	$\Delta R_{APD,exh}$	$\Delta R_{L,exh}$
100	5.91	3.24	3.17	3.08	4.32	2.18	0.97	1.85
101	4.31	2.10	3.07	3.77	2.62	1.30	1.25	2.82
102	5.86	5.23	4.68	4.74	3.21	2.03	1.44	-0.69
103	6.40	5.52	5.27	5.54	2.82	3.76	1.91	3.23
104	7.23	NM	4.75	NM	3.65	NM	0.72	NM
105	4.59	3.70	4.37	3.52	2.39	2.29	2.06	1.76

R_{APD}: APD resistance; R_L: Pulmonary resistance; ΔR: Change in measured resistance relative to baseline resistance; NM: Not Measured.

Table 13: Measured inspiratory (ins) and expiratory (exp) resistances and change in resistances with 5.81 cm H_2O/L/s added only on the exhalation side.

Subject No	$R_{APD,ins}$	$R_{L,ins}$	$R_{APD,exh}$	$R_{L,exh}$	$\Delta R_{APD,ins}$	$\Delta R_{L,ins}$	$\Delta R_{APD,exh}$	$\Delta R_{L,exh}$
100	3.68	1.60	5.66	4.58	2.10	0.54	3.46	3.34
101	2.64	3.06	4.53	3.53	0.94	2.26	2.71	2.58
102	5.09	3.31	6.62	7.25	2.45	0.12	3.38	1.83
103	4.67	4.31	6.56	7.30	1.10	2.54	3.20	5.00
105	3.45	3.38	4.79	3.65	1.24	1.97	2.48	1.89

R_{APD}: APD resistance; R_L: Pulmonary resistance; ΔR: Change in measured resistance relative to baseline resistance.

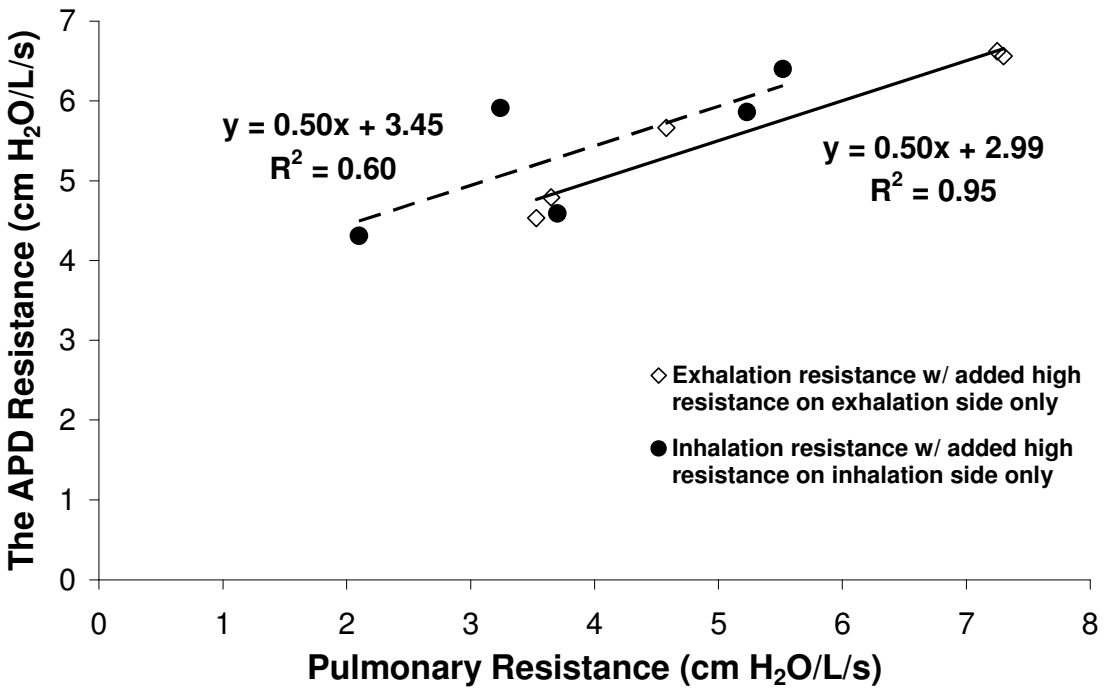

Figure 51: Inspiratory and expiratory resistances of all subjects with one way valve. Solid circles: Inhalation pulmonary and the APD resistances. Open diamond: Exhalation pulmonary and the APD resistances.

Figure 52 shows the mean change with standard deviation in the APD and pulmonary inspiratory and expiratory resistances. When the high respiratory load was applied only on the inhalation side, there was significant difference between the change in inspiratory and expiratory APD resistances and these changes were 3.17 ± 0.72 cm H_2O/L/s (55 % of the added resistance) and 1.39 ± 0.52 cm H_2O/L/s, respectively. Additionally, the average change in inhalation pulmonary resistance was 2.31 ± 0.90 cm H_2O/L/s (40 % of the added resistance), and the change in expiratory pulmonary resistance was 1.79 ± 1.52 cm H_2O/L/s. Again, there was significant difference between the change in inhalation and exhalation pulmonary resistances.

When the resistance was added only to the exhalation side, again, there was significant difference between the change in APD expiratory and inspiratory

resistances. The average resistance change was 3.05 ± 0.43 cm H_2O/L/s (52 % of the added resistance) on the exhalation side and was 1.57 ± 0.67 cm H_2O/L/s on the inhalation side. Additionally, the average change in exhalation and inhalation pulmonary resistance was 2.93 ± 1.31 cm H_2O/L/s (50 % of the added resistance) and 1.49 ± 1.08 cm H_2O/L/s, respectively. There was no significant difference between the changes on the inhalation and exhalation side of pulmonary resistance.

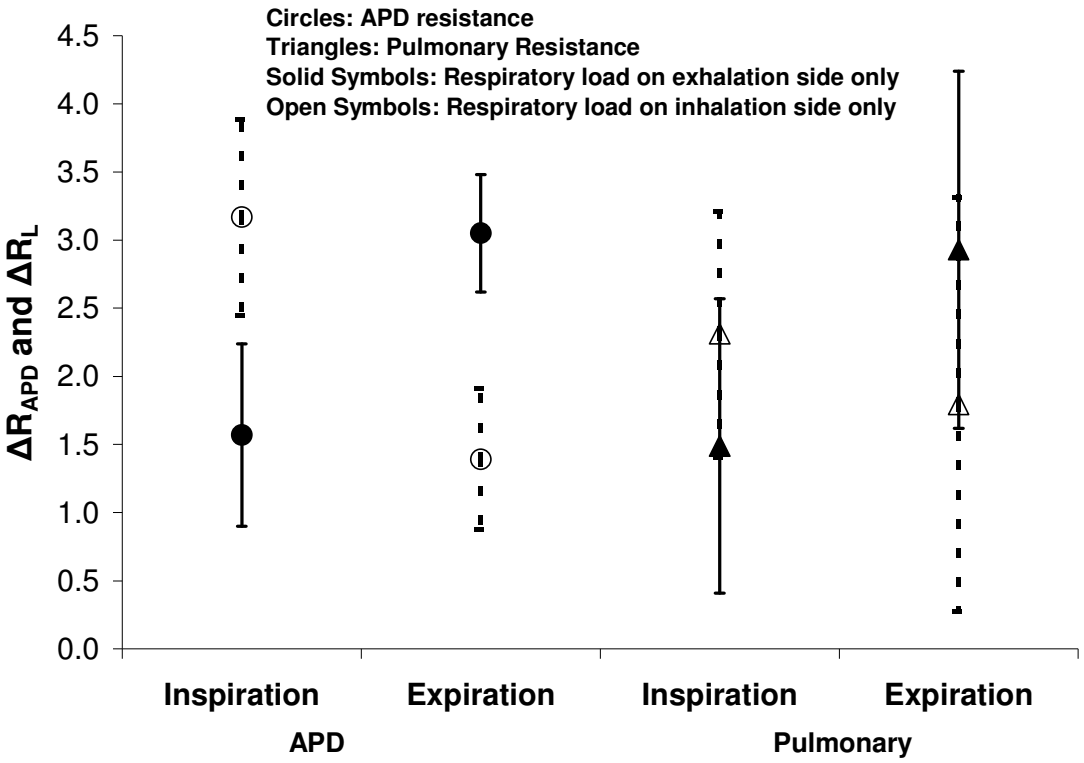

Figure 52: Mean change in inspiratory and expiratory resistances. The error bars show the standard deviation.

5.2 Discussion

The APD consistently showed an increase in resistance with added resistance during inhalation and exhalation. On the other hand, the pulmonary resistance did not show an increase in resistance with added resistance for all subjects. When the added high respiratory load was only on the inhalation or exhalation side, the APD and pulmonary resistances both showed a larger change on the side where the external resistance was added. However, the variance was less in the APD resistance prediction. Even though the APD resistance underestimated the added resistance, the measured change relative to the expected change was higher than the pulmonary resistance prediction of the added resistance. The underestimation of the added resistance by the APD could be due to loss of mouth pressure because of compliance of the airways in healthy subjects. All these experiments demonstrate the ability of the APD to detect small changes in upper airway resistance.

Lourens et al. (2001) studied the effect of a series of resistances on flow limitation in 18 mechanically ventilated COPD patients. The added external resistances increased the flow on iso-volume pressure – flow curves (IVPF) in six patients. They concluded that the resistances counteracted airways compression. A similar effect could explain why the change in exhalation APD resistance was less than the change in inhalation APD resistance (82 % of expected change vs. 76 % of expected change). The increase in mouth pressure with perturbations could be opening the compliant airways during exhalation.

The pulmonary resistance measurements were not as consistent as the APD resistance measurements with added external resistances. The change in pulmonary resistance could be affected by the change in lung volume, functional residual

capacity (FRC), flowrate at which the calculations are made, cardiac artifacts, the subject's ability to keep his glottis open and the ratio of subject's base intrinsic resistance to added resistance. Any of these possible causes might have resulted in inconsistent results.

When Kelsen et al. (1981) tested six normal subjects with external resistive loading ranging from 0.65 to 13.33 cm H_2O/L/s. They observed that with the addition of external resistances FRC increased, and inspiratory flow rate was reduced. The change in FRC means there would be a change in the lung compliance effect. This might increase the variance in pulmonary resistance measurements. Phagoo et al. (1995) compared the sensitivity and reliability of resistances measured with the esophageal balloon technique, body plethysmography, the forced oscillation method and the interrupter method in seven healthy subjects. The airway resistance measured with a body plethysmography showed a variation of 10 ± 3 %, while forced oscillation showed a variation of 10 ± 6 %. A variation of 11 ± 6 % was observed in the interrupter when the pressure occurring after 100 ms of interruption was used to calculate the resistance. Additionally, the esophageal balloon technique had a coefficient of variation of 15 ± 6 %. The variability was attributed to cardiac artifacts (i.e. noise from the heart beat) and change in elastic forces. In this study, cardiac artifacts were also visible in some subjects tested (Figure 53 versus Figure 54), and variation in pulmonary resistance measurements was higher compared to variation in the APD resistance prediction.

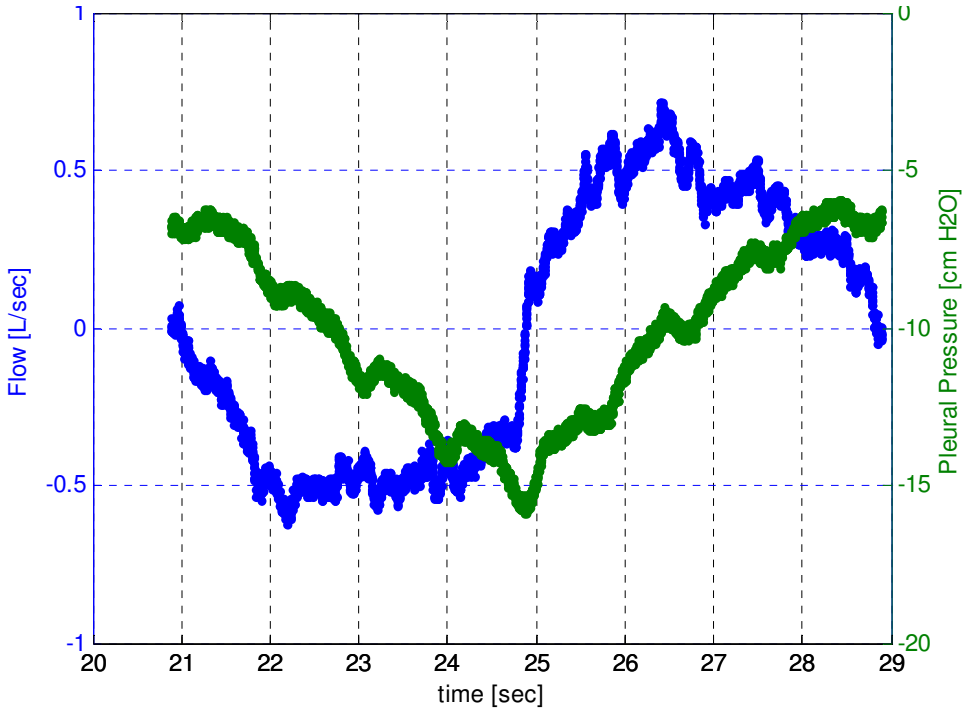

Figure 53: Flow (blue line) and pleural pressure (green line) recording of subject 101 during tidal breathing. The pleural pressure plot clearly shows variation assumed to be cardiac artifacts. Compare this to Figure 54.

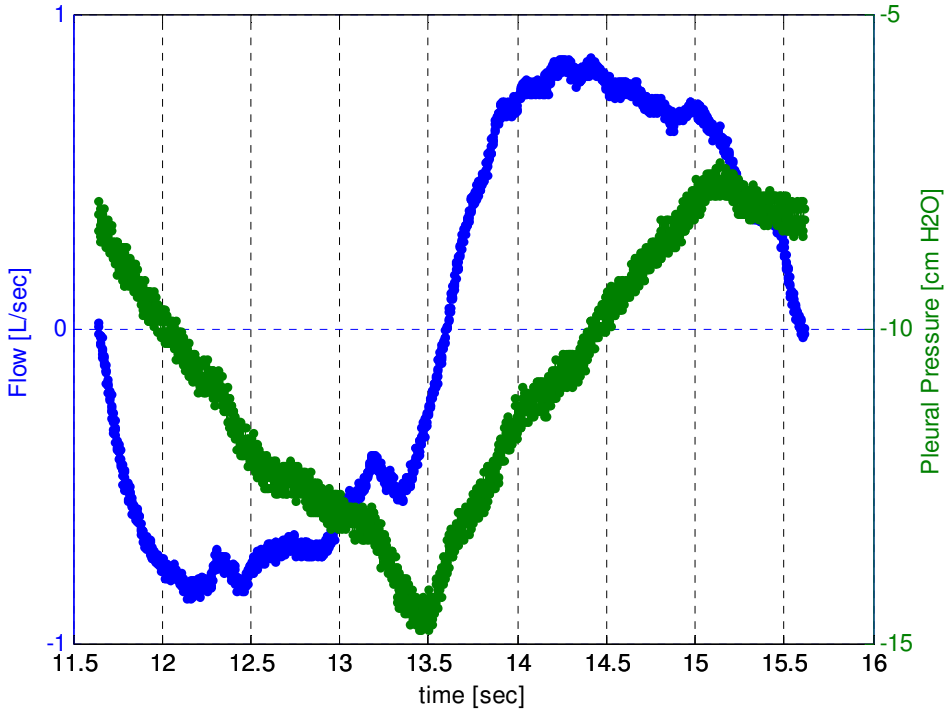

Figure 54: Flow (blue line) and pleural pressure (green line) recording of subject 100 during tidal breathing. Pleural pressure plot does not show any cardiac artifacts. Compare it to Figure 53.

The average pulmonary resistance is commonly used to identify respiratory problems since it does not require knowing the lung elastic recoil pressure and is calculated at isovolume points. Therefore, in addition to calculating separate inhalation and exhalation pulmonary resistances, in this study the average pulmonary resistance was also calculated. Measured average pulmonary resistance always showed an increase when the high resistance was added. But for the low added external resistances, the average pulmonary resistance of one subject decreased and that of another almost did not change. Mead et al. (1953) investigated the pulmonary resistance measurements after adding known flow resistance at the mouth in five healthy subjects. They reported the results in a pressure flow curve rather than giving the exact values of added resistance and the corresponding measured resistances. Their results showed an exact prediction of the added resistance by the pulmonary resistance. On the contrary, in this study, the pulmonary resistance underestimated the added resistance. Adding external resistances to the mouth imitates increasing the upper airway resistance. It is possible that the changes in the upper airway resistance were somehow compensated in the lower airways causing less of a change in the pulmonary resistance measurement. This could especially be observed with the addition of low external resistances. Even though with the addition of high external resistance pulmonary resistance increased, with addition of low resistances, measured pulmonary resistance decreased for some subjects.

When the measured APD resistance was compared to pulmonary resistance, no statistically valid difference was determined. Perhaps the number of subjects tested was too small to draw a conclusion regarding the significance of the differences, and

there was large variance in measurements. Additionally, the measured APD resistance was higher than the measured pulmonary resistance. This is again expected because the pulmonary resistance only includes the airway resistance and lung tissue resistance. On the other hand, it has been shown before that the APD perturbations travel further than the pleural space (Lausted et al., 1999 and Johnson et al., 2004). Lausted et al. (1999) observed the presence of observations on the chest wall. Additionally, when Johnson et al. (2004) used excised sheep lungs, the APD perturbations were observed in the respiratory chamber. These studies show that the APD measures more than pulmonary resistance.

In order to investigate further the observation of perturbations in the pleural space, an esophageal balloon was lowered into the esophagus of subjects and pleural pressure was recorded during tidal breathing when the APD wheel was rotating. The esophageal balloon catheter was a second order system with a flat frequency response up to 5 Hz (detailed explanation is given in Chapter 3), and the APD wheel was rotating at 10 Hz. Therefore, the perturbations of the pulmonary pressure could not be observed due to inadequate frequency response of the esophageal balloon catheter. Pleural pressure curves of subject 100 were compared when the APD was on and off during tidal breathing in Figure 55 and Figure 56. No perturbations are visible on the pleural space when the APD was on in Figure 56.

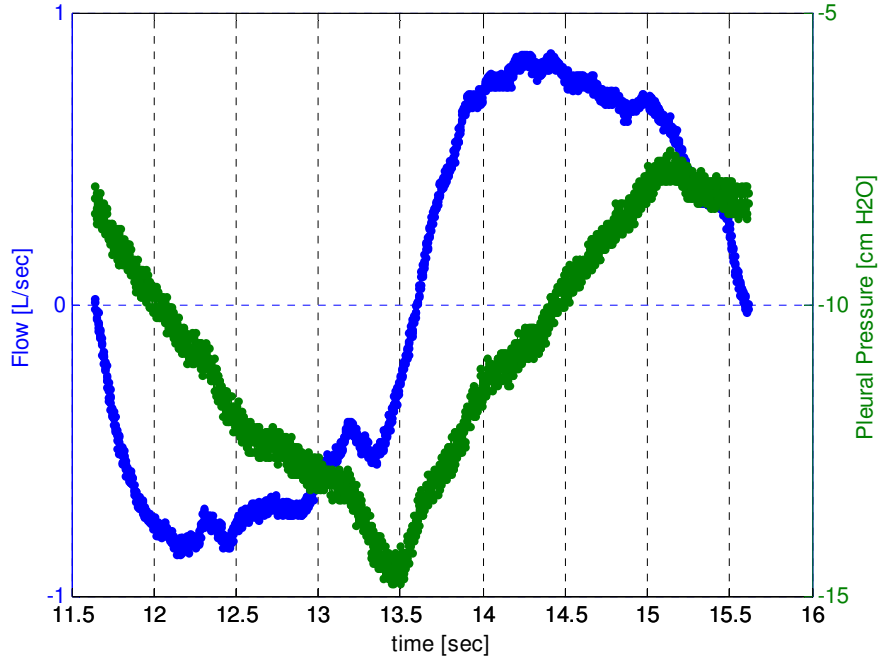

Figure 55: Pleural pressure (green line) and flow curve (blue line) of subject 100 during tidal breathing when the APD was off.

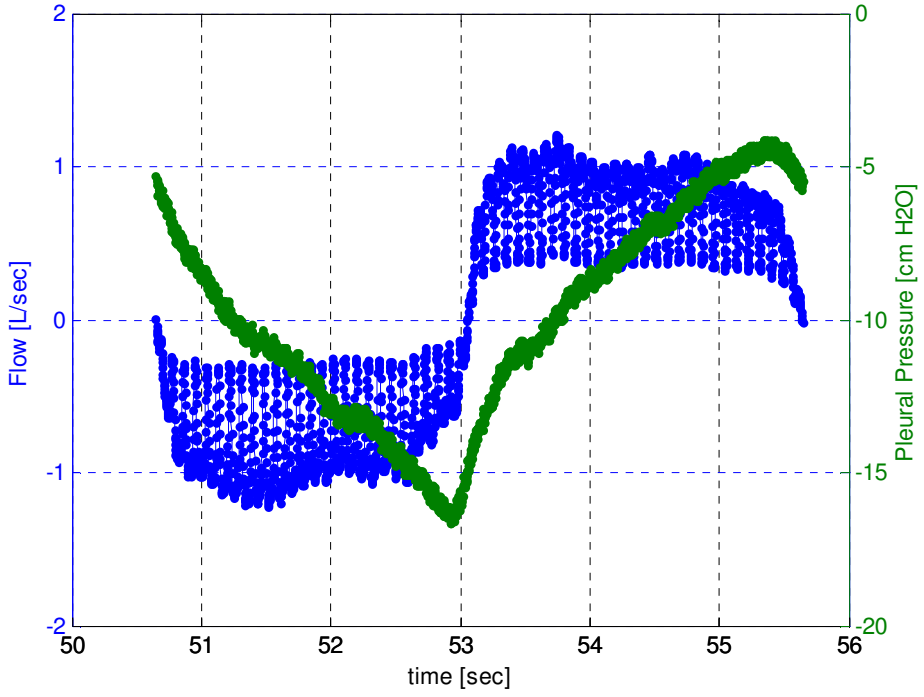

Figure 56: Pleural pressure (green line) and flow curve (blue line) of subject 100 when the APD was on. Note that pleural pressure curve is not any different than the curve in Figure 55. There are no identifiable perturbations in the pleural pressure curve.

5.3 Conclusion

Adding rigid external resistances during inhalation, exhalation and both inhalation and exhalation showed that the APD can reasonably measure added upper airway resistance, and the observations were as good as the pulmonary resistance measurements in healthy subjects. Further investigation is necessary with patients to finalize the ability of the APD to be used as an everyday diagnostic tool.

Chapter 6. Isovolume Pressure - Flow (IVPF) Curves

The IVPF curves were constructed with both the stop – flow and esophageal balloon methods at 25 %, 50 % and 75 % vital capacity (VC). Six subjects were tested with the esophageal balloon method, and five were tested with both methods. The subject is said to have reached limited flow if two straight lines could be fit through the data points as described in Chapter 4. The constructed curves and comparison of both methods are explained below. The detailed statistics are given in Appendix G, and all statistical calculations were made at $\alpha = 0.05$.

6.1 IVPF Curves

6.1.1 Stop – Flow Method

Mouth pressure vs. flow curves were constructed for all subjects at 25 %, 50 % and 75 %VC (Figure 57 through Figure 61). Subject 103 was the only one who had trouble keeping his mouth pressure at a constant value during shutter closing. He could not exert pressures higher than 35 cm H_2O. This made it challenging to get enough data points at different lung volumes. As seen from the figures, all five subjects tested reached the limited flow at 25 %VC. Four out of five subjects reached the limited flow at 50 %VC. At 75 %VC, only three subjects had a clearly identifiable curve that showed the flow limitation. At higher lung volumes (i.e. high vital capacity), larger pressures are required to reach the limited flow (Mead et al.,1967; Fry et al.,1960; Hyatt et al., 1958). Therefore, as lung volume increased, fewer subjects showed flow limitation.

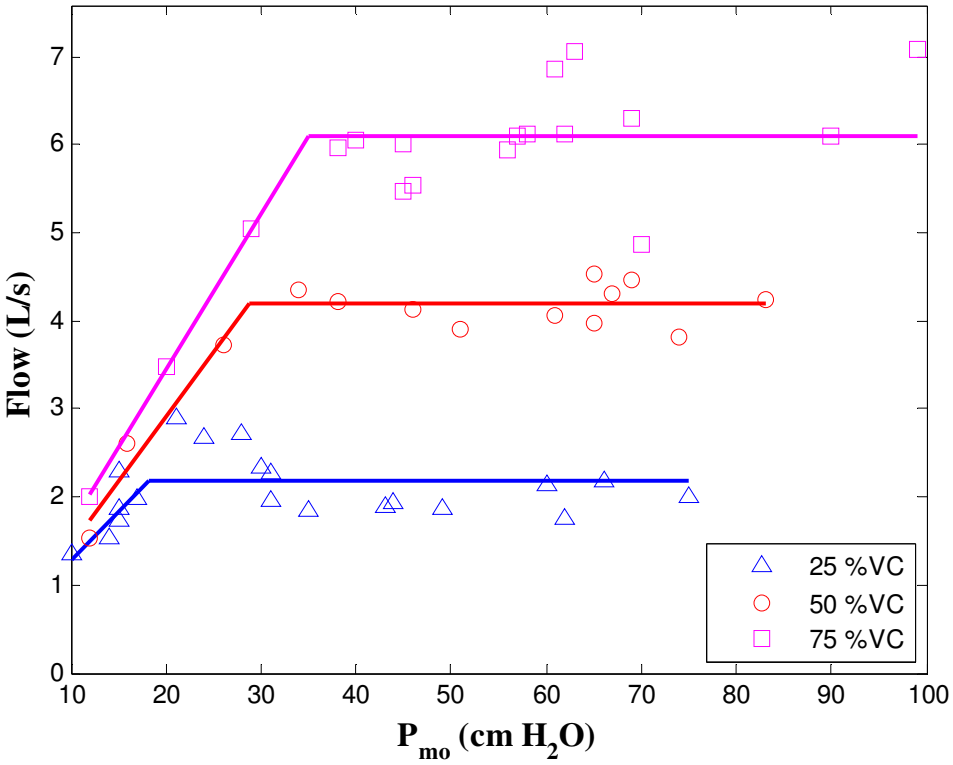

Figure 57: IVPF curves of subject 100 constructed with stop-flow method.

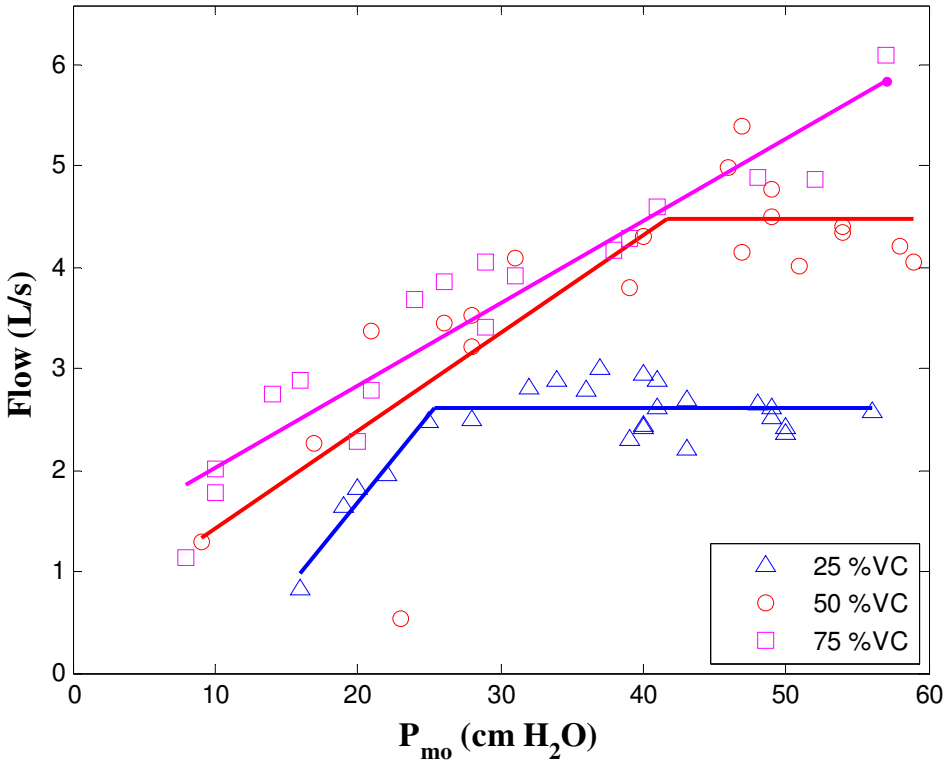

Figure 58: IVPF curves of subject 101 constructed with stop-flow method.

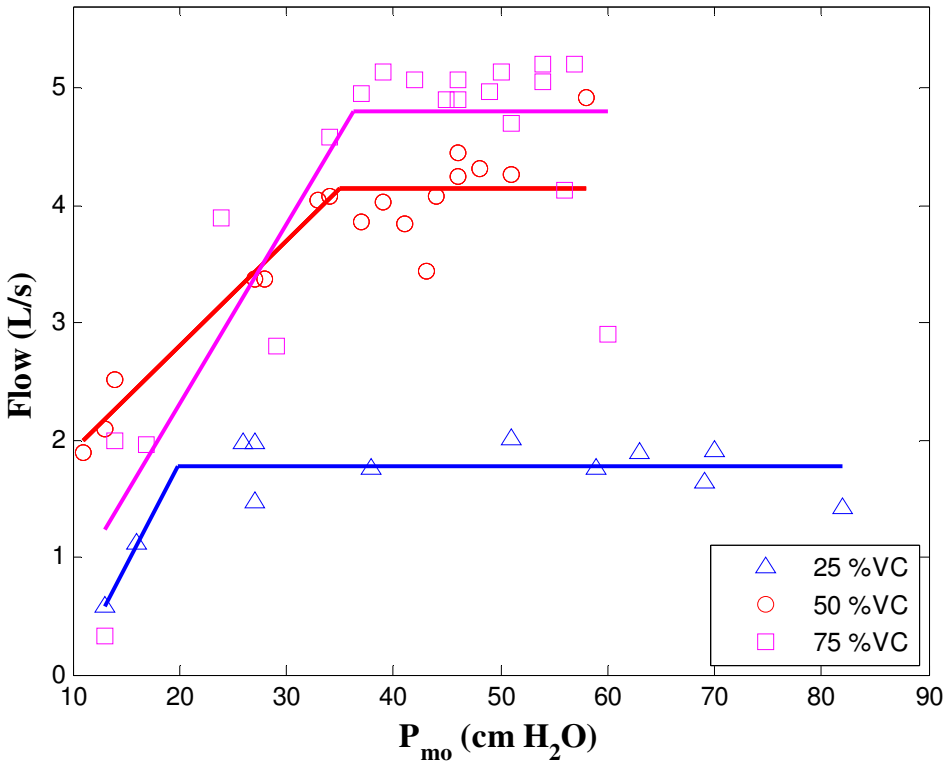

Figure 59: IVPF curves of subject 102 constructed with stop-flow method.

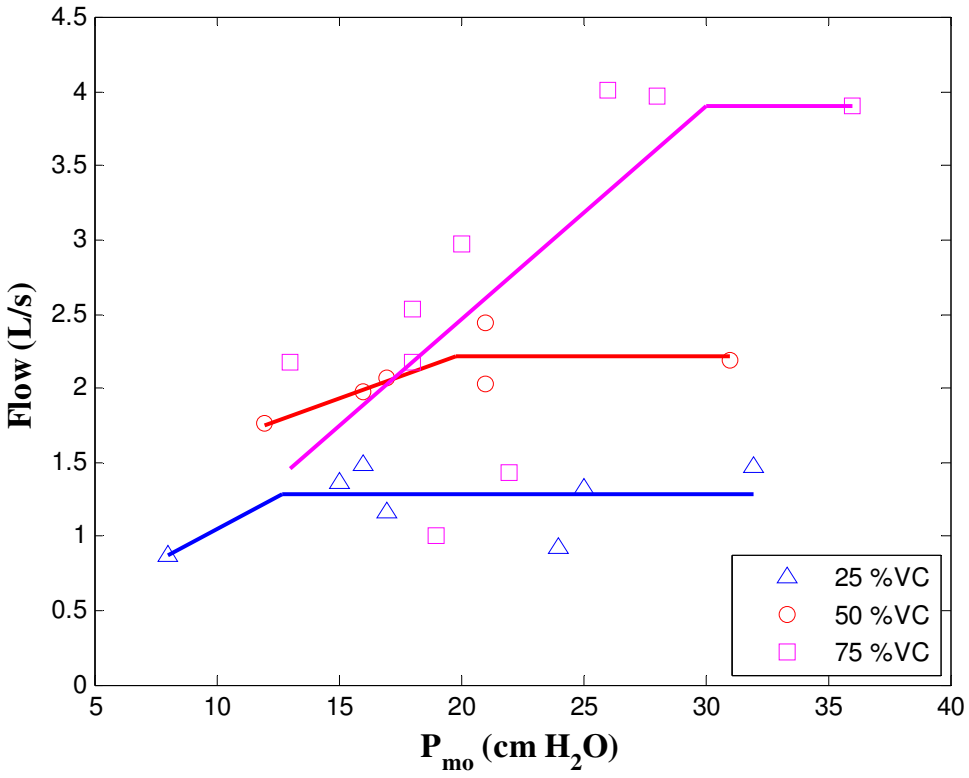

Figure 60: IVPF curves of subject 103 constructed with stop-flow method.

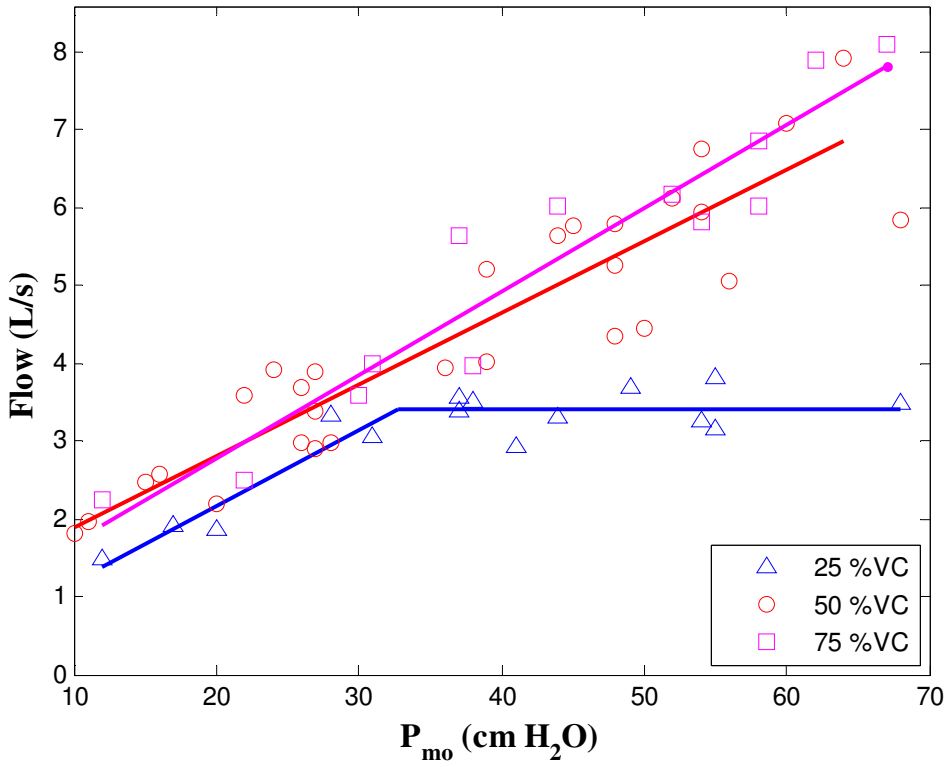

Figure 61: IVPF curves of subject 105 constructed with stop-flow method.

Table 14 summarizes the pressure and flow values at flow limitation for subjects who reached limited flow. The following observations can be made:

- As lung volume increased, so did the pressure, $P_{SF,max}$, at which flow became limited.
- As lung volume increased, one needed higher flows, $Q_{SF,max}$, to reach the flow limitation.

Similar observations about the IVPF curves have been reported before in various studies (Mead et al., 1967; Pride et al., 1967; Fry et al., 1960; Hyatt et al., 1958). Since the stop –flow method showed a similar trend with the pressure and flow values at flow limitation, it makes it more convincing the possibility of using the noninvasive the stop – flow method instead of an invasive esophageal balloon method to construct the IVPF curves.

Table 14: Pressure ($P_{SF,max}$) and flow ($Q_{SF,max}$) values at the point of flow limitation at different lung volumes for all subjects with the stop – flow method.

Subject No	Lung Volume (%VC)	$P_{SF,max}$ (cm H_2O)	$Q_{SF,max}$ (L/s)
100	25	18.1	2.2
	50	28.7	4.2
	75	35.1	6.1
101	25	25.4	2.6
	50	41.8	4.5
	75	No Flow Limitation	
102	25	19.9	1.8
	50	35.0	4.1
	75	36.3	4.8
103	25	12.7	1.3
	50	19.8	2.2
	75	30.0	3.9
105	25	32.7	3.4
	50	No Flow Limitation	
	75	No Flow Limitation	

The data in Table 14 were normalized for each subject by dividing the pressure and flow values at flow limitation by corresponding values at 50 % VC. Figure 62 shows that the relationship between the lung volume and the normalized pressure and flow were linear.

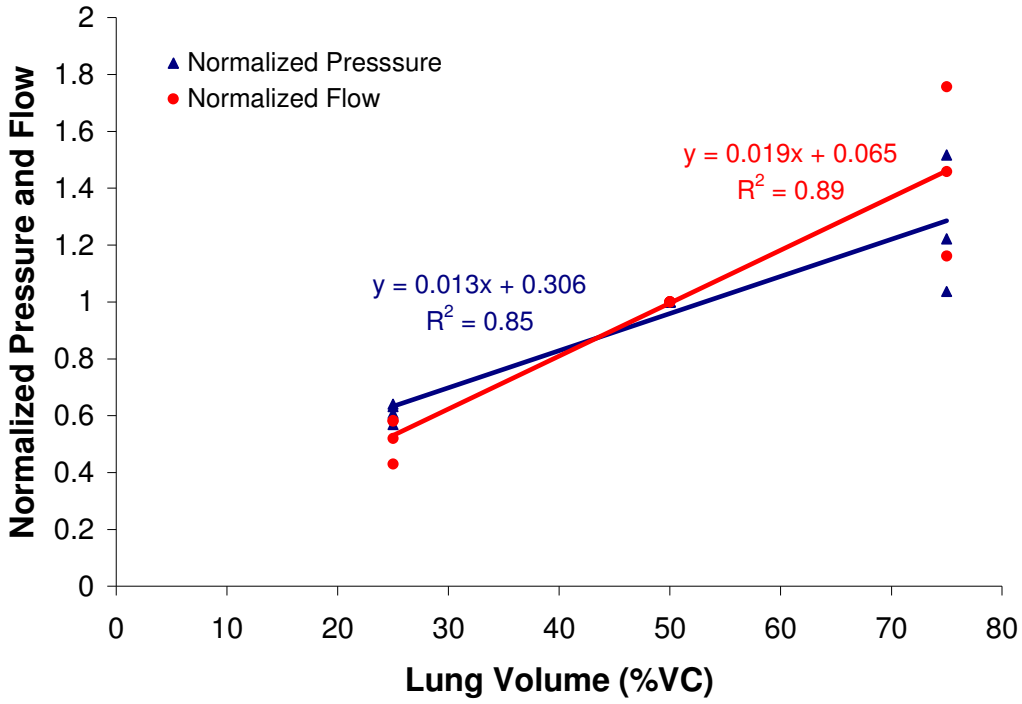

Figure 62: Normalized pressure and flow versus lung volume for stop - flow method.

6.1.2 Esophageal Balloon Method

Transpulmonary pressure (P_{tp}) versus flow curves at 25 %, 50 %, and 75 %VC were plotted for each subject (Figure 63-Figure 68). At 25 % and 50 %VC flow limitation was identifiable for all six subjects tested. At 75 %VC, only two subjects' IVPF curves showed the flow limitation. Again, as lung volume increased, there were fewer subjects with flow limitation because reaching the limiting flow at high lung volumes require greater efforts i.e. greater transpulmonary pressures. IVPF curves with the esophageal balloon were constructed by asking the subjects to exhale with different effort levels after a full inspiration. Even though a subject breathes out as hard as he can, it might not be enough to reach the conditions required for flow limitation.

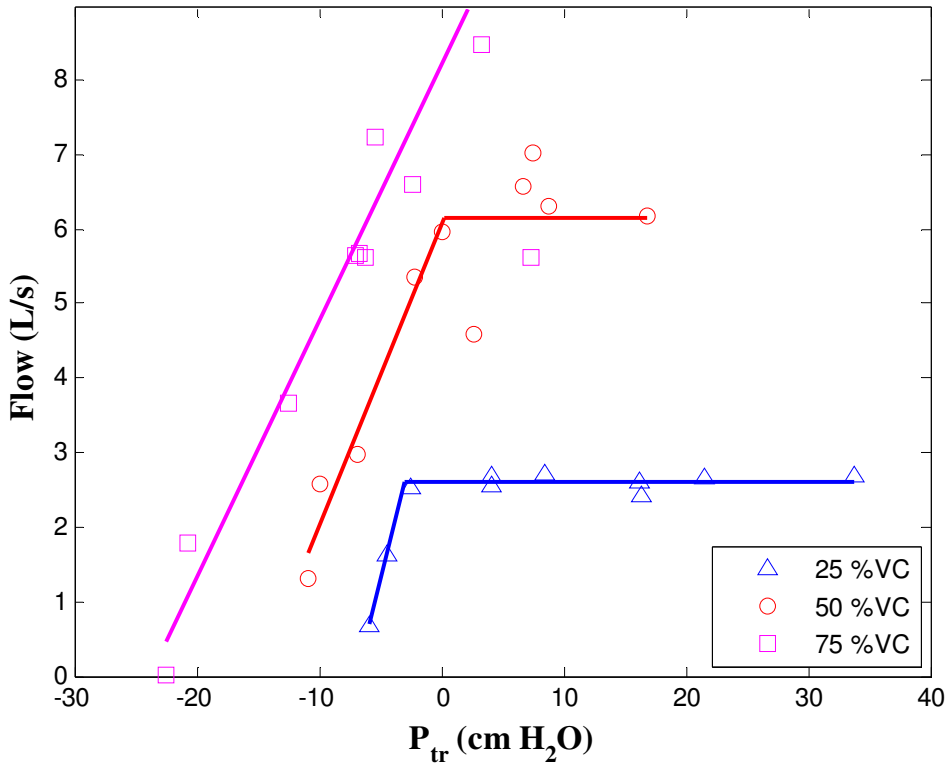

Figure 63: IVPF curve of subject 100 with the esophageal balloon method.

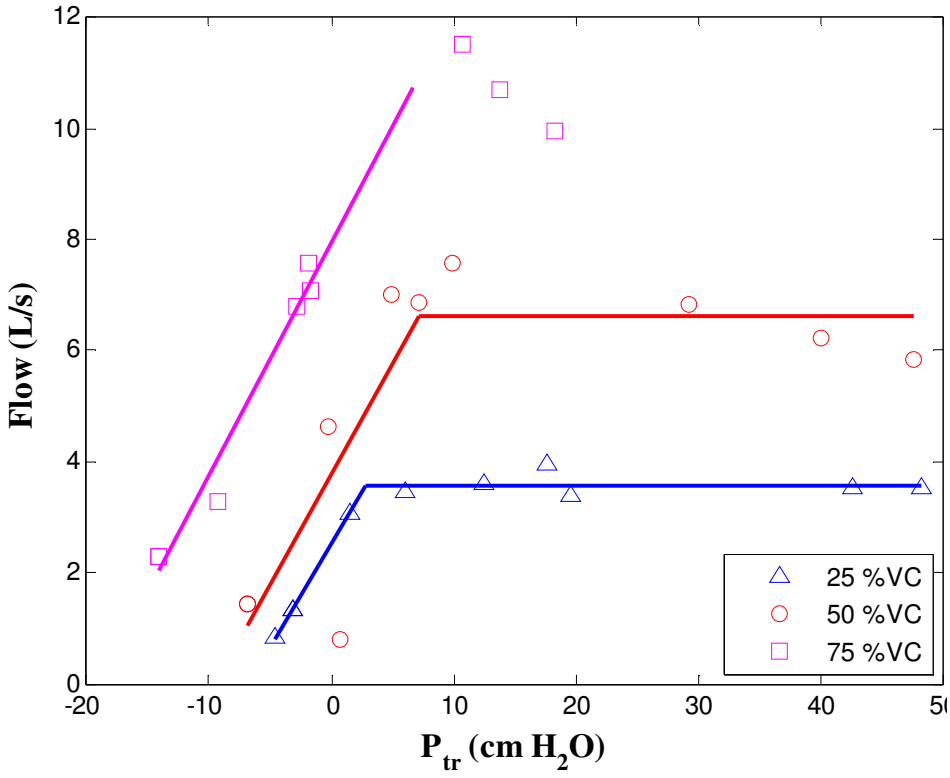

Figure 64: IVPF curve of subject 101 with the esophageal balloon method.

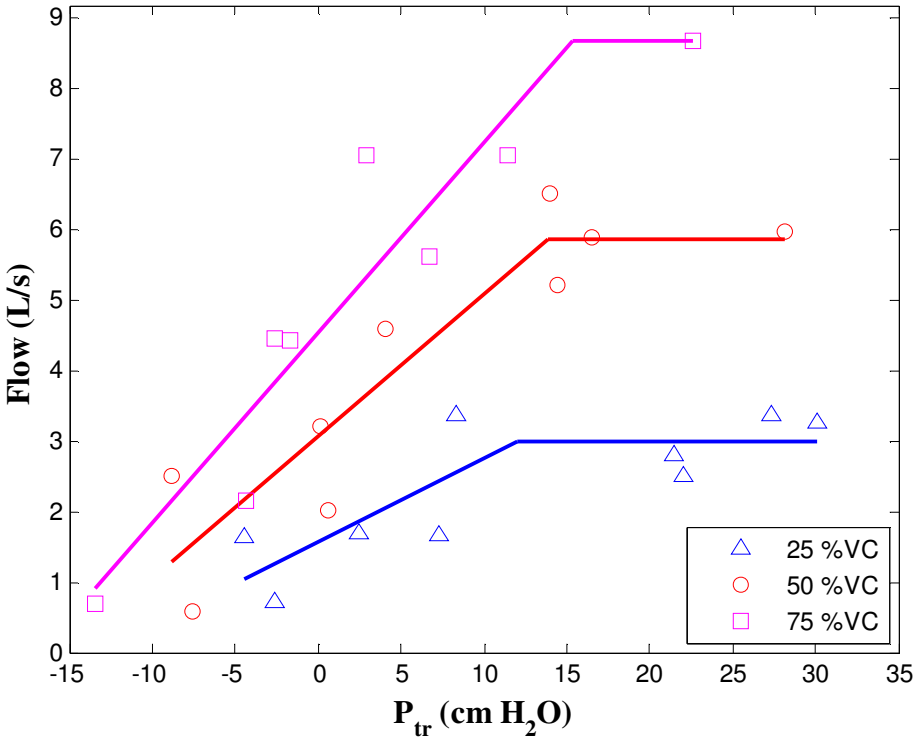

Figure 65: IVPF curve of subject 102 with the esophageal balloon method.

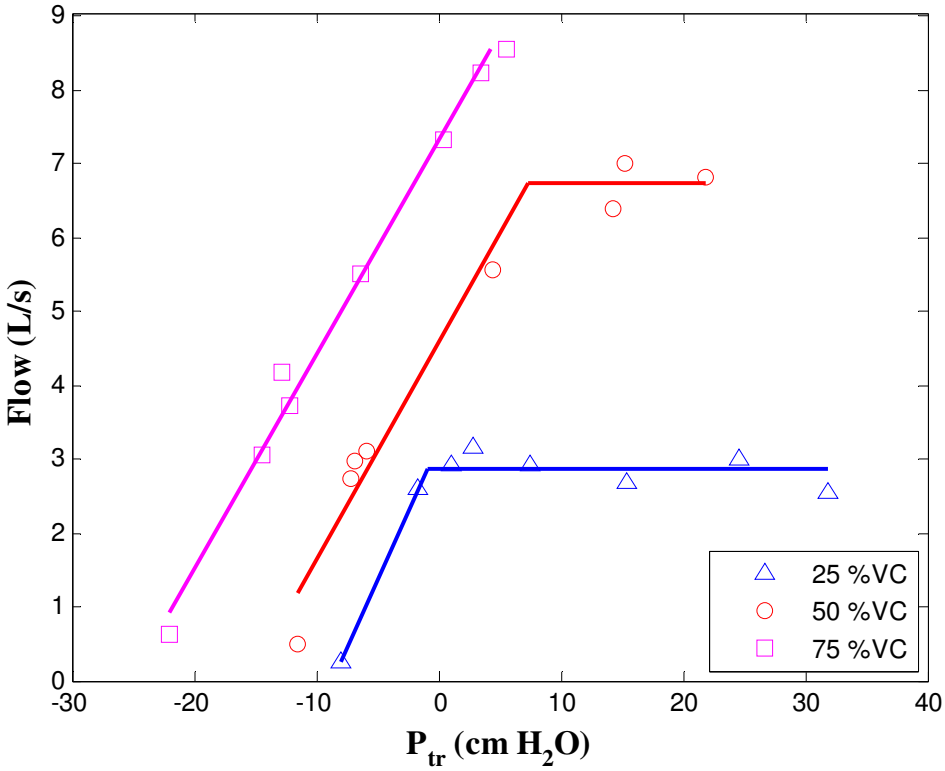

Figure 66: IVPF curve of subject 103 with the esophageal balloon method.

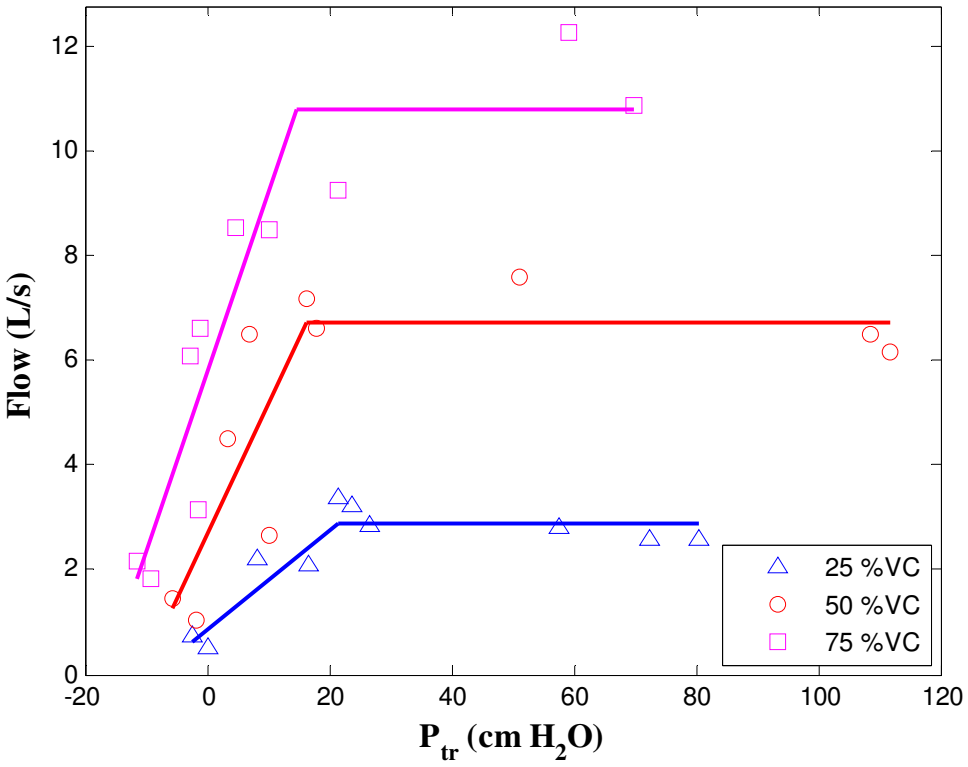

Figure 67: IVPF curve of subject 104 with the esophageal balloon method.

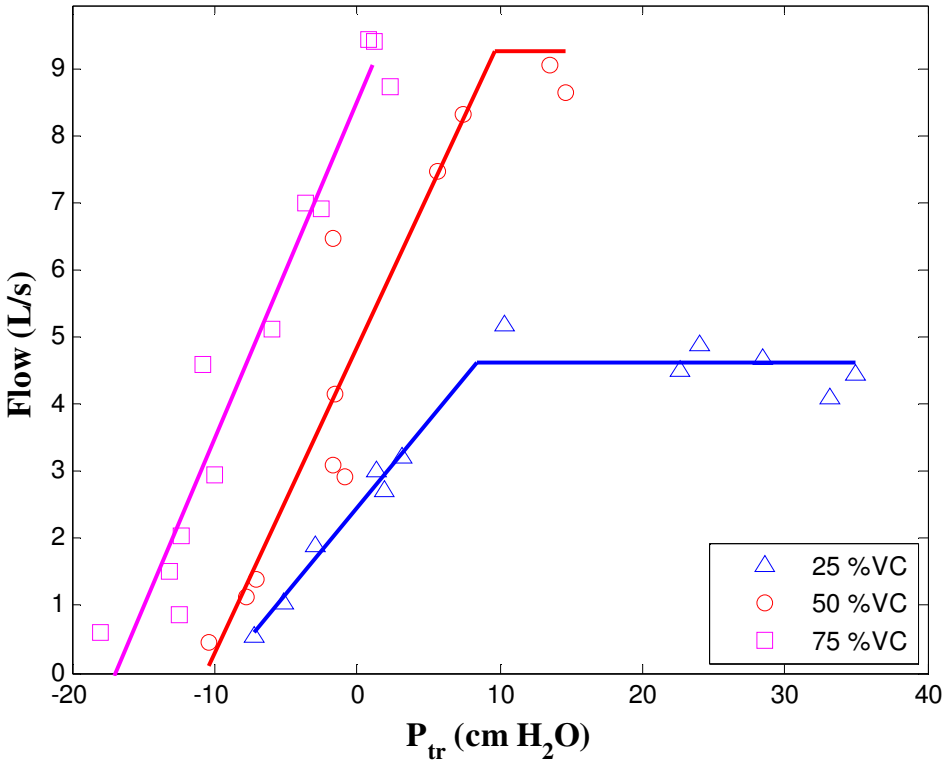

Figure 68: IVPF curve of subject 105 with the esophageal balloon method.

For all subjects except subject 104, as lung volume increased the pressure and flow at which the flow becomes limited was higher (Table 15). For subject 104, even though the flows were higher with increasing lung volume, the pressures decreased. The following observations can be made from Table 15 :

- As lung volume increased, so did the pressure, $P_{EB,max}$, at which flow became limited.
- As lung volume increased, one needed higher flows, $Q_{EB,max}$, to reach the flow limitation.

Both these observations were again as expected and the trend of pressure and flow with lung volume were the same as that of the stop – flow method. The pressure and flow were normalized as explained in section 6.1.1 (Figure 69). Even though the normalized flow versus lung volume values showed a linear trend, the normalized pressure values showed a poor correlation with lung volume. One reason was that subject 100 reached flow limitation at 50 % VC at very low pressure. Therefore, the normalized value at 25 % VC was very high. In Figure 69, this value, which is negative, stands out as an outlier. Additionally, at 25 % VC, the normalized pressure values were scattered with large variation for the rest of the subjects. These anomalies may be responsible for the poor fit between the normalized pressure and lung volume.

Table 15: Pressure ($P_{EB,max}$) and flow ($Q_{EB,max}$) values at the point of flow limitation at different lung volumes for all subjects with the esophageal balloon method.

Subject No	Lung Volume (%VC)	$P_{EB,max}$ (cm H_2O)	$Q_{EB,max}$ (L/s)
100	25	-2.9	2.6
	50	0.3	6.1
	75	No Flow Limitation	
101	25	2.9	3.6
	50	7.2	6.6
	75	No Flow Limitation	
102	25	12.0	3.0
	50	13.9	5.9
	75	15.4	8.7
103	25	-1.0	2.9
	50	7.3	6.7
	75	No Flow Limitation	
104	25	21.6	2.9
	50	16.4	6.7
	75	14.5	10.8
105	25	8.4	4.6
	50	9.7	9.3
	75	No Flow Limitation	

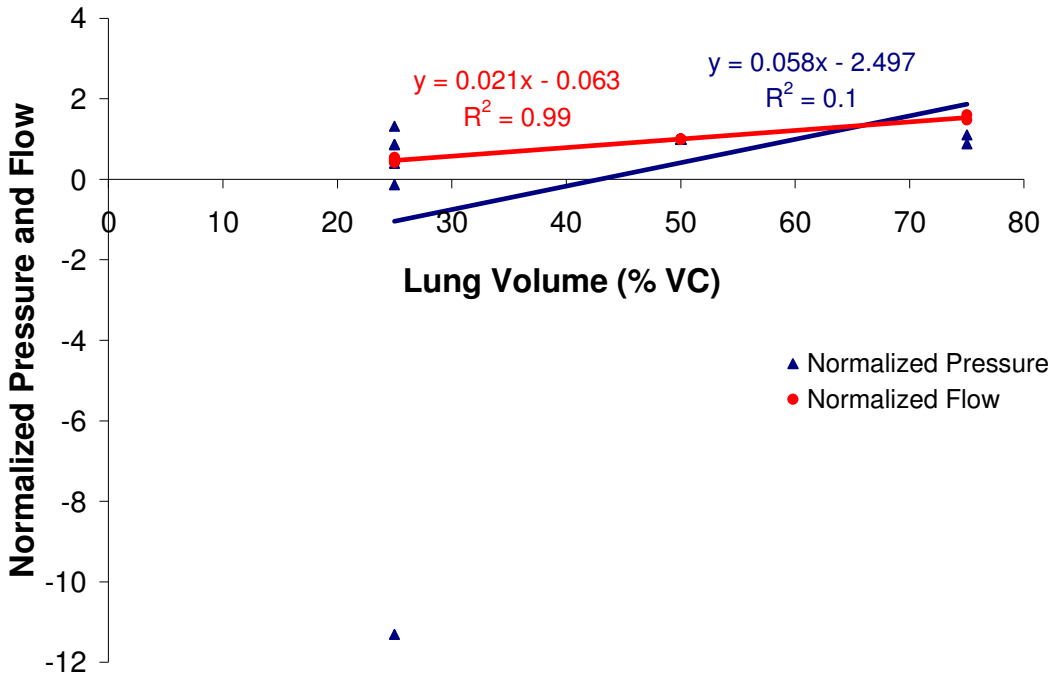

Figure 69: Normalized pressure and flow versus lung volume for the esophageal balloon method.

6.2 Comparing the two Methods

The IVPF curves for the two methods were compared at 25 % and 50 %VC, because flow limitations could be observed accurately with both methods at low lung volumes in four out of five subjects tested (Figure 70-Figure 78).

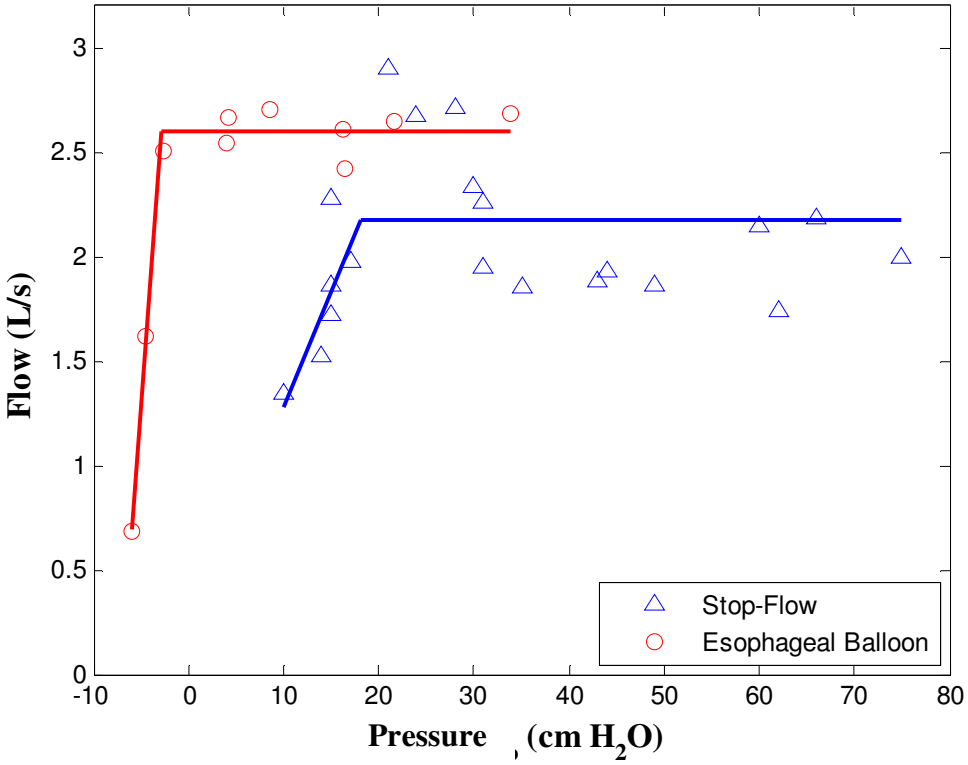

Figure 70: IVPF curve of subject 100 at 25 %VC with the stop – flow and esophageal balloon methods.

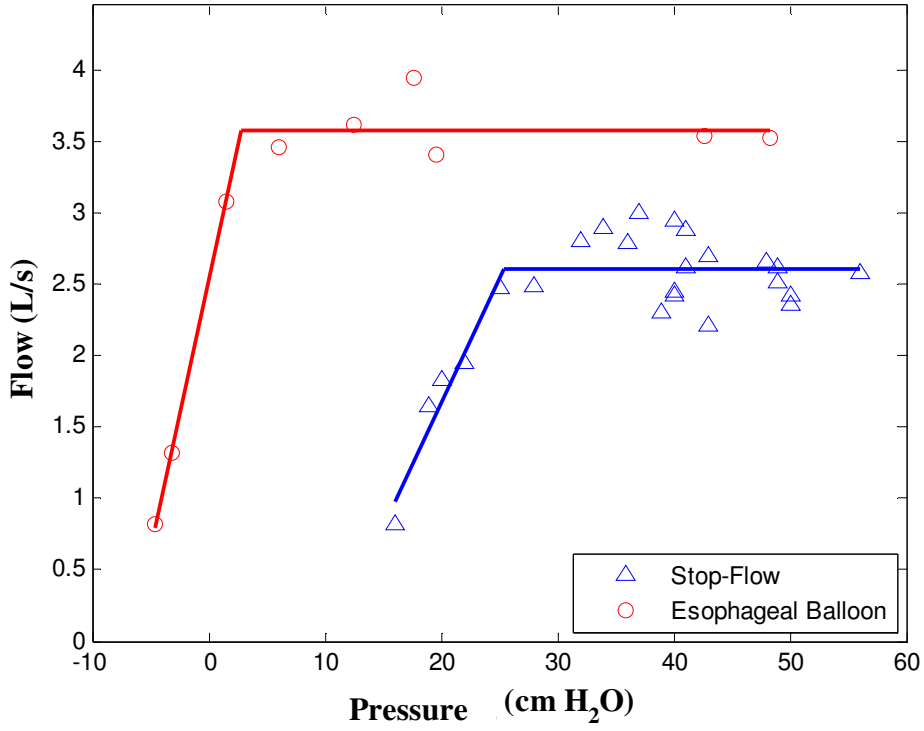

Figure 71: IVPF curve of subject 101 at 25 %VC with the stop – flow and esophageal balloon methods.

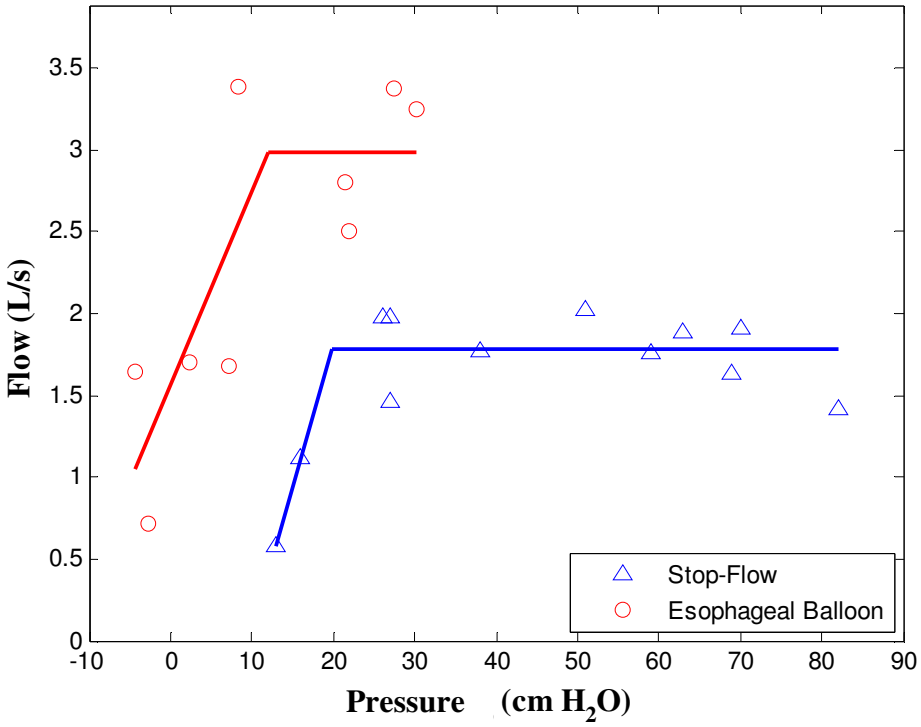

Figure 72: IVPF curve of subject 102 at 25 %VC with the stop – flow and esophageal balloon methods.

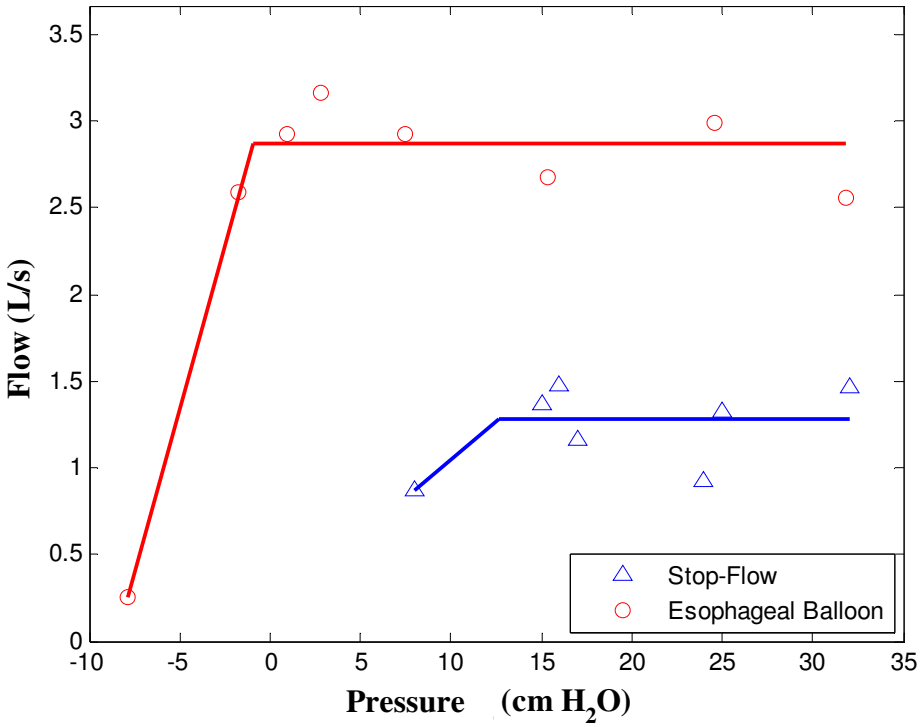

Figure 73: IVPF curve of subject 103 at 25 %VC with the stop – flow and esophageal balloon

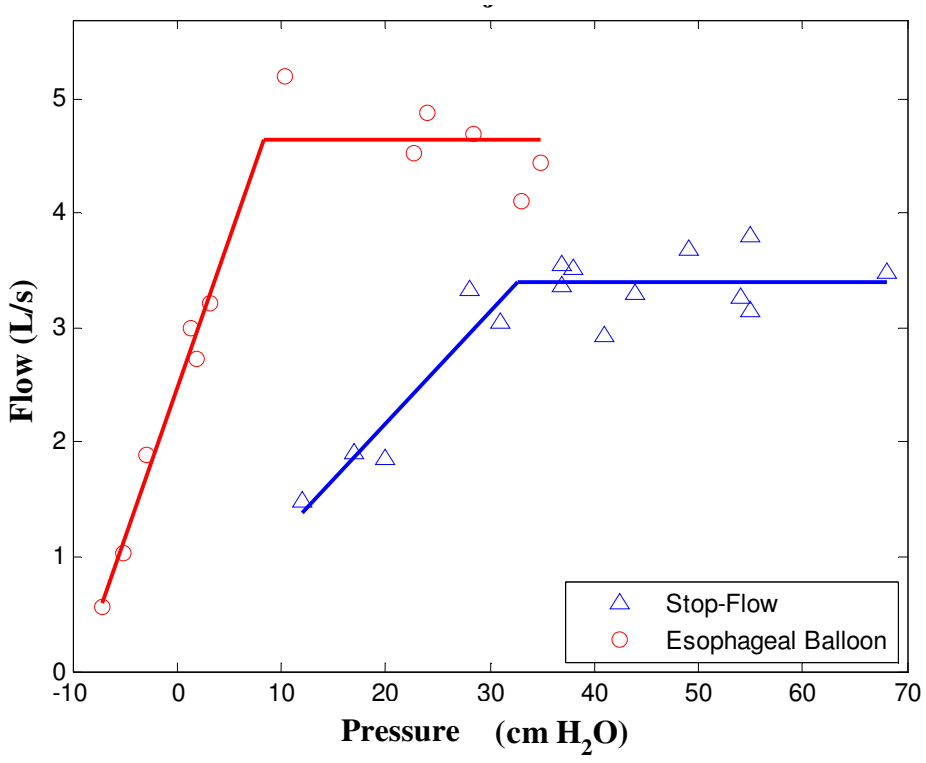

Figure 74: IVPF curve of subject 105 at 25 %VC with the stop – flow and esophageal balloon methods.

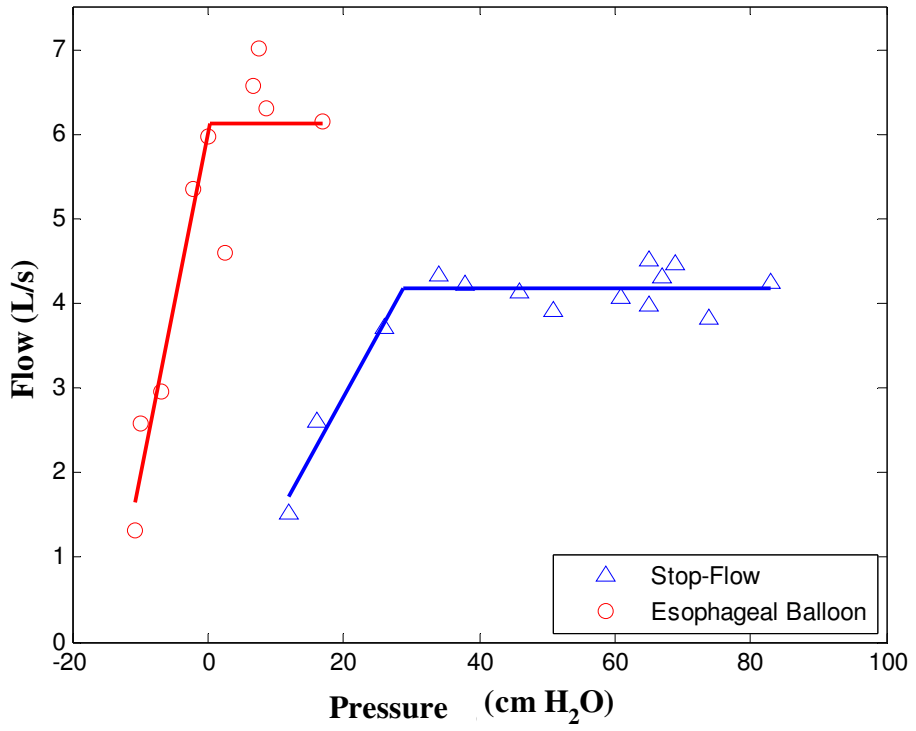

Figure 75: IVPF curve of subject 100 at 50 %VC with the stop – flow and esophageal balloon methods.

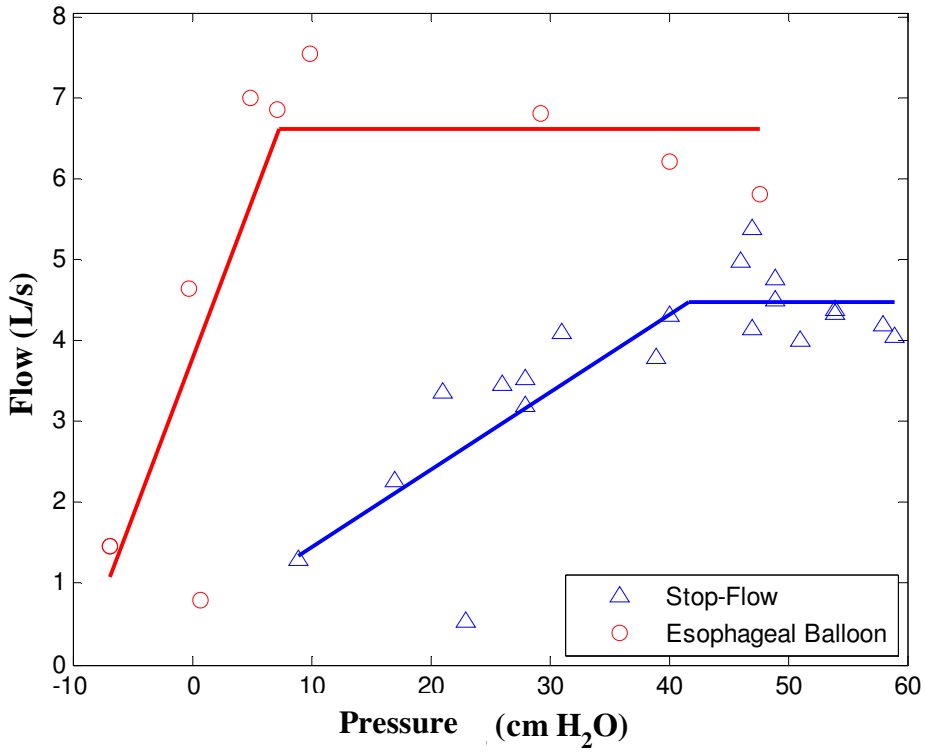

Figure 76: IVPF curve of subject 101 at 50 %VC with the stop – flow and esophageal balloon methods.

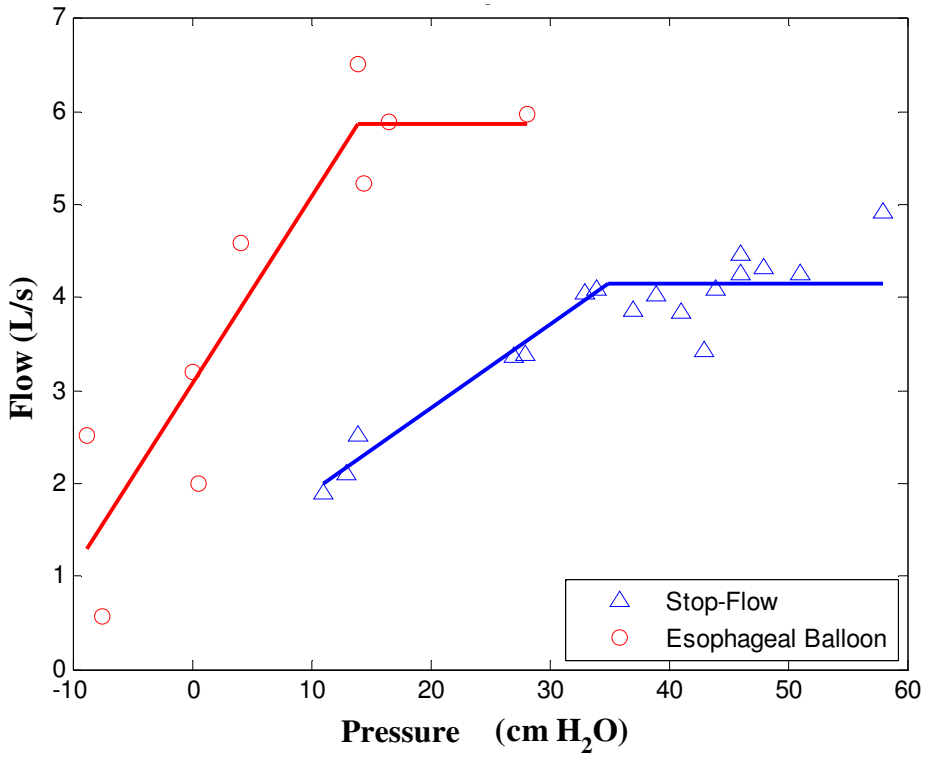

Figure 77: IVPF curve of subject 102 at 50 %VC with the stop – flow and esophageal balloon methods.

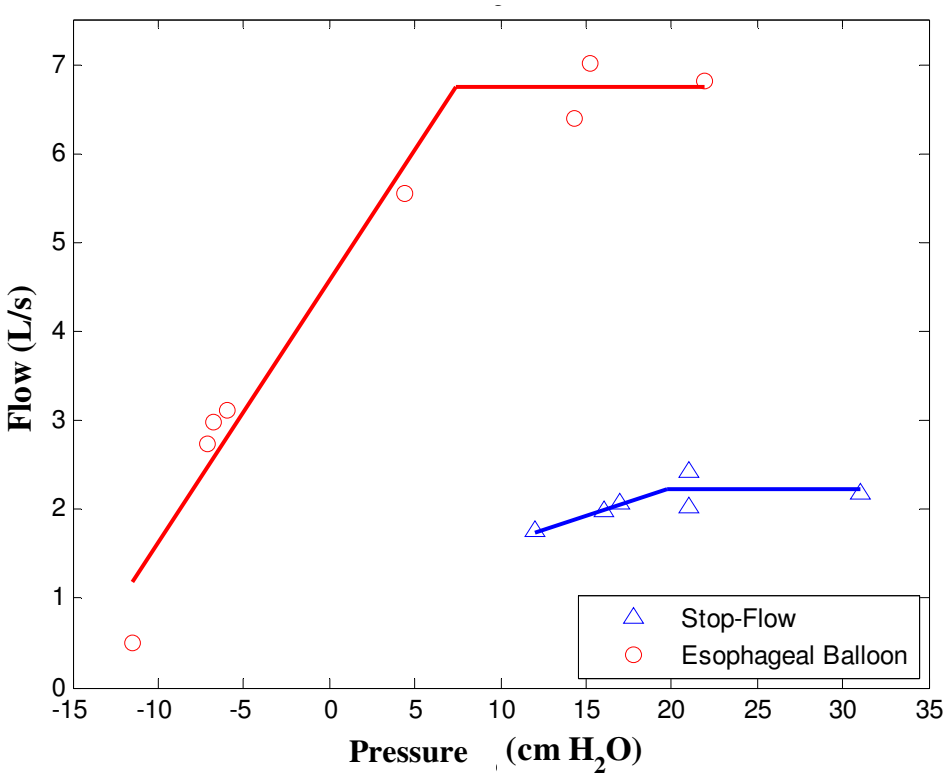

Figure 78: IVPF curve of subject 103 at 50 %VC with the stop – flow and esophageal balloon methods.

.

Table 16 and Table 17 show the pressure and flow values at the onset of flow limitation at 25 % and 50 %VC, respectively. From these tables, two observations can be made:

- $P_{SF,max}$ was always greater than $P_{EB,max}$
- $Q_{SF,max}$ was always lower than $Q_{EB,max}$

The Pearson correlation coefficient (Mendenhall et al., 1992) was calculated to investigate any possible correlation between two methods (Table 18). When $P_{SF,max}$ was compared to $P_{EB,max}$, the Pearson correlation coefficient was higher at 25 % than at 50%. Therefore, there may be a stronger correlation at 25 %VC. When $Q_{SF,max}$ was compared to $Q_{EB,max}$, the correlation coefficient was close in value at 25 % and 50 %VC. However, even though the coefficient was positive at 25 % VC, it was negative

at 50 %VC. Negative coefficient reflects the possible inverse linear relationship between $Q_{SF,max}$ and $Q_{EB,max}$. Therefore, at 25 % VC as $Q_{SF,\ max}$ increased, $Q_{EB,max}$ also increased. On the other hand, at 50 %VC as $Q_{SF,max}$ increased, $Q_{EB,max}$ decreased.

It has been known that the flow limitation mechanisms differ at low and high lung volumes (Hyat et al. (1980), Wilson et al. (1980)). At low lung volumes, viscous effects dominate. On the other hand, at high lung volumes, flow limitation can be predicted with the wave speed theory (Elliott and Dawson (1977)). It is possible that the different trend seen at 25 % and 50 %VC between $Q_{SF,max}$ and $Q_{EB,\ max}$ is due to the difference in flow limitation mechanisms.

Table 16: Pressure (P) and flow (Q) values at the onset of flow limitation for stop - flow (SF) and esophageal balloon (EB) methods at 25 %VC.

Subject No	$P_{SF,max}$ (cm H_2O)	$P_{EB,max}$ (cm H_2O)	$Q_{SF,max}$ (L/s)	$Q_{EB,max}$ (L/s)
100	18.1	-2.9	2.2	2.6
101	25.4	2.9	2.6	3.6
102	19.9	12	1.8	2.9
103	12.7	-0.96	1.3	2.9
105	32.7	8.4	3.4	4.6

Table 17: Pressure (P) and flow (Q) values at the onset of flow limitation for stop - flow (SF) and esophageal balloon (EB) methods at 50 %VC.

Subject No	$P_{SF,max}$ (cm H_2O)	$P_{EB,max}$ (cm H_2O)	$Q_{SF,max}$ (L/s)	$Q_{EB,max}$ (L/s)
100	28.7	0.2	4.2	6.1
101	41.8	7.3	4.5	6.6
102	34.9	13.9	4.1	5.9
103	19.8	7.4	2.2	6.8

Table 18: Pearson correlation coefficient values.

	% VC	Pearson Correlation
$P_{SF,max}$ vs. $P_{EB,max}$	25	0.522
	50	0.262
$Q_{SF,max}$ vs. $Q_{EB,max}$	25	0.854
	50	-0.591

T-tests showed that there was a statistically significant difference between $P_{SF,max}$ and $P_{EB,max}$ at both 25 % and 50 %VC. This was expected since the two methods measure different pressures. $P_{SF,max}$ represents the mouth pressure, and therefore the alveolar pressure before the shutter opening. First, it can never be negative. Conversely, $P_{EB,max}$ represents the transpulmonary pressure (i.e. pleural pressure - mouth pressure) and could be negative.

The main assumption of the stop – flow method is that when the shutter is opened, the alveolar pressure remains the same during the transient time of flow settlement. Most likely the alveolar pressure decreases during this time. During the stop – flow experiments, the pressure before the shutter was correlated with the flow after shutter opening. If the alveolar pressure was changing after shutter opening, the flow after shutter opening might not correlate with the pressure before the shutter opening. If this is the case, the pressure would be overestimated. This would result in higher pressures at flow limitation. This effect was demonstrated by Pride et al., (1967) by measuring the change in alveolar pressure after shutter opening with an esophageal balloon. During the 30 ms of their transient time, the alveolar pressure fell 17 % and 19 % in the two subjects tested. They assumed the transient time was constant for all subjects tested and it was 30 ms. They did not test what happens to the alveolar pressure, if transient times were longer. Most likely, the fall in the alveolar

pressure would be more significant with longer transient region. In this study, the transient time ranged from 30 to 70 ms and varied from one subject to another.

Another significant observation was that the measured flow at flow limitation was lower with the stop – flow method, and the t-test showed that there was no significant difference between $Q_{SF,max}$ and $Q_{EB,max}$ at 25 % VC. On the other hand, $Q_{SF,max}$ were significantly lower than $Q_{EB,max}$ at 50 %VC. One reason why $Q_{SF,max}$ was lower might be due to the change in lung volume after the shutter opening. During the stop – flow method, the shutter was closed at a specified lung volume. When the shutter was opened, it was assumed that the lung volume did not change during the transient time. This assumption was tested by calculating the change in lung volume during the transient time with 15 trials and a single subject. The average change in VC (about 4900 ml) was 170 ± 51 ml. It was decided that the change in lung volume was not significant enough to cause a big difference between $Q_{SF,max}$ and $Q_{EB,max}$. Pride et al. (1967) also mentioned that the lung volume at the time of flow measurement was changing. They attributed this change to the high gas pressure in the lung during flow measurement and gas flowing out of the lung during the transient time.

6.3 Resistance Calculation at the Onset of Flow Limitation

The slope of the line that was drawn to the point of flow limitation was calculated for each subject for the IVPF curves constructed with stop – flow and esophageal balloon methods at 25 % and 50 %VC. The inverse of this slope was the resistance at flow limitation.

Additionally, the APD resistances at various lung volumes were calculated during forced breathing. Figure 79 shows the calculated APD resistance vs. percent vital capacity for one of the subjects tested. The known inverse relationship between resistance and lung volume (Briscoe et al. (1958) and Blide et al. (1964)) were also observed in Figure 79.

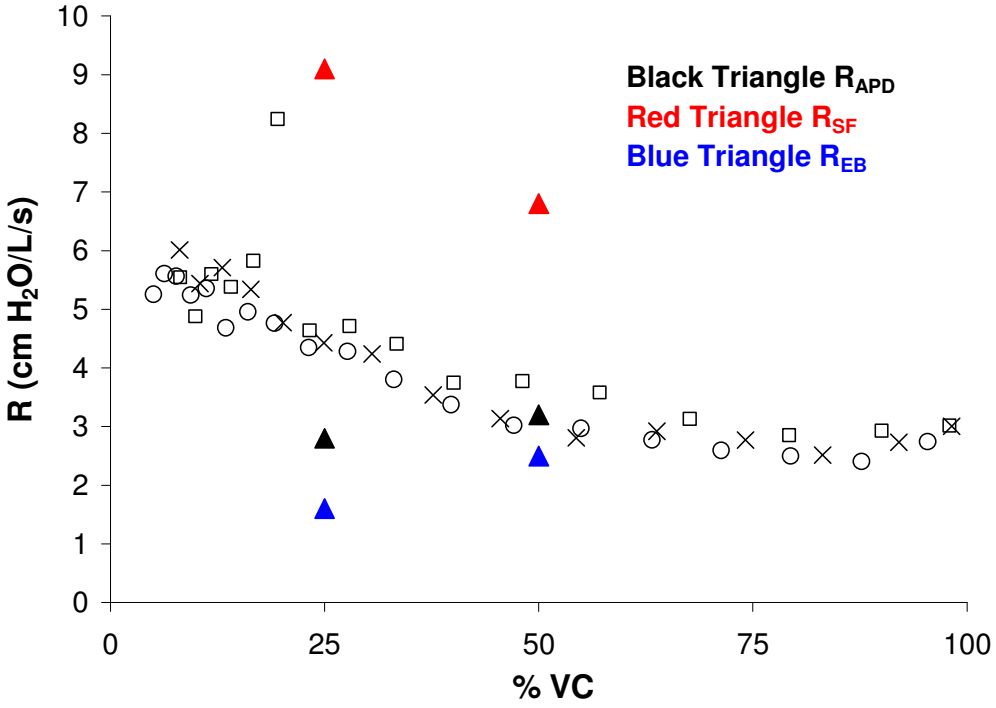

Figure 79: R_{APD} versus %VC for subject 100 for three different runs are represented by the open symbols. The esophageal balloon, stop –flow, and APD resistances are also plotted at 25 and 50 %VC, and are represented by solid symbols. 100 %VC corresponds to TLC.

The objective of this test was to observe the predictability of the resistance with the APD during forced breathing by comparing it to the resistance calculated with both the stop –flow and esophageal balloon methods. At 25 %VC, R_{SF} was higher than R_{EB} for three out of five subjects (Table 19). At 50 %VC, R_{SF} was higher than R_{EB} for all four subjects (Table 20). When R_{SF} was compared to R_{EB}, there was no significant difference between them at 25 %VC. However, at 50 %VC, they were

significantly different. When R_{APD} was compared to R_{SF}, at both 25 and 50 %VC, they were significantly different. Additionally, R_{APD} was compared to R_{EB}, and at both 25 and 50 %VC, there was no significant difference between them.

Table 19: The resistance values (cm H_2O/L/s) at the onset of flow limitation for stop - flow (SF), esophageal balloon (EB), and the APD methods at 25 %VC.

Subject No	R_{SF}	R_{EB}	R_{APD}
100	9.1	1.6	2.8
101	5.8	2.7	3.1
102	5.8	8.5	3.6
103	2.7	11.4	2.9
105	10.3	3.9	2.3

Table 20: The resistance values (cm H_2O/L/s) at the onset of flow limitation for stop - flow (SF), esophageal balloon (EB), and the APD methods at 50 %VC.

Subject No	R_{SF}	R_{EB}	R_{APD}
100	6.8	2.5	3.2
101	10.4	2.6	5.2
102	11.1	5	4.2
103	16.6	3.4	3.2

The Pearson correlation was also calculated to observe any possible correlation between the R_{APD}, R_{EB}, and R_{SF} (Table 21). The results showed that there was poor correlation between them.

Table 21: Pearson correlation coefficient at 25 and 50 %VC.

	% VC	Pearson Correlation
R_{APD} vs. R_{EB}	25	0.364
	50	0.023
R_{APD} vs. R_{SF}	25	-0.565
	50	-0.153

6.4 Discussion

Maximum expiratory flows have been used to diagnose various respiratory diseases since it was first constructed by Hyatt et al. (1958) and Fry et al. (1960). Isovolume pressure – flow curves could also be used for diagnostic purposes if it was as easy to construct as the maximum expiratory flow – volume curves. The classical method of constructing the IVPF curves is invasive and requires the use of an esophageal balloon. In this study, the IVPF curves were constructed with the classical method and the stop – flow method. Even though pressures and flows at the points of flow limitation were higher with increasing lung volume with both methods, there were differences between them. On average, $P_{SF,max}$ was 5.6 and 4.4 times $P_{EB,max}$ at 25 % and 50 %VC, respectively. $Q_{SF,max}$ was 0.68 and 0.59 times $Q_{EB,max}$ at 25 % and 50 %VC, respectively.

The prediction of the resistance during forced breathing was also investigated with the APD. The resistance with the stop – flow and esophageal balloon methods were compared to the resistance calculated with the APD during forced breathing. It was surprising that the APD even measured the resistance during forced breathing. In theory, one expects to see the APD resistance become infinite at the limited flow. The reason is that the APD measures resistance at any point by dividing the change in pressure by the change in flow (Figure 80). That is, the APD measures the instantaneous resistance. Therefore, at the limited flow, when further increase in pressure is not changing the flow any more (i.e., $\Delta\dot{V}$ ~0), $\Delta P/\Delta\dot{V}$ would become infinite.

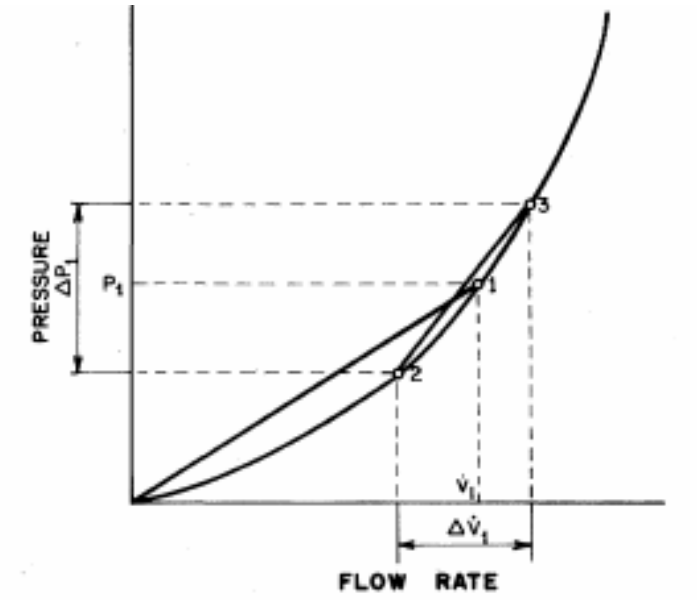

Figure 80: Comparison of different methods of measuring resistance. For example, the body plethysmograph measures airways resistance as $P_1/\dot{V}_1$. On the other hand the APD measures resistance at point 1 as $\Delta P_1/\Delta\dot{V}_1$ (Johnson et al., 1984).

After investigating further the theory behind the APD resistance calculation, an interesting observation was made. The APD resistance calculation works based on the fact that if the peaks of the flow perturbations were connected, the resulting curve (i.e. virtual flow curve) would give the flow that would have existed if the APD was not connected to the system. When the APD was used to find the resistance values during the forced vital capacity (FVC), it was observed that the virtual flow curve does not follow the real FVC curve that was recorded without the APD being connected to the mouth (Figure 81). In fact, the virtual FVC curve had higher flows. One explanation for these high flows is that during the forced breathing, the increase in pressures during the APD perturbations were opening the compressed airways. This preliminary observation needs further investigation to understand the resistance calculations during forced breathing with the APD.

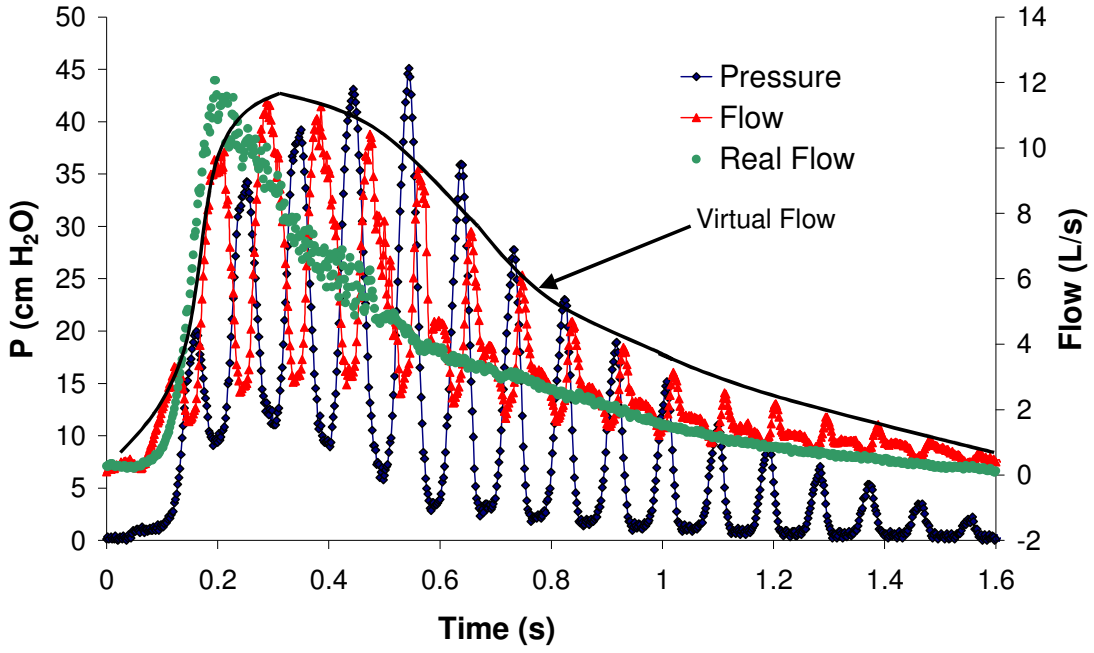

Figure 81: Pressure-Flow curve of a subject during forced breathing when the APD was connected to the mouth. The black line drawn by connecting the peaks of the flow is the virtual flow curve. This curve does not follow the real flow curve (green line) that was observed without the APD being connected to the mouth.

Chapter 7. Conclusion and Future Work

This dissertation was designed to characterize the Airflow Perturbation Device (APD) for resistance measurements. The resistance calculations with the esophageal balloon and the APD were experimentally investigated and compared. Furthermore, experimentally constructed flow limitation curves with the stop – flow and esophageal balloon methods were compared and analyzed.

7.1 Conclusion

1. The APD detects the small changes in upper airways resistance at least as well as classical measurements of pulmonary resistance.
2. When IVPF curves were constructed with the stop – flow method, pressures were overestimated and flow was underestimated. One needs to be aware of these effects if stop – flow is going to be used to assess the mechanics of the lung.
3. When the resistance at flow limitation was compared with the stop – flow, esophageal balloon, and the APD, there was no significant relationship between them. However, it may be that there were not enough data points to conclude a possible correlation due to variations inherent in these techniques.

7.2 Suggestions for Future Work

In this study, the detection of inspiratory and expiratory loads was investigated when various external loads were added to breathing. It has been shown that the ratio of added resistance to the background resistance plays a significant role

in the detection of external loads (Bennet et al. (1962), Wiley et al. (1966), Mahutte et al. (1983)). For future studies that will investigate external load detection, larger external resistances should be used as respiratory loads so that the ratio of added external resistance to the background resistance is larger. Therefore, the observed change in resistance would be larger.

In this research, only six subjects were tested. Therefore, it was challenging to generalize the results. Additionally, all subjects were healthy with no respiratory problems. Another study that compares the pulmonary resistance to the APD resistance in patients with respiratory problems would be useful to establish use of the APD as a diagnostic tool. When chronic patients such as COPD (chronic obstructive pulmonary disease) patients have flow limitation during tidal breathing, the pressure measured at the airway opening might not reflect the true back pressure. Therefore, the exhalation resistance might not be calculated correctly. Those patients might need a slower rotation of the wheel to reach the equilibrium between the mouthpiece and alveolar pressure. The adjustments necessary to measure the resistance with patients with the APD should be tested. Additionally, in this study, rigid external resistances were used to imitate the change in upper airway resistance. Patients with COPD or asthma have lower airway restrictions. Another controlled study that investigates the ability of the APD to detect the lower airway resistance would be useful.

In this research, the stop –flow method was used to construct the IVPF curves. No correlation was found between the stop –flow and the esophageal balloon methods. Perhaps, the variability inherent in these methods did not allow observing a possible correlation with a small number of subjects tested. Additionally, it is possible

that the IVPF curves constructed with both methods are fundamentally different. Another study that focuses more on the differences inherent in these methods could be useful.

Appendix A: Consent Form and Health Questionnaire

Initials _____Date_____

CONSENT FORM

The Relationship between Maximum Flowrate and Resistance
First revised on September 17, 2007
Second revision on February 8, 2008

I, _____, state that I am 18 years of age or older, in good physical health, and have no disease of the lungs or chest, and wish to participate in a research project being conducted by Arthur T. Johnson, Ph.D., and Derya Coursey, M.S., Steven M. Scharf, M.D, Ph.D., at the University of Maryland, College Park.

Purpose: This study has been designed to examine the relationship between lung pressure and maximum flow at various lung volumes. In this study, respiratory resistance, which shows the difficulty of breathing, will be measured with a breathing machine. Then, the relationship between measured resistance values and maximum flow will be investigated.

Methods and Procedures:

Orientation Session

This informed consent document, which describes the test procedures and methods, must be read and signed before participating in this investigation. An investigator will be present to review the informed consent document and to provide any answers to questions regarding this investigation. Next, you will be asked to complete the brief questionnaire, which is a medical history form designed to provide investigators with information regarding your present and past health status.

Please note that there is no financial compensation for completion of any of the exercise tests performed as part of this study and the results of the questionnaire may exclude you from further participation.

During the orientation session, the amount of air you could breathe out during a forced breath will be measured with a flow measuring setup. The test procedure will require you to be seated in front of flow measuring equipment with a mouthpiece attached to your mouth while wearing a nose clip. You will be instructed to breathe normally. When your breathing shows a constant level, you will be directed to breathe in as much as possible until your lungs are completely full and signal the technician. Then, you will blow out as much as possible to the point where your lungs are empty. The same test will be performed until the consecutive results do not differ from each other more than 5%, which might take up to five measurements.

Maximal lung capacity will be the last measurement determined during the orientation session. The test procedure will require you being seated in the constant volume chamber with a mouthpiece attached to your mouth while wearing a nose clip. Next, you will be instructed to take several normal breaths and to signal the technician following the completion of the breathing out of the last breath. At the completion, you will be required to perform a maximal breathing in or out maneuver while refraining from all body movements. Lung volumes are measured and recorded for both the maximal breathing in and out capacities. The same test will be repeated three times.

Test Session

The orientation session will take approximately thirty minutes. You will be scheduled a time after the orientation session. All measurements will be completed with two visits, which will take two hours and a half, and are performed using various breathing machines. It will take approximately three hours to finish all the required tests including the orientation session

During your first visit, the first measurement will be measuring lung pressures. The test procedure will require you be seated in front of a flow measuring set up with a mouthpiece attached to your mouth while wearing a nose clip. You will be instructed to take several normal breaths and to signal the technician after taking a full breath in. Then you will be instructed to slowly breathe out. Once you reach a predetermined lung volume, the mouthpiece will be closed with a shutter. Then, you will be instructed to make a steadily increasing effort to increase the pressure against the closed shutter until it reaches a preset value. Reaching the preset pressure should not take more than two seconds. At this point, the shutter will be opened and you will empty out your lungs. At each lung volume, pressure measurements will be obtained between 10 cm H_2O and 120 cm H_2O. The pressure just before the shutter opening is correlated with the flow just after shutter opening. You could be asked to repeat this procedure up to two times.

The second test of the session will be using one breathing machine to measure the resistance values that show the difficulty of breathing. You will be seated in front of the machine and bite a disposable mouthpiece. A nose clip will close your nose. You will be instructed to press your hands against your cheeks. The resistance is measured through the mouth. You will be instructed to take several normal breaths and to signal the technician following the completion of a full breath in. Then, you will breathe out with various effort levels until your lungs are empty. You might be asked to repeat the same procedure up to four times.

The last test of your first visit will be using one breathing machine to measure the resistance values that show the difficulty of breathing during regular breathing. You will be seated in front of the machine and bite a disposable mouthpiece. A nose clip will close your nose. You will be instructed to press your hands against your cheeks. The resistance is measured through the mouth. You will breathe regularly and after a minute the resistance values appear on the computer monitor. The same procedure will be performed three times.

During your second visit, the tests will require use of an esophageal balloon catheter to measure pressure surrounding the lung. It consists of a fine polyethylene tube (~ 1/32 inches in diameter) whose open end is covered by a very thin-walled air-containing balloon (~3 4/5 inches long and 2/5 inches wide). It is passed through the nose into the lower third of the esophagus. Very little air (less than 1/4 teaspoon of air) is put into the balloon. The catheter will be swallowed into the distal third of the esophagus as follows: less than 1/4 teaspoon of 1% lidocaine, which is a local anesthetic commonly used by dentists as a numbing medicine or agent, is injected into one of your nostrils using a syringe without a needle. You will be asked to sniff this

back. The balloon, with all air removed, is then inserted by an experienced operator to the back of the nose. You will be asked to drink water from a cup through a straw. The balloon is passed until the swallowing mechanism "catches" the balloon. The balloon is swallowed to 11 4/5 inches from the nostrils. Approximately 0.5 ml (0.017 ounce)-1ml (0.034 ounce) of air is injected into the balloon and the end of the catheter connected to a pressure gauge. The tests previously described will be repeated with the esophageal balloon catheter in place and additional measurements will be made through the catheter. Following measurements (a period of approximately 20 minutes), the balloon is removed.

Benefits: You will be entitled to receive test results after completing the project. This study has not been undertaken to benefit volunteers directly, but it is intended to help understand what happens to respiratory resistance when maximum flow rate is reached. This information could be used to understand the change in the respiratory mechanics of diseased people. The testing may also provide new knowledge on respiratory resistance values during forced expiration.

Risks: The use of esophageal balloons to measure pressure surrounding the lung has been in use for over 50 years, and techniques have been standardized since 1964. The main discomfort is some mild irritation of the nose and back of the throat, and gagging. If you gag, you will not be asked to continue the study. Potential risks include nasal bleeding, esophageal perforation and passage of the balloon into the lungs leading to cough. Most of the reported injuries are related to use of esophageal balloon for controlling esophageal bleeding and esophageal dilation. Use of the esophageal balloon technique for measurement of respiratory mechanics should be distinguished from other balloon related techniques. It should be noted that esophageal balloons are standard techniques for the measurement of pleural pressures in assessment of respiratory mechanics in the pulmonary function lab, the intensive care unit, and for assessing respiratory effort in patients undergoing sleep studies. If difficulty is encountered in passing the tube through the nose, the procedure will be stopped. You may experience some degree of dizziness while performing the maximal inhalation or exhalation maneuver and/or may experience slight discomfort when esophageal balloon is used. If you experience dizziness and/or discomfort, you will be given as much time as needed to rest and you will self-pace the remaining tests. Also, you will be given the option of rescheduling to finish the remaining tests if necessary. . Also you are free to withdraw from this investigation at any time without giving any reason and without incurring a penalty. If an emergency medical situation should occur, a physician who is a specialist in pulmonary and critical care medicine will be on hand. A defibrillator also will be available. If appropriate and/or necessary, 911 will be called.

Informed Consent and Confidentiality:

We will do our best to keep your personal information confidential. To help protect your confidentiality, you will be assigned an identification number. All personal information will be concealed by this personal identification number, which will be used whenever references are made regarding this investigation. The identification key that links the identity of the subjects to the subject's numbers will be maintained by storing this

information in the office of the investigators and will be accessible only to individuals directly responsible for the collection and analysis of this data. If we write a report or article about this research project, your identity will be protected to the maximum extent possible. Your information may be shared with representatives of the University of Maryland, College Park or governmental authorities if you or someone else is in danger or if required to do so by law.

Rights: You are free to withdraw from this investigation at any time without giving any reason and without incurring a penalty. This desire may be expressed to an investigator through written or verbal communication.

Medical Care: The University of Maryland does not provide any medical or hospitalization insurance for you in this research study nor will the University of Maryland provide any compensation for any injury sustained as a result of participation in this research study, except as required by law.

Contact Information:
Arthur T. Johnson, Ph.D.
Derya Coursey, M.S.

Biological Resources Engineering (Bldg. #142)
Phone numbers: 301-405-1186 or 301-405-1184
Email: derya@umd.edu or artjohns@umd.edu

Your signature indicates that: you are at least 18 years of age; the research has been explained to you; your questions have been fully answered; and you freely and voluntarily choose to participate in this research project. If you have any questions about your rights as a research subject or wish to report a research-related injury, please contact: Institutional Review Board Office, University of Maryland, College Park, 20742; email: IRB@deans.umd.edu; telephone: 301-405-4212

Signature of Subject _____ Date_____

Name of Subject _____

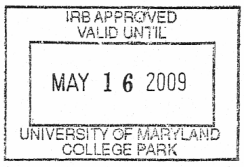

University of Maryland
Health History Questionnaire

Subject Number:_____ **Date**_____

Address_____

_____

Phone# (day)_____ **(night)**_____

Age_____ **Date of Birth**_____ **Gender**_____

Height_____ **Weight**_____ **Race**_____

A. Have you ever been treated by a physician for any of the following ailments? (Please circle your response)

Dizziness or fainting spells	Yes	No
Chronic respiratory illness	Yes	No
Asthma	Yes	No
Shortness of breath	Yes	No
Heart trouble	Yes	No
High or low blood pressure	Yes	No

B. Have you taken medication or seen a physician for any of the following ailments within the last 15 days? (Please circle your response)

Dizziness or fainting spells	Yes	No
Chronic respiratory illness	Yes	No
Asthma	Yes	No
Shortness of breath	Yes	No
Heart trouble	Yes	No
High or low blood pressure	Yes	No
Ear, nose, or throat trouble	Yes	No
Sinusitis	Yes	No
History of allergic diseases	Yes	No
Upper respiratory tract infection	Yes	No
Cold / Flu	Yes	No

C. Please characterize your smoking history by checking the appropriate responses below.

___ Never smoked
___ Stopped more than 10 years ago
___ Smoke up to 1 pack/day
___ Smoke 1-2 packs/day
___ Smoke 3+ packs/day
___ Other:

D. Have you ever had an adverse reaction to any materials listed below:

Rubbers	Yes	No
Latex rubbers	Yes	No
Silicone rubbers	Yes	No
Polyurethane	Yes	No

E. Have you ever had an adverse reaction to lidocaine or similar numbing medications?

Yes No

F. Have you ever had difficulty of swallowing?

Yes No

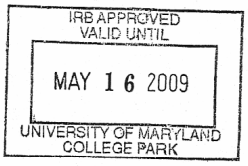

Appendix B. Various Lung Volumes and Capacities

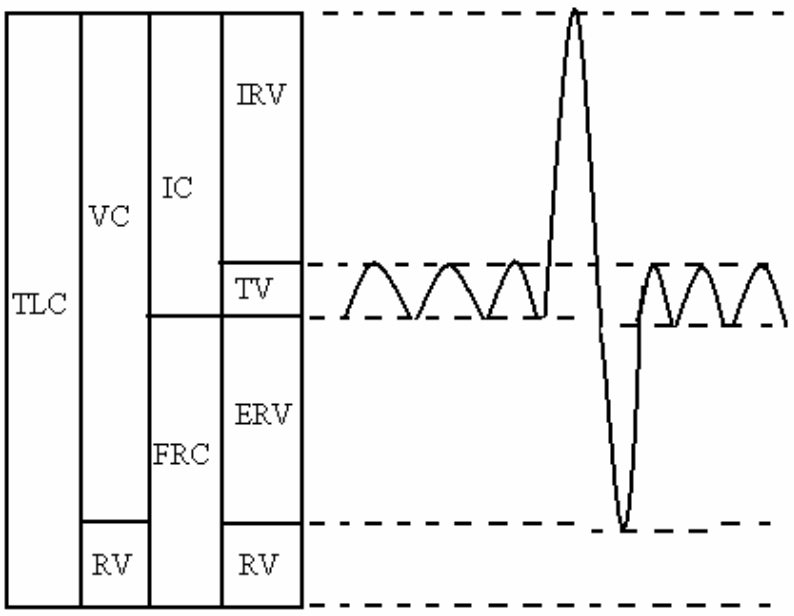

Figure B1: Diagram of various lung volumes

Tidal Volume (TV): The amount of gas inspired or expired with each breath.

Inspiratory Reserve Volume (IRV): Maximum amount of additional air that can be inspired from the end of a normal inspiration.

Expiratory Reserve Volume (ERV): Maximum amount of additional air that can be expired from the end of a normal inspiration.

Residual Volume (RV): The volume of air remaining in the lung after a maximal expiration.

Vital Capacity (VC): The maximum amount of air that can be forcefully expelled from the lungs following a maximal inspiration.

Total Lung Capacity (TLC): The volume of air contained in the lungs at the end of a maximal inspiration. TLC = VC + RV

Functional Residual Capacity (FRC): the volume of air remaining in the lung at the end of a normal expiration.

Inspiratory Capacity (IC): Maximum volume of air that can be inspired from end expiratory position.

Appendix C: Matlab Program to Plot IVPF Curves

```
%%%%%%%%%%%%%%%%%%%%%%%%%%%%%%%%%%%%%%%%%%%%%
% this code uses the following functions for optimization
%%%%%%%%%%%%%%%%%%%%%%%%%%%%%%%%%%%%%%%%%%%%%
function f = doublelinefitter2(x)
global t;
global y;
global xc;

f=0;
% for each point
for i=1:length(t)
   if (t(i) < xc) % if your t value is less than critical value, use the 1st line
      prediction=x(1)*t(i)+x(3);
   else % if your t value is greater than or equal to the critical value, use the 2nd line
      prediction=x(2)*t(i)+x(4);
   end

%    prediction
   % sum up the square of the residuals
   f=f+(prediction-y(i))^2;
end

%%%%%%%%%%%%%%%%%%%%%%%%%%%%%%%%%%%%%%%%%%%%%
function [c,ceq] = deryacon2(x)
global xc;
%c = ...     % Compute nonlinear inequalities at x.
%ceq = ...   % Compute nonlinear equalities at x.
c=[];
ceq=x(1)*xc+x(3)-x(2)*xc-x(4);
%%%%%%%%%%%%%%%%%%%%%%%%%%%%%%%%%%%%%%%%%%%%%

clear all
close all
clc

global t;
global y;
global xc;

% load the data
load SF_data.txt
Pmo=SF_data(:,1);
Qsf=SF_data(:,2);
```

```
t=Pmo;
y=Qsf;

figure(1)
hh=plot(t,y,'b^')
hold on
%max(t)
xc_array=[min(t):(max(t)-min(t))/200:max(t)];

%options = optimset('Display','iter','FunValCheck','on');

for i=1:length(xc_array)
   xc=xc_array(i);
   x0=[.1 0 0 2.5];
% x := slope1 slope2 intercept1 intercept2 intersection
[xx,fval] = fmincon(@doublelinefitter2,x0,[],[],[0 1 0 0],0,[],[],@deryacon2);
myf(i)=fval;
my_var(i,1:4)=xx;
end

figure
plot(xc_array,myf,'b.')
myoptim=find(myf==min(myf));

figure (1)

myxx=[min(t) xc_array(myoptim)];
myxx2=[xc_array(myoptim) max(t)];
plot(myxx,my_var(myoptim,1)*myxx+my_var(myoptim,3),'b-','LineWidth',2)
hold on
plot(myxx2,my_var(myoptim,2)*myxx2+my_var(myoptim,4),'b-','LineWidth',2)

xc_array(myoptim)   %limited pressure
my_var(myoptim,:)  %the first line is the slope

%% Balloon IVPF Curve fitting
load EB_data.txt
Ptp=EB_data(:,1);
Qeb=EB_data(:,2);

t=Ptp;
y=Qeb;

xc_array=[min(t):(max(t)-min(t))/200:max(t)];
```

```
%options = optimset('Display','iter','FunValCheck','on');

for i=1:length(xc_array)
   xc=xc_array(i);
   x0=[.1 0 0 2.5];
% x := slope1 slope2 intercept1 intercept2 intersection
 [xx_eb,fval_eb] = fmincon(@doublelinefitter2,x0,[],[],[0 1 0 0],0,[],[],@deryacon2);
% x := slope1 slope2 intercept1 intercept2 intersection
   myf_eb(i)=fval_eb;
   my_var_eb(i,1:4)=xx_eb;
end

figure
plot(xc_array,myf_eb,'b.')

myoptim_eb=find(myf_eb==min(myf_eb));

figure(1)
m=plot(t,y,'ro')
legend([hh,m],'Stop-Flow','Esophageal Balloon','Location','southeast')
ylim([0 max(y)+.5])
hold on
h=gca
set(get(h,'XLabel'),'String','P_t_r or P_m_o (cm H_2O)',...
                'FontName','times',...
                'FontWeight','bold',...
                'FontSize',12)
set(get(h,'YLabel'),'String','Flow (L/s)',...
                'FontName','times',...
                'FontWeight','bold',...
                'FontSize',12)
set(get(h,'title'),'String','IVPF Curve of Subject 103 at 50 %VC',...
                'FontName','times',...
                'FontWeight','bold',...
                'FontSize',12)
myxx_eb=[min(t) xc_array(myoptim_eb)];
myxx2_eb=[xc_array(myoptim_eb) max(t)];
plot(myxx_eb,my_var_eb(myoptim_eb,1)*myxx_eb+my_var_eb(myoptim_eb,3),'r-
','LineWidth',2)
hold on
plot(myxx2_eb,my_var_eb(myoptim_eb,2)*myxx2_eb+my_var_eb(myoptim_eb,4),'r
-','LineWidth',2)

xc_array(myoptim_eb)   %limited pressure
my_var_eb(myoptim_eb,:)  %the first line is the slope
```

Appendix D: Statistics of Comparison of the APD Resistance to Pulmonary Resistance

The comparison between the stop – flow and esophageal balloon methods were done with t- test for unequal variances at $\alpha = 0.05$. The resulting statistics are given in Tables D1 through D25.

D.1 Baseline Resistances

The comparison of baseline resistances calculated with the APD and esophageal balloon are given in Tables D1 through D3.

Table D1: Statistics for t-test for unequal variances of baseline $R_{APD,\,av}$ and $R_{L,av}$

	$R_{APD,av}$	$R_{L,av}$
Mean	2.686	1.768
Variance	0.718	1.676
Observations	6	6
Hypothesized Mean Difference	0	
df	9	
t Stat	1.453	
P(T<=t) one-tail	0.090	
t Critical one-tail	1.833	
P(T<=t) two-tail	0.180	
t Critical two-tail	2.262	

Table D2: Statistics for t-test for unequal variances of baseline $R_{APD,ins}$ and $R_{L,ins}$

	$R_{APD,ins}$	$R_{L,ins}$
Mean	2.547	1.437
Variance	0.779	0.966
Observations	6	6
Hypothesized Mean Difference	0	
df	10	
t Stat	2.059	
P(T<=t) one-tail	0.033	
t Critical one-tail	1.812	
P(T<=t) two-tail	0.066	
t Critical two-tail	2.228	

Table D3: Statistics for t-test for unequal variances of baseline $R_{APD,exh}$ and $R_{L,exh}$

	$R_{APD,exh}$	$R_{L,exh}$
Mean	2.827	2.347
Variance	0.715	2.611
Observations	6	6
Hypothesized Mean Difference	0	
df	8	
t Stat	0.645	
P(T<=t) one-tail	0.269	
t Critical one-tail	1.860	
P(T<=t) two-tail	0.537	
t Critical two-tail	2.306	

D.2 Addition of Inspiratory and Expiratory Resistances

Both low and high resistances were added during tidal breathing. Statistics for the change in inhalation (ΔR_{ins}), exhalation (ΔR_{exh}), and average (ΔR_{av}) resistances relative to the baseline resistance with both the APD and esophageal balloon were calculated. Additionally, those changes were compared to expected resistance change.

D.2.1 Average Resistance

D.2.1.1 Addition of Low Resistance

Table D4: Statistics for t-test for unequal variances of $\Delta R_{APD,av}$ and $\Delta R_{L,av}$ when low resistance was added.

	$\Delta R_{APD,av}$	$\Delta R_{L,av}$
Mean	0.939	0.252
Variance	0.576	0.750
Observations	6	5
Hypothesized Mean Difference	0	
df	8	
t Stat	1.385	
P(T<=t) one-tail	0.102	
t Critical one-tail	1.860	
P(T<=t) two-tail	0.203	
t Critical two-tail	2.306	

Table D5: Statistics for t-test for unequal variances of Added resistance and $\Delta R_{APD,av}$ and when low resistance was added.

	Added Resistance	$\Delta R_{APD,av}$
Mean	1.167	0.939
Variance	0.005	0.576
Observations	6	6
Hypothesized Mean Difference	0	
df	5	
t Stat	0.732	
P(T<=t) one-tail	0.249	
t Critical one-tail	2.015	
P(T<=t) two-tail	0.497	
t Critical two-tail	2.571	

Table D6: Statistics for t-test for unequal variances of Added resistance and $\Delta R_{L,av}$ and when low resistance was added.

	Added Resistance	$\Delta R_{L,av}$
Mean	1.167	0.252
Variance	0.005	0.750
Observations	6	5
Hypothesized Mean Difference	0	
df	4	
t Stat	2.355	
P(T<=t) one-tail	0.039	
t Critical one-tail	2.132	
P(T<=t) two-tail	0.078	
t Critical two-tail	2.776	

D.2.1.2 Addition of High Resistance

Table D7: Statistics for t-test for unequal variances of $\Delta R_{APD,av}$ and $\Delta R_{L,av}$ when high resistance was added.

	$\Delta R_{APD,av}$	$\Delta R_{L,av}$
Mean	1.687	1.466
Variance	0.547	1.002
Observations	6	5
Hypothesized Mean Difference	0	
df	7	
t Stat	0.410	
P(T<=t) one-tail	0.347	
t Critical one-tail	1.895	
P(T<=t) two-tail	0.694	
t Critical two-tail	2.365	

Table D8: Statistics for t-test for unequal variances of Added resistance and $\Delta R_{APD,av}$ and when high resistance was added.

	Added Resistance	$\Delta R_{APD,av}$
Mean	2.167	1.687
Variance	0.011	0.547
Observations	6	6
Hypothesized Mean Difference	0	
df	5	
t Stat	1.573	
P(T<=t) one-tail	0.088	
t Critical one-tail	2.015	
P(T<=t) two-tail	0.176	
t Critical two-tail	2.571	

Table D9: Statistics for t-test for unequal variances of Added resistance and $\Delta R_{L,av}$ and when high resistance was added.

	Added Resistance	$\Delta R_{L,av}$
Mean	2.167	1.466
Variance	0.011	1.002
Observations	6	5
Hypothesized Mean Difference	0	
df	4	
t Stat	1.559	
P(T<=t) one-tail	0.097	
t Critical one-tail	2.132	
P(T<=t) two-tail	0.194	
t Critical two-tail	2.776	

D.2.2 Inhalation Resistance

D.2.2.1 Addition of Low Resistance

Table D10: Statistics for t-test for unequal variances of $\Delta R_{APD,ins}$ and $\Delta R_{L,ins}$ when low resistance was added.

	$\Delta R_{APD,ins}$	$\Delta R_{L,ins}$
Mean	0.958	-0.012
Variance	0.482	0.745
Observations	6	5
Hypothesized Mean Difference	0	
df	8	
t Stat	2.025	
P(T<=t) one-tail	0.039	
t Critical one-tail	1.860	
P(T<=t) two-tail	0.077	
t Critical two-tail	2.306	

Table D11: Statistics for t-test for unequal variances of Added resistance and $\Delta R_{APD,ins}$ and when low resistance was added.

	Added Resistance	$\Delta R_{APD,ins}$
Mean	1.167	0.958
Variance	0.005	0.482
Observations	6	6
Hypothesized Mean Difference	0	
df	5	
t Stat	0.73	
P(T<=t) one-tail	0.25	
t Critical one-tail	2.02	
P(T<=t) two-tail	0.50	
t Critical two-tail	2.57	

Table D12: Statistics for t-test for unequal variances of Added resistance and $\Delta R_{L,ins}$ and when low resistance was added.

	Added Resistance	$\Delta R_{L,ins}$
Mean	1.167	-0.012
Variance	0.005	0.745
Observations	6	5
Hypothesized Mean Difference	0	
df	4	
t Stat	3.045	
P(T<=t) one-tail	0.019	
t Critical one-tail	2.132	
P(T<=t) two-tail	0.038	
t Critical two-tail	2.776	

D.2.2.2 Addition of High Resistance

Table D13: Statistics for t-test for unequal variances of $\Delta R_{APD,ins}$ and $\Delta R_{L,ins}$ when high resistance was added.

	$\Delta R_{APD,ins}$	$\Delta R_{L,ins}$
Mean	1.779	1.046
Variance	0.496	0.849
Observations	6	5
Hypothesized Mean Difference	0	
df	7	
t Stat	1.460	
P(T<=t) one-tail	0.094	
t Critical one-tail	1.895	
P(T<=t) two-tail	0.188	
t Critical two-tail	2.365	

Table D14: Statistics for t-test for unequal variances of Added resistance and $\Delta R_{APD,ins}$ and when high resistance was added.

	Added Resistance	$\Delta R_{APD,ins}$
Mean	2.167	1.779
Variance	0.011	0.496
Observations	6	6
Hypothesized Mean Difference	0	
df	5	
t Stat	1.333	
P(T<=t) one-tail	0.120	
t Critical one-tail	2.015	
P(T<=t) two-tail	0.240	
t Critical two-tail	2.571	

Table D15: Statistics for t-test for unequal variances of Added resistance and $\Delta R_{L,ins}$ and when high resistance was added.

	Added Resistance	$\Delta R_{L,ins}$
Mean	2.167	1.046
Variance	0.011	0.849
Observations	6	5
Hypothesized Mean Difference	0	
df	4	
t Stat	2.705	
P(T<=t) one-tail	0.027	
t Critical one-tail	2.132	
P(T<=t) two-tail	0.054	
t Critical two-tail	2.776	

D.2.3 Exhalation Resistance

D.2.3.1 Addition of Low Resistance

Table D16: Statistics for t-test for unequal variances of $\Delta R_{APD,exh}$ and $\Delta R_{L,exh}$ when low resistance was added.

	$\Delta R_{APD,exh}$	$\Delta R_{L,exh}$
Mean	0.918	0.274
Variance	0.851	1.911
Observations	6	5
Hypothesized Mean Difference	0	
df	7	
t Stat	0.890	
P(T<=t) one-tail	0.201	
t Critical one-tail	1.895	
P(T<=t) two-tail	0.403	
t Critical two-tail	2.365	

Table D17: Statistics for t-test for unequal variances of Added resistance and $\Delta R_{APD,exh}$ and when low resistance was added.

	Added Resistance	$\Delta R_{APD,exh}$
Mean	1.167	0.918
Variance	0.005	0.851
Observations	6	6
Hypothesized Mean Difference	0	
df	5	
t Stat	0.657	
P(T<=t) one-tail	0.270	
t Critical one-tail	2.015	
P(T<=t) two-tail	0.540	
t Critical two-tail	2.571	

Table D18: Statistics for t-test for unequal variances of Added resistance and $\Delta R_{L,exh}$ and when low resistance was added.

	Added Resistance	$\Delta R_{L,exh}$
Mean	1.167	0.274
Variance	0.005	1.911
Observations	6	5
Hypothesized Mean Difference	0	
df	4	
t Stat	1.442	
P(T<=t) one-tail	0.111	
t Critical one-tail	2.132	
P(T<=t) two-tail	0.223	
t Critical two-tail	2.776	

D.2.3.2 Addition of High Resistance

Table D19: Statistics for t-test for unequal variances of $\Delta R_{APD,exh}$ and $\Delta R_{L,exh}$ when high resistance was added.

	$\Delta R_{APD,exh}$	$\Delta R_{L,exh}$
Mean	1.595	1.652
Variance	0.805	1.941
Observations	6	5
Hypothesized Mean Difference	0	
df	7	
t Stat	-0.080	
P(T<=t) one-tail	0.469	
t Critical one-tail	1.895	
P(T<=t) two-tail	0.939	
t Critical two-tail	2.365	

Table D20: Statistics for t-test for unequal variances of Added resistance and $\Delta R_{APD,exh}$ and when high resistance was added.

	Added Resistance	$\Delta R_{APD,exh}$
Mean	2.167	1.595
Variance	0.011	0.805
Observations	6	6
Hypothesized Mean Difference	0	
df	5	
t Stat	1.551	
P(T<=t) one-tail	0.091	
t Critical one-tail	2.015	
P(T<=t) two-tail	0.181	
t Critical two-tail	2.571	

Table D21: Statistics for t-test for unequal variances of Added resistance and $\Delta R_{L,exh}$ and when high resistance was added.

	Added Resistance	$\Delta R_{L,exh}$
Mean	2.167	1.652
Variance	0.011	1.941
Observations	6	5
Hypothesized Mean Difference	0	
df	4	
t Stat	0.824	
P(T<=t) one-tail	0.228	
t Critical one-tail	2.132	
P(T<=t) two-tail	0.456	
t Critical two-tail	2.776	

D.3 High Respiratory Load only on Inhalation or Exhalation

D.3.1 High Respiratory Load on Inhalation Side

Table D22: Statistics for t-test for unequal variances of $\Delta R_{APD,ins}$ and $\Delta R_{APD,exh}$ when high respiratory load was on inhalation side.

	$\Delta R_{APD,ins}$	$\Delta R_{APD,exh}$
Mean	3.168	1.392
Variance	0.518	0.273
Observations	6	6
Hypothesized Mean Difference	0	
df	9	
t Stat	4.893	
P(T<=t) one-tail	0.0004	
t Critical one-tail	1.833	
P(T<=t) two-tail	0.0009	
t Critical two-tail	2.262	

Table D23: Statistics for t-test for unequal variances of $\Delta R_{L,ins}$ and $\Delta R_{L,exh}$ when high respiratory load was on inhalation side.

	$\Delta R_{L,ins}$	$\Delta R_{L,exh}$
Mean	2.312	1.794
Variance	0.805	2.322
Observations	5	5
Hypothesized Mean Difference	0	
df	6	
t Stat	0.655	
P(T<=t) one-tail	0.268	
t Critical one-tail	1.943	
P(T<=t) two-tail	0.537	
t Critical two-tail	2.447	

D.3.2 High Respiratory Load on Exhalation Side

Table D24: Statistics for t-test for unequal variances of $\Delta R_{APD,ins}$ and $\Delta R_{APD,exh}$ when high respiratory load was on exhalation side.

	$\Delta R_{APD,ins}$	$\Delta R_{APD,exh}$
Mean	1.566	3.046
Variance	0.445	0.185
Observations	5	5
Hypothesized Mean Differenc	0	
df	7	
t Stat	-4.168	
P(T<=t) one-tail	0.002	
t Critical one-tail	1.895	
P(T<=t) two-tail	0.004	
t Critical two-tail	2.365	

Table D25: Statistics for t-test for unequal variances of $\Delta R_{L,ins}$ and $\Delta R_{L,exh}$ when high respiratory load was on exhalation side.

	$\Delta R_{L,ins}$	$\Delta R_{L,exh}$
Mean	1.486	2.928
Variance	1.176	1.717
Observations	5	5
Hypothesized Mean Differenc	0	
df	8	
t Stat	-1.896	
P(T<=t) one-tail	0.047	
t Critical one-tail	1.860	
P(T<=t) two-tail	0.095	
t Critical two-tail	2.306	

Appendix E: Average APD and Pulmonary Resistance Plots

The resistance value on the y axis when the added resistance is zero corresponds to the subject's intrinsic resistance.

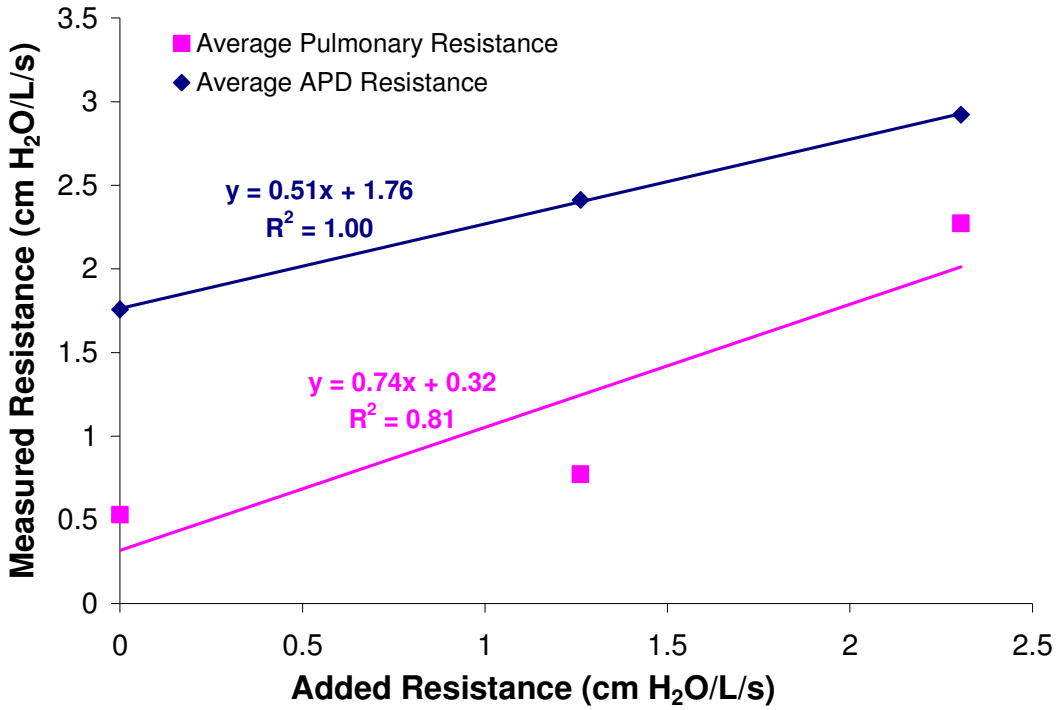

Figure E1: Added Resistance versus pulmonary and APD resistances for subject 101.

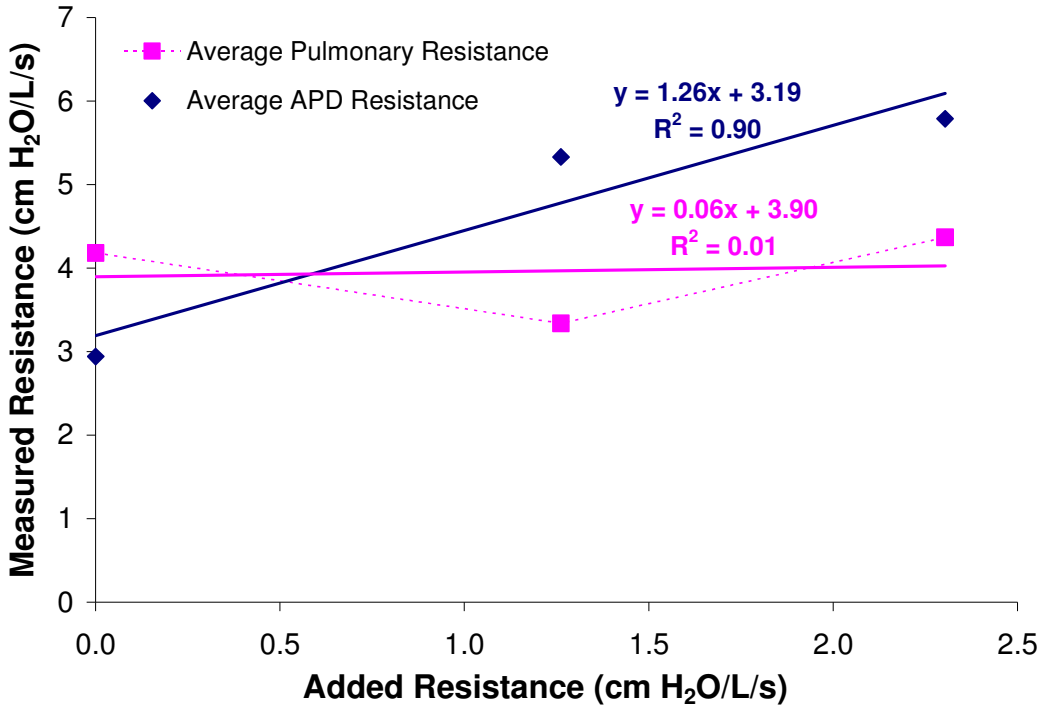

Figure E2: Added Resistance versus pulmonary and APD resistances for subject 102. Even though measured APD resistance shows an increase with added resistance, pulmonary resistance does not change significantly.

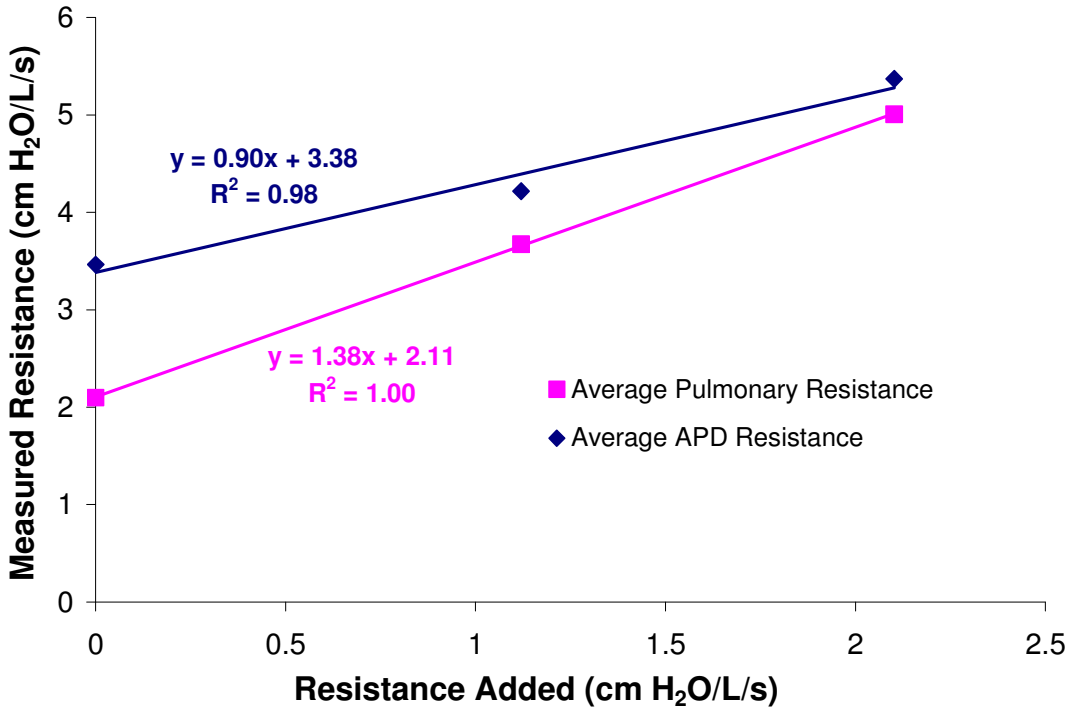

Figure E3: Added Resistance versus pulmonary and APD resistances for subject 103.

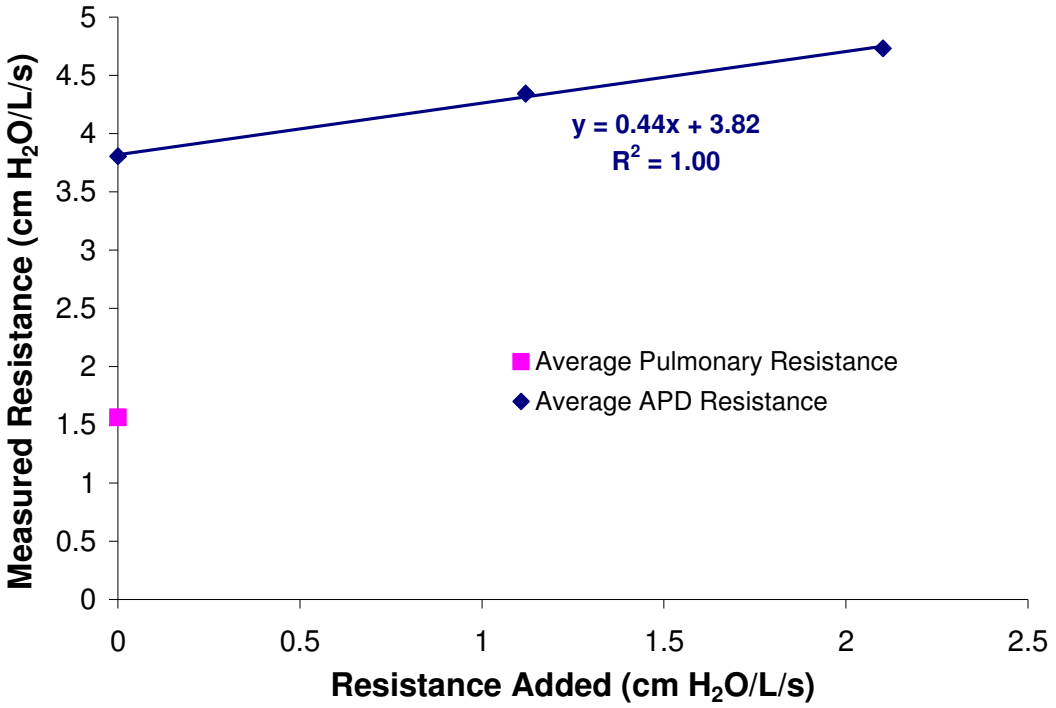

Figure E4: Added Resistance versus pulmonary and APD resistances for subject 104. He was the first subject tested. Therefore, not all measurements are done with him.

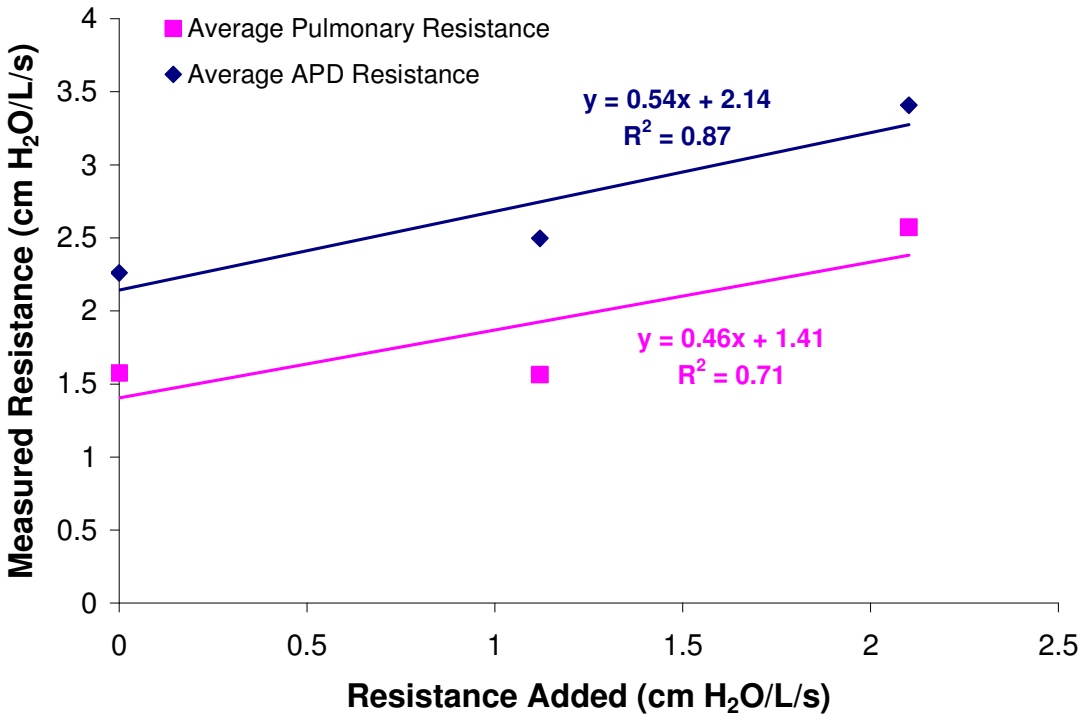

Figure E5: Added Resistance versus pulmonary and APD resistances for subject 105.

Appendix F: Inhalation and Exhalation APD and Pulmonary Resistance Plots

The resistance value on the y axis when the added resistance is zero corresponds to the subject's intrinsic resistance.

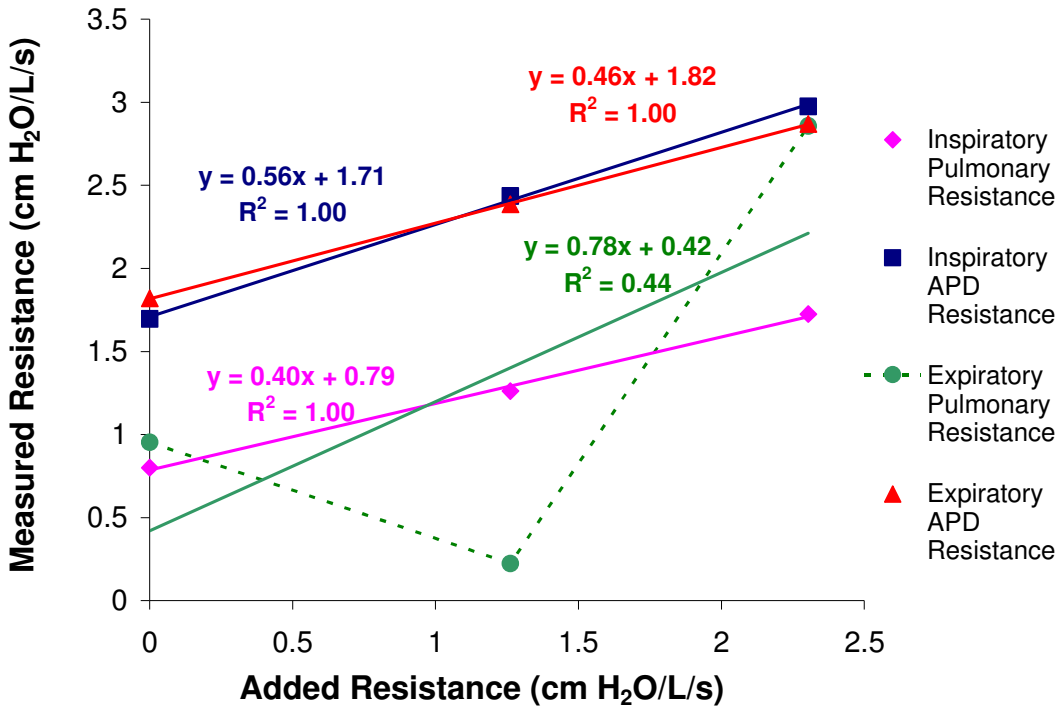

Figure F1: Added Resistance versus pulmonary and APD inhalation and exhalation resistances for subject 101.

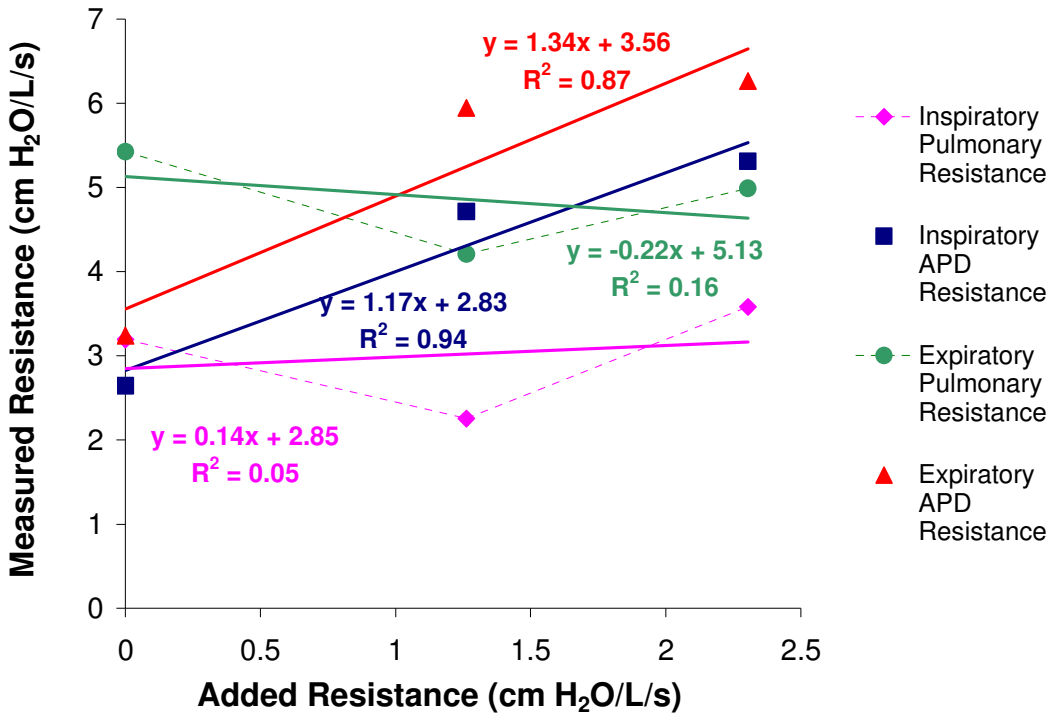

Figure F2: Added Resistance versus pulmonary and APD inhalation and exhalation resistances for subject 102. Pulmonary inspiratory and expiratory resistances show a very poor correlation with added resistance.

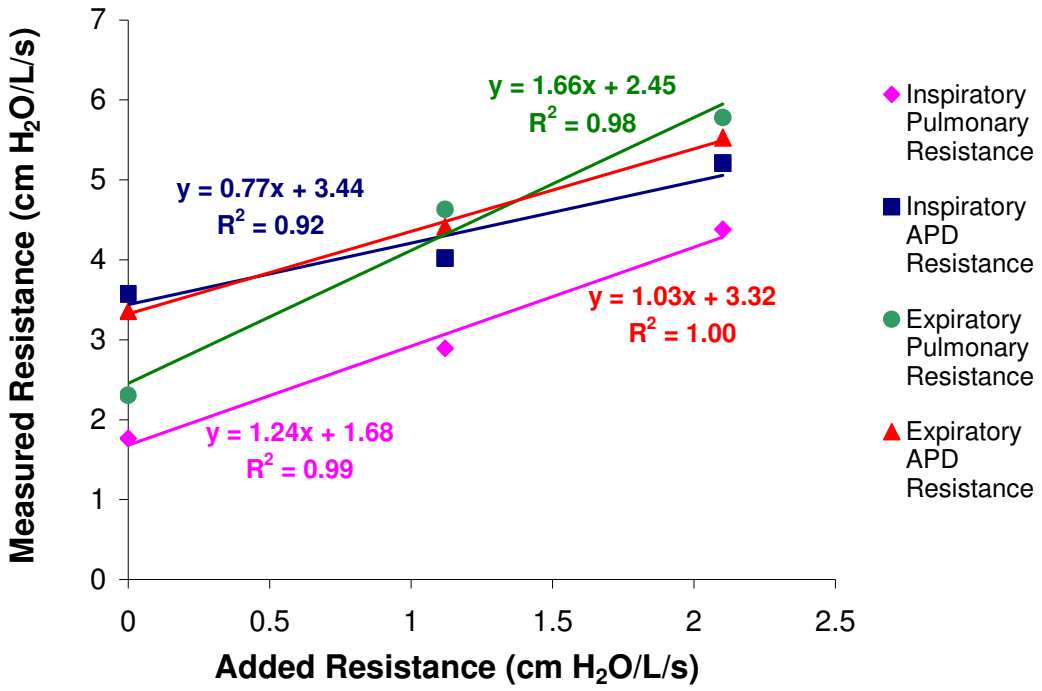

Figure F3: Added Resistance versus pulmonary and APD inhalation and exhalation resistances for subject 103.

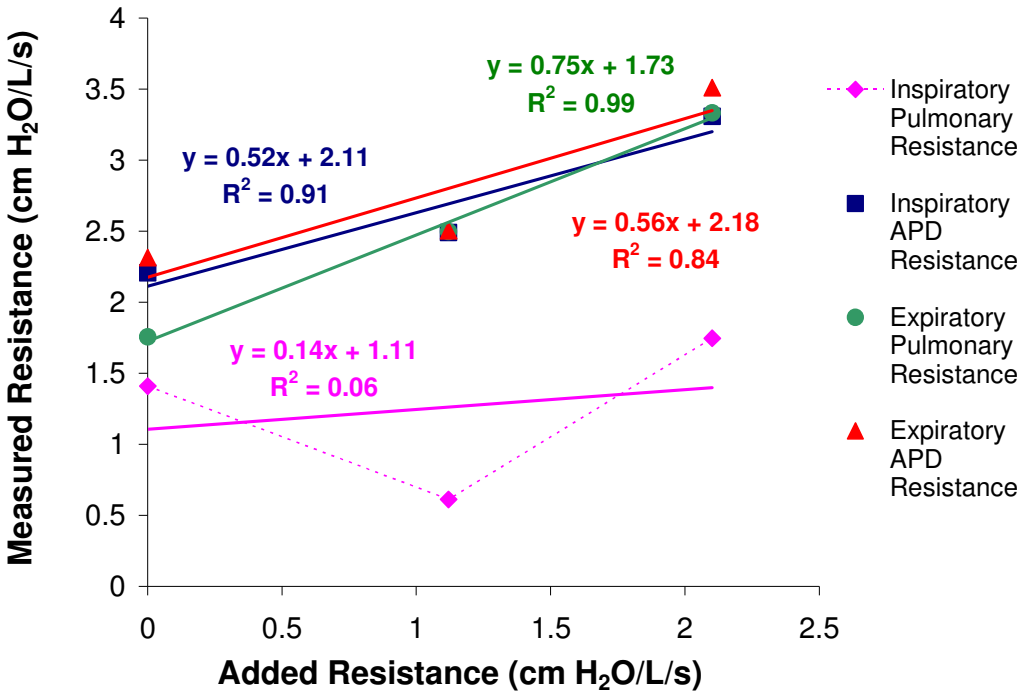

Figure F4: Added Resistance versus pulmonary and APD inhalation and exhalation resistances for subject 105. Pulmonary inspiratory resistance showed a very poor correlation with added resistance.

Appendix G: Statistics of IVPF Curves

The comparison between the stop – flow and esophageal balloon methods were done with t- test for unequal variances at $\alpha = 0.05$. The resulting statistics are given in Tables G1 through G10.

G1. Comparing the Stop – Flow and Esophageal Balloon Methods

The pressures (P) and flows (Q) at flow limitation with the stop – flow (SF) and esophageal balloon (EB) methods were compared at 25 % and 50 % VC (Tables G1 through G4).

Table G1: Statistics for t-test for unequal variances of $P_{SF,max}$ and $P_{EB,max}$ at 25 %VC

	$P_{SF,max}$	$P_{EB,max}$
Mean	21.76	3.888
Variance	57.968	39.180
Observations	5	5
Hypothesized Mean Difference	0	
df	8	
t Stat	4.055	
P(T<=t) one-tail	0.002	
t Critical one-tail	1.860	
P(T<=t) two-tail	0.004	
t Critical two-tail	2.306	

Table G2: Statistics t-test for unequal variances of $Q_{SF,max}$ and $Q_{EB,max}$ at 25 %VC

	$Q_{SF,max}$	$Q_{EB,max}$
Mean	2.26	3.32
Variance	0.638	0.647
Observations	5	5
Hypothesized Mean Difference	0	
df	8	
t Stat	-2.091	
P(T<=t) one-tail	0.035	
t Critical one-tail	1.860	
P(T<=t) two-tail	0.070	
t Critical two-tail	2.306	

Table G3: Statistics t-test for unequal variances of $P_{SF,max}$ and $P_{EB,max}$ at 50 %VC

	$P_{SF,max}$	$P_{EB,max}$
Mean	31.3	7.2
Variance	87.407	31.313
Observations	4	4
Hypothesized Mean Difference	0	
df	5	
t Stat	4.424	
P(T<=t) one-tail	0.003	
t Critical one-tail	2.015	
P(T<=t) two-tail	0.007	
t Critical two-tail	2.571	

Table G4: Statistics t-test for unequal variances of $Q_{SF,max}$ and $Q_{EB,max}$ at 50 %VC

	$Q_{SF,max}$	$Q_{EB,max}$
Mean	3.75	6.35
Variance	1.097	0.177
Observations	4	4
Hypothesized Mean Difference	0	
df	4	
t Stat	-4.608	
P(T<=t) one-tail	0.005	
t Critical one-tail	2.132	
P(T<=t) two-tail	0.010	
t Critical two-tail	2.776	

G.2 Comparison of Resistances

The resistances (R) at the point of flow limitation with the stop – flow (SF), esophageal balloon (EB), and the APD were compared at 25 % and 50 % VC (Tables G5 through G10).

Table G5: Statistics t-test for unequal variances of R_{SF} and R_{EB} at 25 %VC

	R_{SF}	R_{EB}
Mean	6.74	5.62
Variance	9.083	17.337
Observations	5	5
Hypothesized Mean Difference	0	
df	7	
t Stat	0.487	
P(T<=t) one-tail	0.320	
t Critical one-tail	1.895	
P(T<=t) two-tail	0.641	
t Critical two-tail	2.365	

Table G6: Statistics t-test for unequal variances of R_{SF} and R_{APD} at 25 %VC

	R_{SF}	R_{APD}
Mean	6.74	2.94
Variance	9.083	0.223
Observations	5	5
Hypothesized Mean Difference	0	
df	4	
t Stat	2.785	
P(T<=t) one-tail	0.025	
t Critical one-tail	2.132	
P(T<=t) two-tail	0.050	
t Critical two-tail	2.776	

Table G7: Statistics t-test for unequal variances of R_{EB} and R_{APD} at 25 %VC

	R_{EB}	R_{APD}
Mean	5.62	2.94
Variance	17.337	0.223
Observations	5	5
Hypothesized Mean Difference	0	
df	4	
t Stat	1.430	
P(T<=t) one-tail	0.113	
t Critical one-tail	2.132	
P(T<=t) two-tail	0.226	
t Critical two-tail	2.776	

Table G8: Statistics t-test for unequal variances of R_{SF} and R_{EB} at 50 %VC

	R_{SF}	R_{EB}
Mean	11.225	3.375
Variance	16.389	1.336
Observations	4	4
Hypothesized Mean Difference	0	
df	3	
t Stat	3.729	
P(T<=t) one-tail	0.017	
t Critical one-tail	2.353	
P(T<=t) two-tail	0.034	
t Critical two-tail	3.182	

Table G9: Statistics t-test for unequal variances of R_{SF} and R_{APD} at 50 %VC

	R_{SF}	R_{APD}
Mean	11.225	3.95
Variance	16.389	0.917
Observations	4	4
Hypothesized Mean Difference	0	
df	3	
t Stat	3.498	
P(T<=t) one-tail	0.020	
t Critical one-tail	2.353	
P(T<=t) two-tail	0.040	
t Critical two-tail	3.182	

Table G10: Statistics t-test for unequal variances of R_{EB} and R_{APD} at 50 %VC

	R_{EB}	R_{APD}
Mean	3.375	3.95
Variance	1.336	0.917
Observations	4	4
Hypothesized Mean Difference	0	
df	6	
t Stat	-0.766	
P(T<=t) one-tail	0.236	
t Critical one-tail	1.943	
P(T<=t) two-tail	0.473	
t Critical two-tail	2.447	

References

American Lung Association. http://www.lungusa.org. Accessed on November 20, 2008.

Aldrich, T. K., Shapiro, S. M., Sherman, M. S., Prezant, D. J., "Alveolar Pressure and Airway Resistance During Maximal and Submaximal Respiratory Efforts," American Review of Respiratory Diseases, 140:899-906, 1989.

Blide, R. W., Kerr, H. D., Spicer, W. S. Jr., "Measurement of Upper and Lower Airway Resistance and Conductance in Man," Journal of Applied Physiology, 19(6): 1059-1069, 1964.

Briscoe, W. A., Dubois, A. B., "The Relationship between Airway Resistance, Airway Conductance and Lung Volume in Subjects of Different Age and Body Size," Journal of Clinical Investigation, 37: 1279-1284, 1959.

Baydur, A., Behrakis, P. K., Zin, W. A., Jaeger, M., Milic-Emili, J., "A Simple Method for Assesing the Validity of the Esophageal Balloon Technique," American Review of Respiratory Diseases, 126:788-791, 1982.

Bates, J. H. T., Baconnier, P., Milic-Emili, J., "A Theoretical Analysis of Interrupter Technique for Measuring Respiratory Mechanics," Journal of Applied Physiology, 64:2204-2214, 1988.

Bennet, E. D., Jayson, M. I. V., Rubenstein, D., Campell, E. J. M., "The Ability of Man to Detect Added Non-Elastic Loads to Breathing," Clinical Science, 23:155-162, 1962.

Clements, J. A., Sharp, J. T., Johnson, R. P., Elam, J. O., "Estimation of Pulmonary Resistance by Repetitive Interruption of Airflow," Journal of Clinical Investigation, 38:1262-1270, 1959.

Dawson, S. V., Elliott, E. A., "Wave-speed Limitation on Expiratory Flow - A unifying Concept," Journal of Applied Physiology: Respiratory, Enviromental and Exercise Physiology, 43:498-515, 1977.

Dechman, G., Sato, J., Bates, J. H. T., "Factors Affecting the Accuracy of Esophageal Balloon Measurement of Pleural Pressure in Dogs," Journal of Applied Physiology, 72:383-388, 1992.

DuBois, A. B., Botelho, S. Y., Comroe, J. H. Jr., "A New Method for Measuring Airway Resistance in Man Using a Body Plethysmograph: Values in Normal Subjects and in Patients with Respiratory Disease," Journal of Clinical Investigation, 35: 327-335, 1956.

Elliott, E. A., Dawson, S. V., "Test of Wave-Speed Theory of Flow Limitation in Elastic Tubes," Journal of Applied Physiology, 43(3): 516-522, 1977.

Ferris, B. G., Mead, J., Opie, L. H., "Partitioning of Respiratory Flow Resistance in Man," Journal of Applied Physiology, 19(4):653-658, 1964.

Frank, N. R., Mead, J., Ferris, B. G., "The Mechanical Behavior of the Lungs in Healthy Elderly Persons," Journal of Clinical Investigation, 36 (12): 1680 -1687, 1957.

Fry, D. L., Hyatt, R. E., "Pulmonary Mechanics: A Unified Analysis of the Relationship Between Pressure, Volume and Gasflow in the Lungs of Normal and Diseased Human Subjects," American Journal of Medicine, 29:672-689, 1960.

Fry, D. L., "Theoretical Considerations of the Bronchial Pressure-Flow-Volume Relationshops with Particular Reference to the Maximum Expiratory Flow Volume Curve," Physics in Medicine and Biology, 3(2):174-194, 1958.

Hankinson, J. L., Odencrantz, J. R., Fedan, K. B., "Spirometric Reference Values From a Sample of the General US Population," American Journal of Respiratory and Critical Care Medicine, 159: 179-187, 1999.

Hyatt, R. E., Wilson, T. A., Bar-Yishay, E., "Prediction of Maximal Expiratory Flow in Excised Human Lungs," Journal of Applied Physiology, 48(6):991-998, 1980.

Hyatt, R. E., Schilder, D. P., Fry, D.L., "Relationship Between Maximum Expiratory Flow and Degree of Lung Inflation," Journal of Applied Physiology, 13:331-336, 1958.

Jackson, A. C., Milhorn, H. T., Norman, J. R., "A Reevaluation of the Interrupter Technique for Airway Resistance Measurement," Journal of Applied Physiology, 36:264-268, 1974.

Johnson, A. T., Sahota, M. S., "Validation of Airflow Perturbation Device Resistance Measurements in Excised Sheep Lungs," Physiological Measurements, 25:679-690, 2004.

Johnson, A. T., Lin, C-S, Hochheimer, J. N., "Airflow Perturbation Device for Measuring Airway Resistance of Humans and Animals," IEEE Transactions on Biomedical Engineering, 31:622-626, 1984.

Kelsen, S. G., Prestel, T. F., Cherniack, N. S., Chester, E. H., Deal, E. C. Jr., "Comparison of the Respiratory Responses to External Resistive Loading and Bronchoconstriction", Journal of Clinical Investigation, 67: 1761-1768, 1981.

Killian, K. J., Mahutte, C. K., Howell, J. B. L., Campbell, E. J. M., "Effect of Timing, Flow, Lung Volume, and Threshold Pressures on Resistive Load Detection," Journal of Applied Physiology, 49(6):958-963, 1980.

Lausted, C. G., Johnson, A. T., "Respiratory Resistance Measured by an Airflow Perturbation Device," Physiological Measurements, 20:21-35, 1999.

Lausted, C. G., Johnson, A.T., "Airflow Perturbation Device for Measuring Human Respiratory Resistance," Proceedings of the IEEE 24th Annual Northeast Conference, 97-99, 1998.

Lourens, M. S., van den Berg, B., Verbraak, A. F. M., Hoogsteden, H. C., Bogaard, J. M., "Effect of Series of Resistance Levels on Flow Limitation in Mechanically Ventilated COPD Patients," Respiration Physiology, 127: 39-52, 2001.

Macklem, P. T., Wilson, N. J., "Measurement of Intrabronchial Pressure in Man," Journal of Applied Physiology, 20(4): 653-663, 1965.

Mahutte, C. K., Campbell, J. M., Killian, K. J., "Theory of Resistive Load Detection," Respiration Physiology, 51: 131-139, 1983.

Mead, J., Turner, J. M., Macklem, P. T., Little, J. B., "Significance of the Relationship Between Lung Recoil and Maximum Expiratory Flow," Journal of Applied Physiology, 22:95-108, 1967.

Mead, J., Whittenberger, J. L., "Evaluation of Airway Interruption Technique as a Method for Measuring Pulmunary Air-Flow Resistance," Journal of Applied Physiology, 6:408-416, 1954.

Mead, J., Whittenberger, J. L., "Physical Properties of Human Lungs," Journal of Applied Physiology, 5:779-796, 1953.

Mendenhall, W., Sincich, T., "Statistics for Engineering and the Sciences," Dellen Publishing Company, San Fransisco, 3rd edition, 1992.

Milic-Emili, J., Mead, J., Glauser, E. M., "Improved Technique for Estimating Pleural Pressure from Esophageal Balloon," Journal of Applied Physiology, 19 (2):207-211, 1964.

Miyamoto, Y., Nakabayashi, T, Mikami, T., "Electronic Device for the Recording of Isopressure Flow-Volume (I.P.F.V.) Curves," Medical and Biological Engineering Computing, 16:83-89, 1978.

Neergard, K. von., Wirz, K., "Die Messung der Stromungwiderstande in den Atemwegen des Menschen insbesondere bie Asthma und Emphysem," Z Klin Med 105:51–82, 1927.

Ohya, N., Huang, J., Fukunaga, T., Toga, H., "Airway Pressure-Volume Curve Estimated by Flow Interruption During Forced Expiration," Journal of Applied Physiology, 67(6):2631-2638, 1989.

Ohya, N., Huang, J., Fukunaga, T., Toga, H., "Mouth Pressure Curve on Abrupt Interruption of Airflow during Forced Expiration," The Tohoku Journal of Experimental Medicine, 155(1):104-105, 1988.

Peslin, R., Navajas, D., Rotger, M., Farré, R., "Validity of the Esophageal Balloon Technique at High Frequencies," Journal of Applied Physiology, 74(3): 1039-1044, 1993.

Phagoo, S. B., Watson, R. A., Silverman, M., Pride, N. B., "Comparison of Four Methods of Assessing Airflow Resistance Before and After Induced Airway Narrowing in Normal Subjects," Journal of Applied Physiology, 79 (2): 518-525, 1995.

Pride, N. B., Permutt, S., Riley, R. L., Bromberger, B., "Determinants of Maximal Expiratory Flow from the Lungs," Journal of Applied Physiology, 23:646-662, 1967.

Shephard, R. J., "Mechanical Characteristics of the Human Airway in Relation to Use of the Interrupter Valve," Clinical Science, 25:253-280, 1963.

Smaldone, G. C., Bergofsky, E. H., "Delineation of Flow-Limiting Segment and Predicted Airway Resistance by Movable Catheter," Journal of Applied Physiology, 40(6):943-952, 1976.

Vincent, N. J., Knudson, R., Leith, D. E., Macklem, P. T., Mead, J., "Factors Influencing Pulmonary Resistance," Journal of Applied Physiology, 29(2):236-243, 1970.

Wiley, R. L., Zechman, F. W., "Perception of Added Airflow Resistance," Respiration Physiology, 2:73-87, 1966.

Wilson, T. A., Hyatt, R. E., Rodarte, J. R., "The Mechanisms that Limit Expiratory Flow," Lung, 159:193-200, 1980.

Zamel, N., Jones, J. G., Bach, S. M., Newberg, L., "Analog Computation of Alveolar Pressure and Airway Resistance During Maximum Expiratory Flow," Journal of Applied Physiology, 36(2):240-245, 1974.